Index

Introduction....1
Objectives of the Report....1
History of the Tourism Development of the Area and of the Need for Coastal Waters Protection....1
Brief Description of the Wastewater Systems and Receiving Waters....1
Description and Characterization of the Sewage System and Presentation of the Basic Design Data....3
Description of the systems....3
Funchal....3
Câmara de Lobos....4
Basic Design Data....5
Perspectives of Evolution of the Sewage System....5
Funchal....5
Câmara de Lobos....6
Climate in Madeira Island....7
Temperature and precipitation....7
Wind regime....7
Description of Receiving Waters....12
Location and bathymetry....12
General circulation....14
Canarias Current....14
Tidal Wave....17
Local circulation....22
Model Implementation....30
Density Driven Flow....32
Tidal circulation....38
Local Wind Variability....42
Transport Scenarios....44
Residual circulation....47
Avaliation of the effects in the receptor mean....54
Description and Microbiological Characterization of Beaches....54
Primary Production in Madeira Coastal Areas....56
Nitrates....56

Chlorophyll-a ..... 57
Transparency ..... 58
Dissolved oxygen ..... 58
Indicator Bacteria ..... 59
ASSESSMENT OF THE EFFECTS ON THE RECEIVING WATERS ..... 60
Simulation data ..... 62
Available light assessment ..... 63
ASSESSMENT OF THE BEHAVIOUR OF INITIAL DILUTION ..... 64
General considerations ..... 64
Physical considerations ..... 64
Biological considerations ..... 64
Methodology for simulation with CORMIX ..... 65
Results of the Discharge Effects Simulation ..... 66
SYSTEM ASSESSMENT: EFFECTS ON THE RECEIVING WATERS ..... 67
Introduction ..... 67
Eutrophication assessment ..... 68
Methodology Used ..... 69
Water quality simulation results ..... 70
North wind simulation ..... 71
South wind simulation ..... 74
West wind simulation ..... 77
East wind simulation ..... 80
No wind simulation ..... 83
Microbiological effects on bathing waters ..... 85
North wind simulation ..... 86
South wind simulation ..... 88
West wind simulation ..... 90
East wind simulation ..... 92
No wind simulation ..... 95
Assessment of the Effects of the Systems as Regards Compliance with EU Directives 96
Summary and conclusion ..... 98
References ..... 99

Index Figures

Figure 1 – Monthly mean windstress for January. Maximum vector plotted is 4.24x10-2 Pa. .....9

Figure 2 - Monthly mean windstress for April. Maximum vector plotted is $8.24x10^{-2}$ Pa. .....10

Figure 3 – Monthly mean windstress for July. Maximum vector plotted is $1.07x10^{-1}$ Pa. .....11

Figure 4 – Monthly mean windstress for October. Maximum vector plotted is $4.47x10^{-2}$ Pa. .....12

Figure 5 – Funchal bay location.....13

Figure 7 – T-S Diagram for Madeira region.....14

Figure 8 - Schematic representation of the circulation in the NorthEast Atlantic. Numbers represent transports in Sv ($1Sv=10^6m^3s^{-1}$). Adapted from Siedler and Onken (1996). .....15

Figure 9 – Velocity flow filed at 30 m depth an output of the model OCCAM obtain in the framework of the EU project CANIGO. .....16

Figure 10 – Surface geostrophic circulation around Madeira. Maximum velocity plotted is 5 cm $s^{-1}$. .....17

Figure 12- Amplitudes and phases of the major lunar tide M2 from Global Ocean Tides model FES95.2. This model predicts tidal sea level variations at any time and point in the deep ocean to within around 3 cm rms. Cophase lines are drawn with a 30° interval (0° phase has thicker lines) (Le Provost, 1998).....19

Figure 13 – Tidal circulation in the North Atlantic during a spring tide: a) 0h after high tide, b) 2h after high tide, c) 4h after high tide, d) 6h after high tide, e) 8h after high tide, f) 10 after high tide. .....21

Figure 14 – Location of the current meters. .....24

Figure 13 – Current meter data for the F1 location at 15 meters from the bottom and 40 m from surface. The measurements were made along 4 days, between 21 and 26 of June of 1990 . The properties represent in each graphic form the top are: salinity, temperature, pressure, current direction, current absolute velocity, X (WE) velocity component and finally Y (SN) velocity component. .....25

Figure 16 – Current meter data for the F1 location at 40 meters from the bottom and 15 m from surface. The measurements were made along 4 days, between 21 and 26 of June of 1990 . The properties represented in each graphic starting from the top are:

salinity, temperature, pressure, current direction, current absolute velocity, X (WE) velocity component and Y (SN) velocity component. .....26
Figure 17 – Current meter data for the F2 location at 15 meters from the bottom and 10 m from surface. The measurements were made along 4 days, between 21 and 26 of June of 1990 . The properties represent in each graphic starting from the top are: salinity, temperature, pressure, current direction, current absolute velocity, X (WE) velocity component and finally Y (SN) velocity component. .....27
Figure 18 – Current meter data for the F4 location at 15 meters from the bottom and 60 m from surface. The measurements were made along 4 days, between 21 and 26 of June of 1990 . The properties represent in each graphic form the top are: salinity, temperature, pressure, current direction, current absolute velocity, X (WE) velocity component and finally Y (SN) velocity component.....28
Figure 19 – Currentmeter data spectral analysis for the F2 location at 15 meters from the bottom and 10 m from surface. The measurements were made along 4 days, between 21 and 26 of June of 1990 . .....29
Figure 18 – Hydrodynamic model grid: a) entire domain, b) zoom of the archipelago, c) zoom of the Madeira island.....31
Figure 19– Surface residual circulation driven by summer climatological density at the Madeira archipelago scale. Colours represent temperature, isolines bathymetry and arrows velocity. .....33
Figure 20– Surface residual circulation driven by summer climatologic density at the Madeira island scale. The colours represent temperature, the isolines bathymetry and the arrows velocity. .....33
Figure 21– Surface residual circulation driven by summer climatologic density at the Funchal bay scale. The colours represent temperature, the isolines bathymetry and the arrows velocity. .....34
Figure 22– Residual circulation at 25 meters depth at the Funchal bay scale. The currents in this case are driven by summer climatologic density. The colours represent temperature, the isolines bathymetry and the arrows velocity. .....34
Figure 23– Residual circulation at 45 meters depth at the Funchal bay scale. The currents in this case are driven by summer climatologic density. The colours represent temperature, the isolines bathymetry and the arrows velocity. .....35
Figure 24– Residual circulation at 80 meters depth at the Funchal bay scale. The currents in this case are driven by summer climatologic density. The colours

represent temperature, the isolines bathymetry and the arrows velocity.....35
Figure 25 – Surface circulation driven by climatologic density and real wind at 5 meters depth at 30 of July of 1994 at the Madeira archipelago scale. The colours represent temperature, the isolines bathymetry and the arrows velocity.....36
Figure 26 – Surface circulation driven by climatologic density and real wind at 5 meters depth at 30 of July of 1994 at the Madeira island scale. The colours represent temperature, the isolines bathymetry and the arrows velocity.....37
Figure 27 – Surface circulation driven by climatologic density and real wind at 80 meters depth at 30 of July of 1994 at the Madeira island scale. The colours represent temperature, the isolines bathymetry and the arrows velocity.....37
Figure 28 – Residual surface circulation driven by climatologic density and real wind for along a 30 days period (July of 1994) at the Island scale at 5 meters depth. The colours and the isolines represent bathymetry and the arrows velocity. .....38
Figure 29 – Comparison between Funchal tidal gauge and model results along 8 days.39
Figure 30 – Tidal circulation along a spring tidal cycle with compute by the Mohid2000 model. The grey solid lines represent the bathymetry and the colours the water level: a) 0h after high tide, b) 2 after high tide, c) 4h after high tide, d) 6h after high tide, e) 8h after high tide, f) 10h after high tide. .....40
Figure 31 – Model water level and X velocity (WE) results for station F1. The velocity is compute 5 meters from surface.....41
Figure 32 –Model water level and X velocity (WE) results for station F2. The velocity is compute 5 meters from surface.....41
Figure 33 – Model water level and X velocity (WE) results for station F4. The velocites is compute 5 meters from surface.....42
Figure 34 - No separation, laminar boundary layer .....43
Figure 35 – Vortex pair with central return flow.....43
Figure 36 - wake formation with wave disturbances along the current/wake interface..44
Figure 37 - von Karman vortex street. .....44
Figure 38 - Examples of vortex streets behind an island observed in the atmosphere. The island of Guadelupe is seen to produce a von Karman vortex street. Two vortices are visible in the first image, the vortices on the other side of the vortex street cannot be seen because of a break in the cloud cover; the image is adapted from NASA (1968). .....44
Figure 39 – Model X velocity at 5 meters depth at F1 station evolution a long a period

of 8 days for several scenarios: No wind, west wind, east wind, north wind, south wind and schematic wake wind.....46
Figure 40 – Model Y velocity at 5 meters depth at F1 station evolution a long a period of 8 days for several scenarios: No wind, west wind, east wind, north wind, south wind and schematic wake wind.....46
Figure 41 – Model X velocity at 5 meters depth at F4 station evolution a long a period of 8 days for several scenarios: No wind, west wind, east wind, north wind, south wind and schematic wake wind.....47
Figure 42 – Model Y velocity at 5 meters depth at F4 station evolution a long a period of 8 days for several scenarios: No wind, west wind, east wind, north wind, south wind and schematic wake wind.....47
Figure 43 - Sketch of the flow field around a cylinder (circular island), showing the frictional boundary layer and the forces experienced by a water particle as it moves along a streamline (Tomczak, 1996). .....48
Figure 44 – Surface residual circulation forced by tide for a period of 8 days along the Madeira coast line. .....50
Figure 45 - Surface residual circulation forced by tide for a period of 8 days in the Desertas islands. .....50
Figure 46 – Surface residual circulation forced by tide for a period of 8 days along Madeira south coast .....51
Figure 47 – Surface residual circulation forced by tide and north wind for a period of 8 days along Madeira south coast . .....51
Figure 48 – Surface residual circulation forced by tide and south wind for a period of 8 days along Madeira south coast . .....52
Figure 49 –Residual circulation at 20 meters depth forced by tide and south wind for a period of 8 days along Madeira south coast .....52
Figure 50– Surface residual circulation forced by tide and west wind for a period of 8 days along Madeira south coast . .....53
Figure 51 – Surface residual circulation forced by tide and east wind for a period of 8 days along Madeira south coast . .....53
Figure 52 – Surface residual circulation forced by tide and schematic wake wind for a period of 8 days along Madeira south coast .....54
Figure 53 - Distribution of total coliforms (NMP/100 ml) in Barreirinha beach .....55
Figure 54- Distribution of fecal coliforms (NMP/100 ml) in Barreirinha beach .....55

Figure 55 - Distribution of fecal streptococci (NMP/100 ml) in Barreirinha beach.....55
Figure 56 – Squematic presentation of the sampling stations .....57
Figure 57 - Space variation of the concentration of Chlorophyll-a in October 1998 .....57
Figure 58 – Spacial variation of dissolved oxigen concentration in October 1998.....58
Figure 59 – Distribution of total coliforms near the Funchal outfall.....59
Figure 60 – Distribution of fecal coliforms near the Funchal and Câmara de Lobos outfall.....59
Figure 61 – Distribution of fecal streptococcis near the Funchal and Câmara de Lobos outfall.....60
Figure 62 Simulation with North wind. Increase ammonia concentration caused by wastewater discharge after primary treatment. .....71
Figure 63 Simulation with North wind. Increase nitrate concentration caused by wastewater discharge after primary treatment. .....71
Figure 64 Simulation with North wind. Increase $BOD_5$ concentration caused by wastewater discharge after primary treatment. .....72
Figure 65 Simulation with North wind. Increase phytoplankton concentration caused by wastewater discharge after primary treatment. .....72
Figure 66 Simulation with North wind. Decrease oxygen (percentage) caused by wastewater discharge after primary treatment. .....73
Figure 67- Simulation with South wind. Increase ammonia concentration caused by wastewater discharge after primary treatment. .....74
Figure 68 Simulation with South wind. Increase nitrate concentration caused by wastewater discharge after primary treatment. .....74
Figure 69 Simulation with South wind. Increase $BOD_5$ concentration caused by wastewater discharge after primary treatment. .....75
Figure 70 Simulation with South wind. Increase phytoplankton concentration caused by wastewater discharge after primary treatment. .....75
Figure 71 Simulation with South wind. Decrease oxygen (percentage) caused by wastewater discharge after primary treatment. .....76
Figure 72- Simulation with West wind. Increase ammonia concentration caused by wastewater discharge after primary treatment. .....77
Figure 73 Simulation with West wind. Increase nitrate concentration caused by wastewater discharge after primary treatment. .....77
Figure 74 Simulation with West wind. Increase $BOD_5$ concentration caused by

wastewater discharge after primary treatment. .....78
Figure 75 Simulation with West wind. Increase phytoplankton concentration caused by wastewater discharge after primary treatment. .....78
Figure 76 Simulation with West wind. Decrease oxygen (percentage) caused by wastewater discharge after primary treatment. .....79
Figure 77- Simulation with East wind. Increase ammonia concentration caused by wastewater discharge after primary treatment. .....80
Figure 78 Simulation with East wind. Increase nitrate concentration caused by wastewater discharge after primary treatment. .....80
Figure 79 Simulation with East wind. Increase $BOD_5$ concentration caused by wastewater discharge after primary treatment. .....81
Figure 80 Simulation with East wind. Increase phytoplankton concentration caused by wastewater discharge after primary treatment. .....81
Figure 81 Simulation with East wind. Decrease oxygen (percentage) caused by wastewater discharge after primary treatment. .....82
Figure 82- Simulation with no wind. Increase ammonia concentration caused by wastewater discharge after primary treatment. .....83
Figure 83 Simulation with no wind. Increase nitrate concentration caused by wastewater discharge after primary treatment.....83
Figure 84 Simulation with East wind. Increase $BOD_5$ concentration caused by wastewater discharge after primary treatment. .....84
Figure 85 Simulation with no wind. Increase phytoplankton concentration caused by wastewater discharge after primary treatment. .....84
Figure 86 Simulation with no wind. Decrease oxygen (percentage) caused by wastewater discharge after primary treatment. .....85
Figure 87Faecal coliforms concentration after an 8 days run with North wind. The characteristics of the effluent are: a concentration of $10^3$ coliforms/ 100 ml after initial dilution and a $T_{90}$ of 2 hours. .....86
Figure 88 Faecal coliforms concentration after an 8 days run with North wind. The characteristics of the effluent are: a concentration of $10^3$ coliforms/ 100 ml after initial dilution and a $T_{90}$ of 6 hours. .....86
Figure 89 Faecal coliforms concentration after an 8 days run with North wind. The characteristics of the effluent are: a concentration of $10^3$ coliforms/ 100 ml after initial dilution and a $T_{90}$ infinite. .....87

Figure 90Faecal coliforms concentration after an 8 days run with South wind. The characteristics of the effluent are: a concentration of $10^3$ coliforms/ 100 ml after initial dilution and a $T_{90}$ of 2 hours. .....88
Figure 91 Faecal coliforms concentration after an 8 days run with South wind. The characteristics of the effluent are: a concentration of $10^3$ coliforms/ 100 ml after initial dilution and a $T_{90}$ of 6 hours. .....88
Figure 92 Faecal coliforms concentration after an 8 days run with South wind. The characteristics of the effluent are: a concentration of $10^3$ coliforms/ 100 ml after initial dilution and a $T_{90}$ infinite. .....89
Figure 93Faecal coliforms concentration after an 8 days run with West wind. The characteristics of the effluent are: a concentration of $10^3$ coliforms/ 100 ml after initial dilution and a $T_{90}$ of 2 hours. .....90
Figure 94 Faecal coliforms concentration after an 8 days run with West wind. The characteristics of the effluent are: a concentration of $10^3$ coliforms/ 100 ml after initial dilution and a $T_{90}$ of 6 hours. .....90
Figure 95 Faecal coliforms concentration after an 8 days run with West wind. The characteristics of the effluent are: a concentration of $10^3$ coliforms/ 100 ml after initial dilution and a $T_{90}$ infinite. .....91
Figure 96Faecal coliforms concentration after an 8 days run with East wind. The characteristics of the effluent are: a concentration of $10^3$ coliforms/ 100 ml after initial dilution and a $T_{90}$ of 2 hours. .....92
Figure 97 Faecal coliforms concentration after an 8 days run with East wind. The characteristics of the effluent are: a concentration of $10^3$ coliforms/ 100 ml after initial dilution and a $T_{90}$ of 6 hours. .....92
Figure 98 Faecal coliforms concentration after an 8 days run with East wind. The characteristics of the effluent are: a concentration of $10^3$ coliforms/ 100 ml after initial dilution and a $T_{90}$ infinite. .....93
Figure 99Faecal coliforms concentration after an 8 days run without wind. The characteristics of the effluent are: a concentration of $10^3$ coliforms/ 100 ml after initial dilution and a $T_{90}$ of 2 hours. .....95
Figure 100 Faecal coliforms concentration after an 8 days run without wind. The characteristics of the effluent are: a concentration of $10^3$ coliforms/ 100 ml after initial dilution and a $T_{90}$ of 6 hours. .....95
Figure 101 Faecal coliforms concentration after an 8 days run without wind. The

characteristics of the effluent are: a concentration of $10^3$ coliforms/ 100 ml after initial dilution and a $T_{90}$ infinite. .....96

Index Tables

Table 1 ..... 5
Table 2 ..... 5
Table 3 – Amplitudes and phases of tidal harmonic constituents in Funchal harbor (Direcção Geral de Portos) ..... 18
Table 4 - Typical values found for a flat plate oriented perpendicular to the flow, other shapes are also consider. ..... 43
Table 5 – Flow in each outfall ..... 62
Table 6– Characterisation of affluent at the ETAR ..... 62
Table 7 - Reduction of pollutant loads in accordance primary treatment ..... 62
Table 8 - Seawater ambient conditions. ..... 63
Table 9 - Parameters used for simulation of the initial dispersion, in stratification conditions ..... 66
Table 10– Concentrations obtained after initial dispersion ..... 67

# FUNCHAL, SANTA CRUZ, CÂMARA DE LOBOS & CALHETA

# WASTEWATER SYSTEMS

---

## Consolidated Report on the Assessment of Effects on the Receiving Waters

---

**FUNCHAL, DECEMBER 2000**

# Introduction

## Objectives of the Report

The aim of this report is to analyse the effect of urban wastewater discharges in the coastal waters from agglomerations of between 15,000 and 150,000 population equivalent.

## History of the Tourism Development of the Area and of the Need for Coastal Waters Protection

Madeira Island is located at about 1,000 km of the Iberian coasts, in Atlantic Ocean. It is characterized by a steeped topography and presents a tempered climate, with very soft average temperatures throughout all the year, and an abundant rainfall. This island presents great natural beauty and a high tourist potential, mainly, because of the conjugation of two factors: its beauty and the temperate climate that occurs practically all year.

In terms of geographic distribution it presents population agglomerations of reduced dimension and, because of the eminently agricultural features of this island associated to its steeped topography, a significant part of the population lives scattered. The main exception to this scenario is the city of the Funchal that presents a population distribution almost uniform.

The economic development of Funchal's region, established mainly on the exploration of the tourist and commercial activities, served as catalyser to the urban concentration and to the demographic expansion of the municipality.

Due to the great tourist potential of this island, it has had an increasing concern to preserve its greater attractions, such as its natural beauty and the quality of oceanic waters. It is an example of this, the region of Porto Moniz, with a population equivalent of 2,200, where is been developed the project of a tertiary wastewater treatment plant with ultraviolet, to preserve the quality of the coastal waters and its natural swimming pools.

## Brief Description of the Wastewater Systems and Receiving Waters

The Funchal Wastewater System serves a catchment's area of 2,400 hectares including most of Funchal municipality. The population served by the system is estimated at 140,000 population equivalents, of resident and fluctuant population.

This system includes the following key components, described in more detail in Chapter 2 of this document:

a) **Main Gravity Interceptor**, located downtown, receives the sewage collected and transported by the existing collecting system.
b) **Outlets Facilities,** which allows the separation of the storm flows.
c) **Wastewater Treatment Plant (ETAR)**, consisting of a primary screening, removal of grit, oils and grease and a final fine screening.
d) **Lift station**, composed by a central lift located in the wastewater treatment plant building allows the effluent lift to the terrestrial emissary.
e) **Terrestrial Emissary**, developed in tunnel throughout an extension of about 1,800 meters, finishing perpendicularity to the coast near Garajau.
f) **Submarine Outfall**, of a total length of 650 m, with a 140 m diffuser, which discharge the effluent at 60 m in depth.

The Câmara de Lobos Wastewater System serves most of Câmara de Lobos municipality and also receives the industrial wastewater proceeding from the West Zone Industrial Park. Before being mixed with the domestic wastewater, the industrial effluent suffers a preliminary treatment at the industrial unit. The population served by the system is estimated at 23,600 population equivalents.

This system is similar to the Funchal Wastewater System and includes the following key components, described in more detail in Chapter 2 of this document:

a) **Wastewater Treatment Plant (ETAR)**, consisting of a primary screening, removal of grit, oils and grease and a final screening.
b) **Lift Station**, composed by a central lift located in the wastewater treatment plant building allows the effluent lift to the submarine outfall.
c) **Submarine Outfall**, of a total length of 1,000 m, which discharge the effluent at 60 m in depth.

Figure 1 shows the location of the Funchal and Câmara de Lobos Wastewater System.

In accordance with the relevant legislation, Madeira's coast, in particular the south coast of the island where the outfalls are located is classified as a **less sensitive zone**. This situation is essentially the result of the location of the island (in the meddle of the Atlantic Ocean), its high coastal edges slopes and high transparency deeps.

# Description and Characterization of the Sewage System and Presentation of the Basic Design Data

## Description of the systems

### Funchal

The wastewater system of Funchal serves an attendance area of about 2,400 ha, that encloses the city of the Funchal, as well as the adjacent hillsides. The drainage, treatment and final disposal system of the Funchal includes as main components the ones that fallow:

**Main Interceptor**, located downtown, receives the sewage transported by the existing transportation system. This is a combined drainage system, witch means that transports domestic wastewater as well as pluvial flows. With the objective of not exceed the capacity of the transport and treatment system, there are some outlets facilities which allows the separation of the storm flows. These structures lead the wastewater to the domestic sewage system and allow the discharge of the extra flows, which occurs in the winter, to the ocean. Next, is shown a resumed characterisation of the outlet structures of the system.

**Outlet D1**, located after the S. Luzia small river, allows the discharge of the runoff whenever the flows exceed the maximum limit of six times the domestic average flow.

**Outlet D2**, located after the João Gomes small river, allows the discharge of the runoff whenever the flows exceed the maximum limit of six times the domestic average flow.

**Outlet D3**, located before the wastewater treatment plant, allows the relief of the volumes from the system always that they exceed the maximum limit of three times the domestic average volume.

**Wastewater Treatment Plant**, consisting of a primary screening, removal of grit, oils and grease and a final screening. The affluent is transported directly to a screening chamber with three grids each one with a unitary capacity of 2.1 $m^3/s$. The distance between grids is of 20 mm, value that assures enough protection for the bolters. After passing this screen, the effluent passes through a circular grid removal, 10 meters in diameter, with scraper and lateral tank for sand retraction. The sand is leaded for two grid classifiers units through a rise screw. The final stage of the treatment consists of a fine screening. There are three fine rotary drum screens. One of them has a perforated screen plate with openings of 1.5 mm and the remainders have openings of 0.5 mm.

**Lift Station**, composed by a central lift located in the wastewater treatment plant

building and by a conduit that makes the connection to the terrestrial emissary. The lift station is equipped with four submergible groups and has a pumping well with a volume adequate to a start/stopping cycle of six times per hour. The lift conduit has an extension of about 235 meters, with a diameter of 1,200 mm. The total head lost is 15.00 meters.

**Terrestrial Emissary**, starts in the Funchal National number 2 High school yard and is developed in tunnel throughout an extension of about 1,800 m, finishing perpendicularity to the coast near Garajau. The tunnel presents a circular section of ϕ 2,300 mm, with an interior diameter of 1,700 mm.

**Submarine Outfall**, constructed in High Density Polythene (HDPE), with 1,200 mm in diameter, is developed after the terrestrial emissary. It presents a total length of 650 m, with a 140 m diffuser. The diffuser is divided in three distinct fragments: the initial fragment, with ϕ 1,000 mm, presents 20 ports of ϕ 80 mm each; the middle fragment, with ϕ 800 mm, presents 20 ports of ϕ 100 mm and the final fragment, of ϕ 500 mm, presents 20 orifices of ϕ 100 mm.

Before the construction of Funchal's wastewater system, the drainage of urban wastewater was done through a set of collectors that discharge the effluent directly in the ocean in front of the city, being the main outputs located between the S. João and St.ª Luzia small rivers and near the old fisher market. The effluent from the tourist zone was discharged in the St.ª Luzia small river.

## Câmara de Lobos

The old zone of Câmara de Lobos is served by a combined collecting system. The remaining zones, as well as the bordering regions, have separated wastewater collecting system and pluvial collecting systems. This collecting systems also serves part of the populations of the Estreito de Câmara de Lobos.

The treatment and final disposal system of Câmara de Lobos is similar to Funchal wastewater system, consisting of a wastewater treatment plant based on physical processes, followed by a submarine outfall, which promotes the discharge of the effluent in the ocean, far away from the shoreline.

The processes and operations of this wastewater treatment plant consist of a mechanical screening, followed by a physical removal of grit and a fine screening of 0.3 mm. It has a sand classifier. The odor treatment is made by a system of activated coal.

The submarine outfall, with a diameter of 350 mm and a length of 1,000 meters, discharges at the bathymetry of -60 m.

The effluent that reaches the treatment plant is a mixture of domestic wastewater with industrial wastewater proceeding from the West Zone Industrial Park (WZIP), located in the Ribeira dos Socorridos. Before being mixed with the domestic wastewater, the industrial effluent suffers a preliminary treatment at the industrial unit, in accordance with the WZIP's regulation.

### Basic Design Data

The following tables present the basic design data of the wastewater systems of Funchal and Câmara de Lobos. Table 1 presents the populations and the systems flows, while Table 2 presents pollutant loads.

**Table 1**

| Parameters | Location | |
|---|---|---|
| | Funchal | Câmara de Lobos |
| Population Equivalent [hab] | 140,000 | 23,600 |
| Average Flow [$m^3$/d] | 22,000 | 4,320 |
| Average Flow [$m^3$/s] | 0.255 | 0.050 |

**Table 2**

| Parameters | Location | |
|---|---|---|
| | Funchal | Câmara de Lobos |
| $BOD_5$ [kg/d] | 8,400 | 1,416 |
| DOC [kg/d] | 18,900 | 3,186 |
| TSS [kg/d] | 12,600 | 2,124 |
| N [kg/d] | 1,400 | 236 |
| P [kg/d] | 420 | 71 |

The data of Câmara de Lobos include the industrial flows from the WZIP industrial zone. The industrial contributions, in pollutant load terms, have a small significance because the industrial effluents have a preliminary treatment before the input in the domestic system, in accordance with the WZIP's regulation.

## Perspectives of Evolution of the Sewage System

### Funchal

Before the existing system of drainage, treatment and final disposal of wastewaters of Funchal's municipality begin to work, the effluent discharge was made directly to the city's Bay. This system was composed by a set of combined collectors that, during the rainy times, discharged part of the diluted effluent directly to small rivers. The domestic effluent was discharged in the ocean, practically all concentrate, in a restricted area between Saint Luzia and João Gomes small rivers.

The conception of the Wastewater System of Funchal's municipality, such as it presents currently, dates of the beginning of the decade of 90. This system was constructed with the principal propose of safeguarding the quality of the sea waters that bathe the edge of the Front Sea of the Funchal and, also, the tourist activity, main income source of all the region.

The main objectives of the system are:

- To intercept and to deviate from some water strings the wastewater discharges.
- To deviate the wastewater discharges from the Funchal's Bay, to safeguard the quality of beach waters, to protect the public health and to avoid compromising the tourist potential of the region.
- To contribute for the valorization and ambient protection of the receptor mean, using its assimilation capacity.

The topography of Funchal's city, characterized by steeped zones with high inclinations and lack of flat, ample places and moved away enough where a conventional wastewater treatment plant could be installed, had led to the adoption of the actual wastewater system.

The Funchal wastewater treatment plant is located in the middle of city historical center, in a very beautiful place and with a high tourist potential. The implantation and the architecture of this treatment plant were thought in form to cause the minor visual impact.

The location of the submarine outfall was chosen with the intention of deviate from the Funchal west region (in which develops the main zone of hotel occupation of the "Front Sea" and where the tourist industry is centered) the discharge of domestic wastewater.

The impacts resulting of the implantation of a convention wastewater treatment plant would have to be analyzed. These impacts are mainly of psychological order (understand the impact that can produce in the tourist population), since the tourism is the most important activity in the economy of the island and, because of that, the protection of the natural environment is very important. Another query is the fact that the improvement of the wastewater treatment presents other environmental costs, such as the sludge management process, that cannot be neglected.

### Câmara de Lobos

Before the existing wastewater system of Câmara de Lobos's municipality start to work, the effluent discharge was made directly to the ocean, near the access to the Wharf of the village. This system was constituted of a set of domestic collectors, with exception

to the restricted area of the downtown of the village, where the network was combined.

The conception of the Wastewater System of Câmara de Lobos, such as it presents currently, had been foreseen due to some limitations of topographical and geographic order. Thus, the topographical features of the zone of the final discharge, the high population density of the village and the extension of the geographic area to enclose on the system, had implied the implantation of the treatment plant in a zone conquest to the sea, through a platform. This solution was adopted in order to minimize the negative effect of aesthetic order and the lack of available space.

The adoption of a traditional wastewater treatment plant in land would cause a significant increase of the platform necessary area, together with an upgrade of the amount sludge produced, with the respective problems of management and final disposal.

## Climate in Madeira Island

### Temperature and precipitation

The temperature and precipitation values are quite different between the south and north coasts. The south coast has larger temperatures and lower precipitation values. The annual average values of temperature also decrease form the coast to the interior proportionally to the increase of altitude. In the *Lugar de Baixo* (15 m) the annual average value is 19.4 ºC while in Funchal (58 m) is 18.8ºC, in Santana (380 m) is 15.2 ºC, in Queimadas (860 m) 12.7 ºC and finally 9.7 ºC in Arieiro (1610 m). The monthly average temperature does not change much along the year. In Funchal the highest values are observed in the summer, 22.2 ºC in August, and the lowest in the winter, 15.9 ºC in February.

The annual average precipitation values increase also in altitude: 533 mm in Funchal and 3084 mm in Arieiro. The monthly average values have a strong variation along the year. The period between October and March is the rainiest one.

### Wind regime

The predominant meteorological conditions near Madeira archipelago are constrained by the subtropical Azores high pressure system. In this region, the Azores high transports tropical air leading to northeasterly winds during the entire year in a zone between 35ºN and 20ºN and extending to the west as far as 20ºW. The Azores high has annual variations of intensity and localization. During summer it moves to NE relatively

to its mean position to the SW of Azores archipelago and it becomes stronger (pressures in the center ranging from 1025 to 1035 mb). During winter the Azores high is located to the South of its mean position and is weaker (1020 to 1030 mb in the center). Between November and March, the Subpolar Frontal System has also effects in the Madeira region. Other regional features affecting the meteorological conditions in Madeira are the standing low pressure systems that sometimes is formed between October and March between the Iberian Peninsula and the Azores and Canary Islands. This low pressure system extends its influence to 20ºN and usually lasts for a week, leading to the occurrence of high nebulosity and rain over Madeira. Thus, predominant winds in Madeira region are from the North/Northeast in most of the situations. One exception is when the Azores High is located to the South of Azores and oriented from West to East. In this situation the winds are moderated and from the west. Other exceptions occur when:

A strong high pressure system is developed to the North of Madeira and is oriented from West to East. This high pressure system is associated with a low pressure system over Africa and near Madeira, that induces winds from the East that transport warm and dry air. Although this situation is not very common, it occurs from February to April and from August to October and usually lasts for 3 days (sometimes 7 days).

The passage of frontal systems, although not very common, may induce strong winds from the South. This phenomenon specially occurs if the frontal system passage occurs during Autumn or Winter.

In Figure 1 toFigure 4, the monthly mean windstress in January, April, July and October is shown. No marked seasonal variations in windstress direction are evident. However, the intensity of windstress increases from winter to summer in response to the increase of the strength of the Azores high.

Finally we should note that local wind patterns over the southern part of Madeira Island may be completely different due to the formation of Lee regions associated with the orography of the Island. This phenomenon has been described in other islands like the Gran Canaria (Barton, 2000).

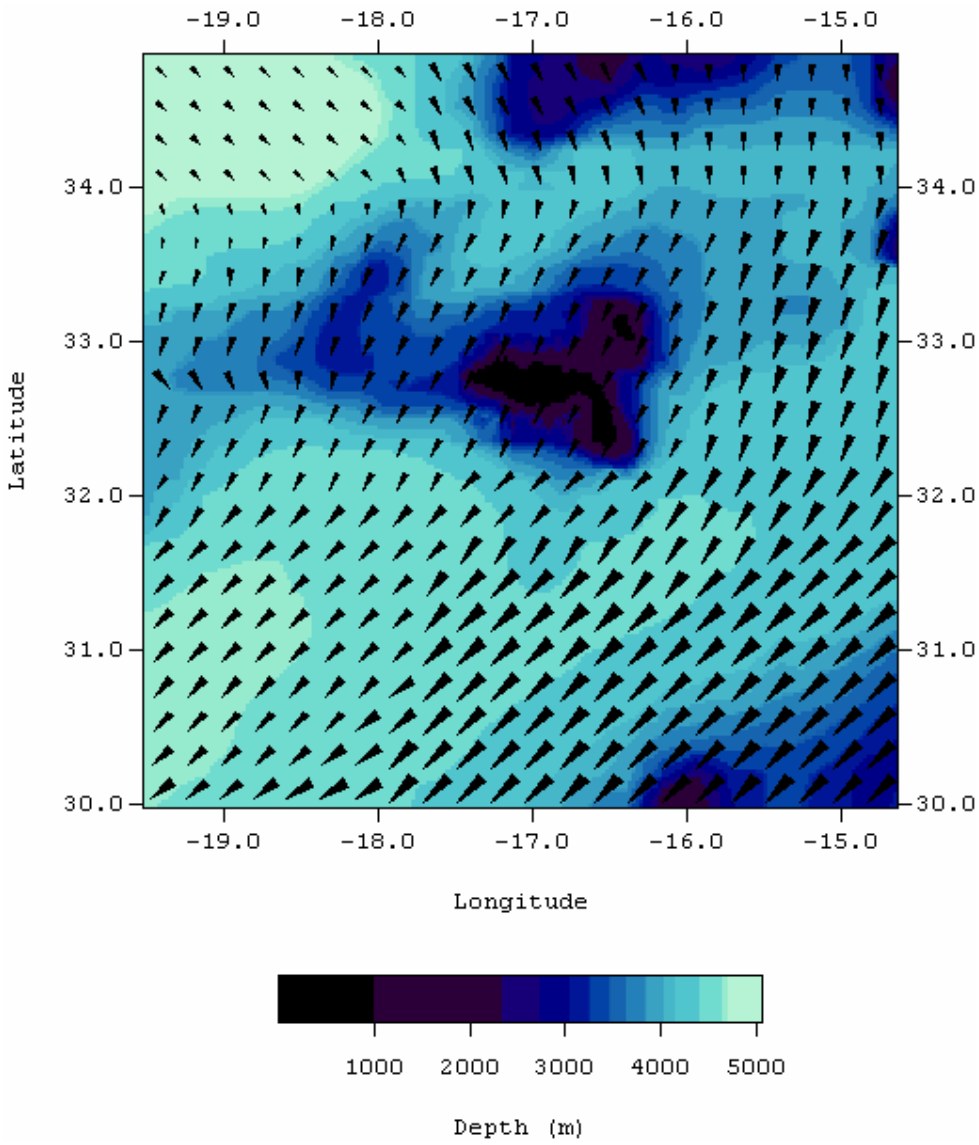


**Figure 1** – Monthly mean windstress for January. Maximum vector plotted is 4.24x10-2 Pa.

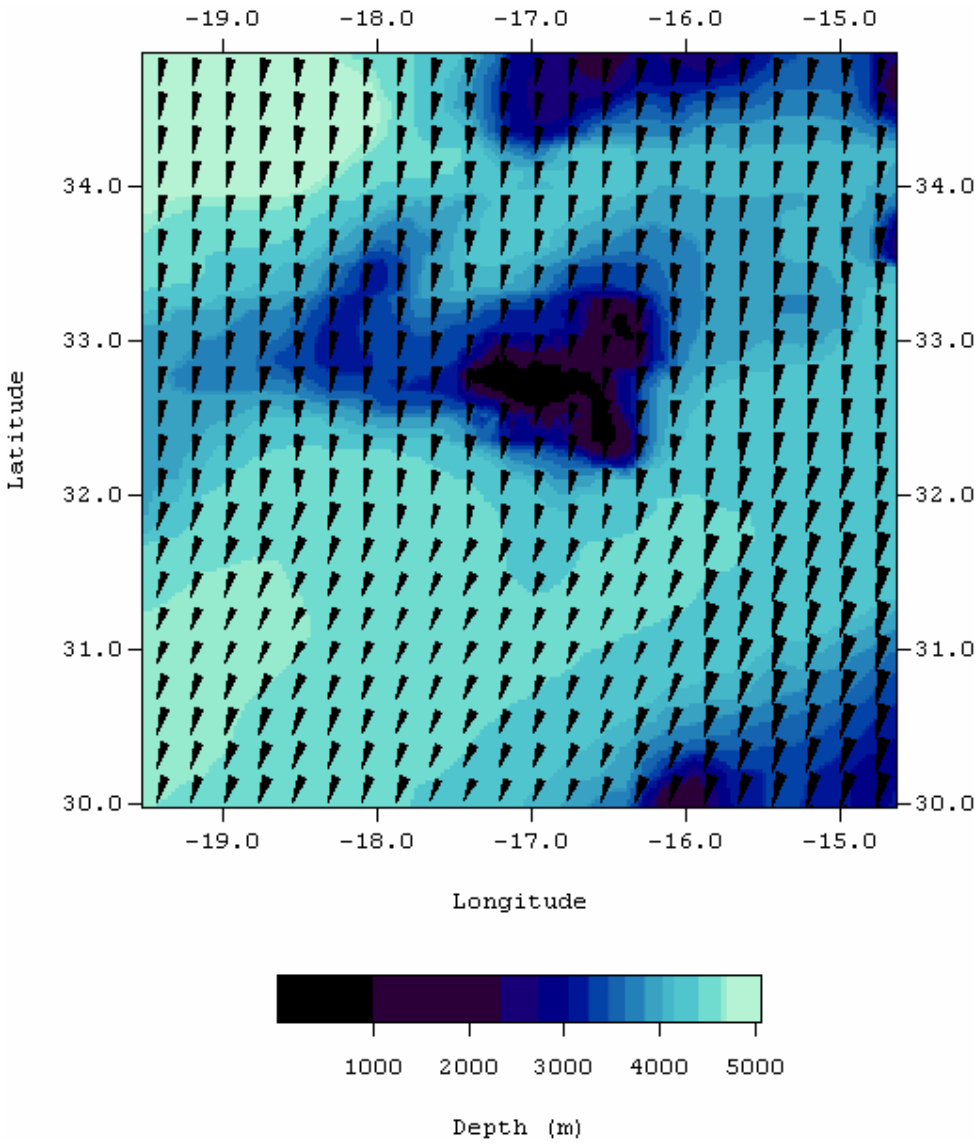


**Figure 2 -** Monthly mean windstress for April. Maximum vector plotted is $8.24 \times 10^{-2}$ Pa.

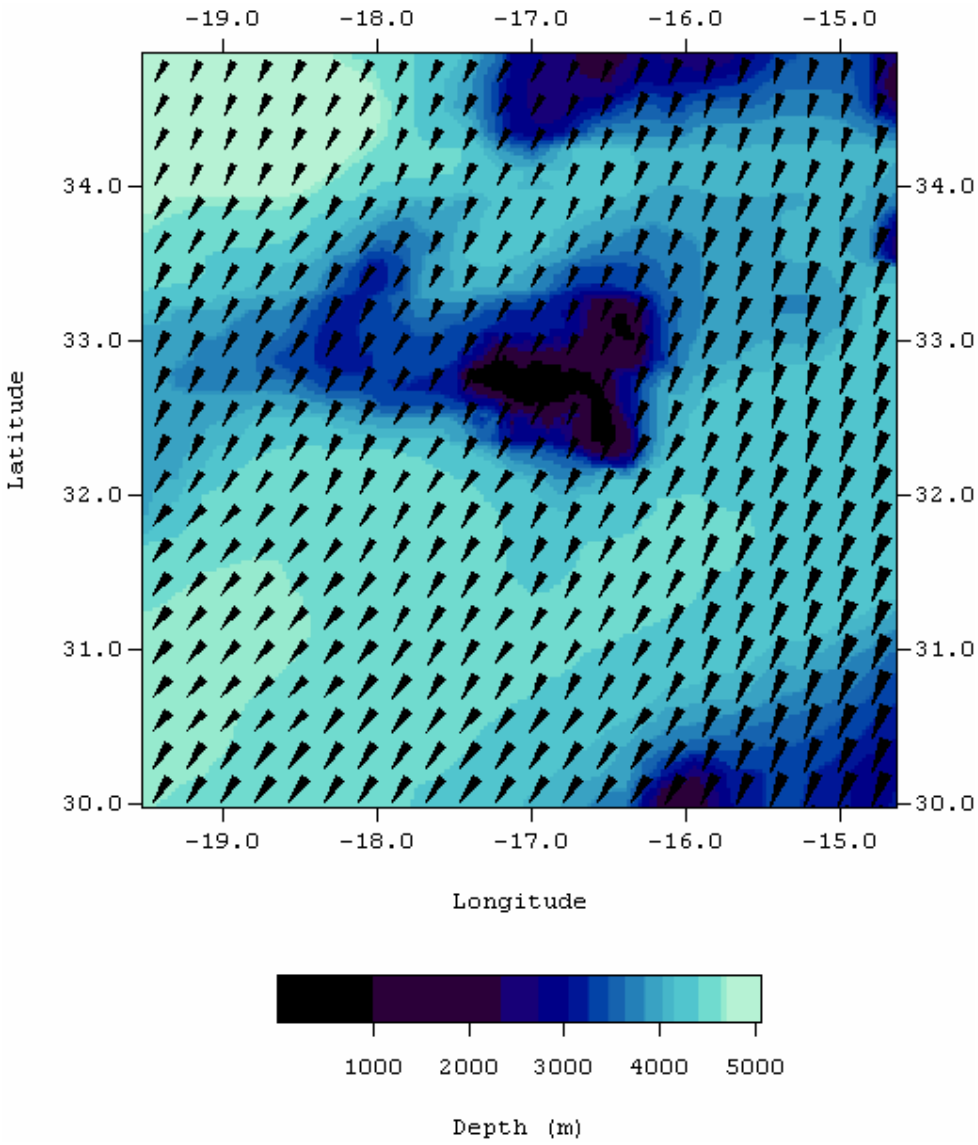


**Figure 3** – Monthly mean windstress for July. Maximum vector plotted is $1.07 \times 10^{-1}$ Pa.

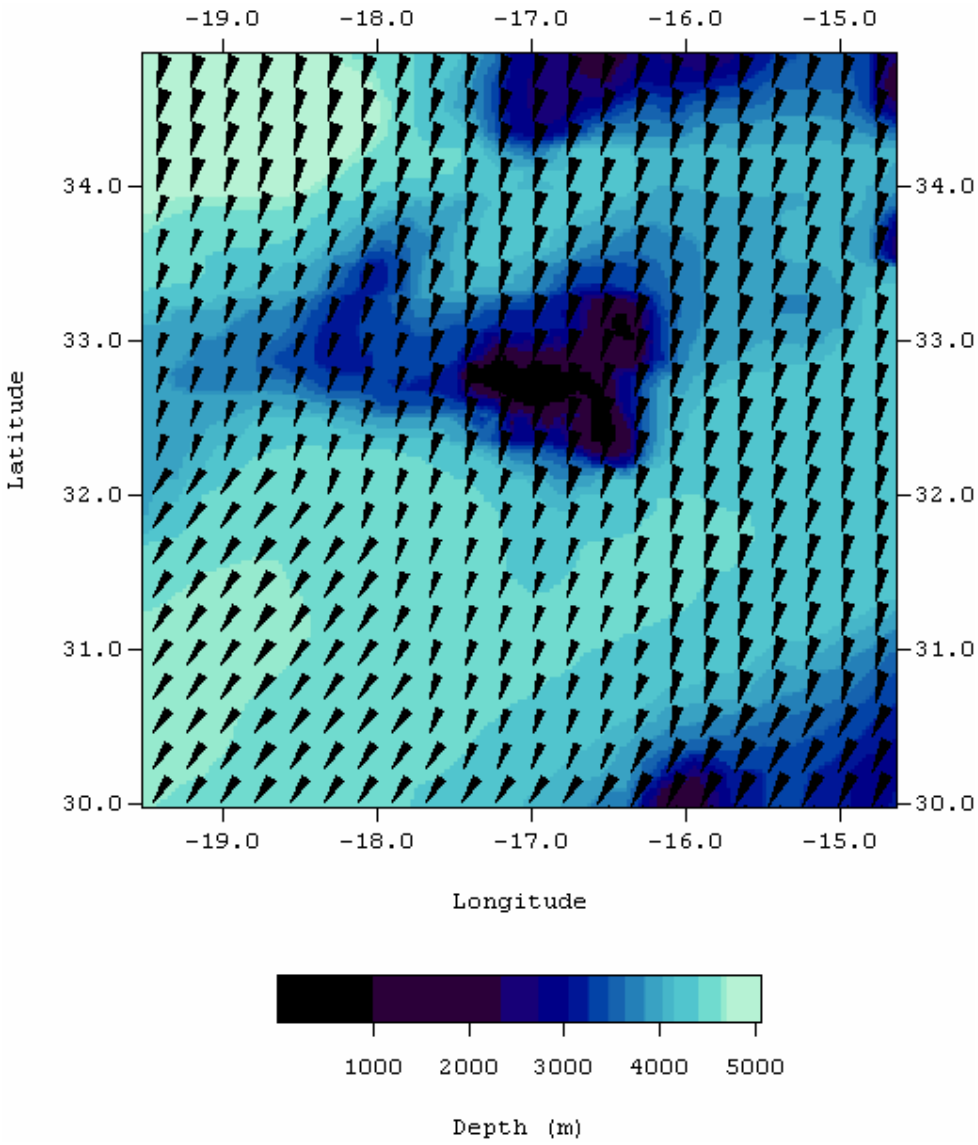


**Figure 4** – Monthly mean windstress for October. Maximum vector plotted is $4.47 \times 10^{-2}$ Pa.

## Description of Receiving Waters

### Location and bathymetry

Madeira is a semi-tropical island, situated in the Atlantic Ocean, off the coast of Africa. The outfalls are implemented mainly in the island South Coast. The main one is implemented in the Funchal Bay (Figure 5). The bottom topography where the outfalls are situated is very steep for example the 500 m bathymetric is located 3 km from the coastline. These large depths will induce large initial dilutions. Preliminary results produce with the Cormix model ("CORnell MIXing System") indicated values of initial dilutions of 2000.

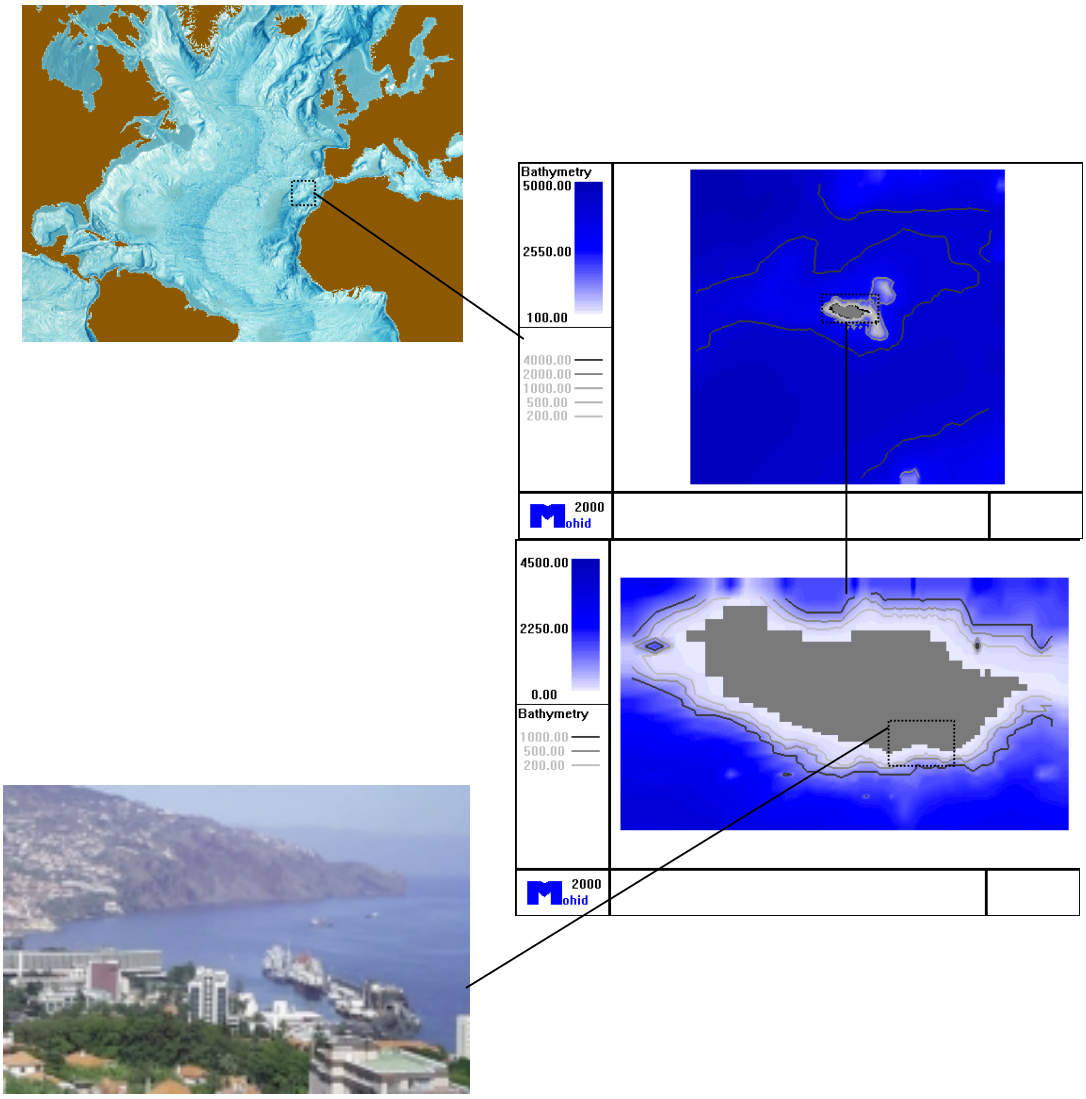


**Figure 5 –** Funchal bay location.

## General circulation

The water masses present near Madeira archipelago are the usual in the North Atlantic. Below the surface mixed layer, the North Atlantic Central Water (NACW) is found, with temperatures ranging from 8 to 19ºC and salinities from 35.1 to 36.7. At depths between 900 and 1200 m, the Mediterranean Water is found, which is characterised by an increase in salinity to values of the order of 35.5-35.8. At greater depths, we found the deep and bottom waters with temperatures lower than 5ºC and salinity lower than 35.2 (see Figure 6).

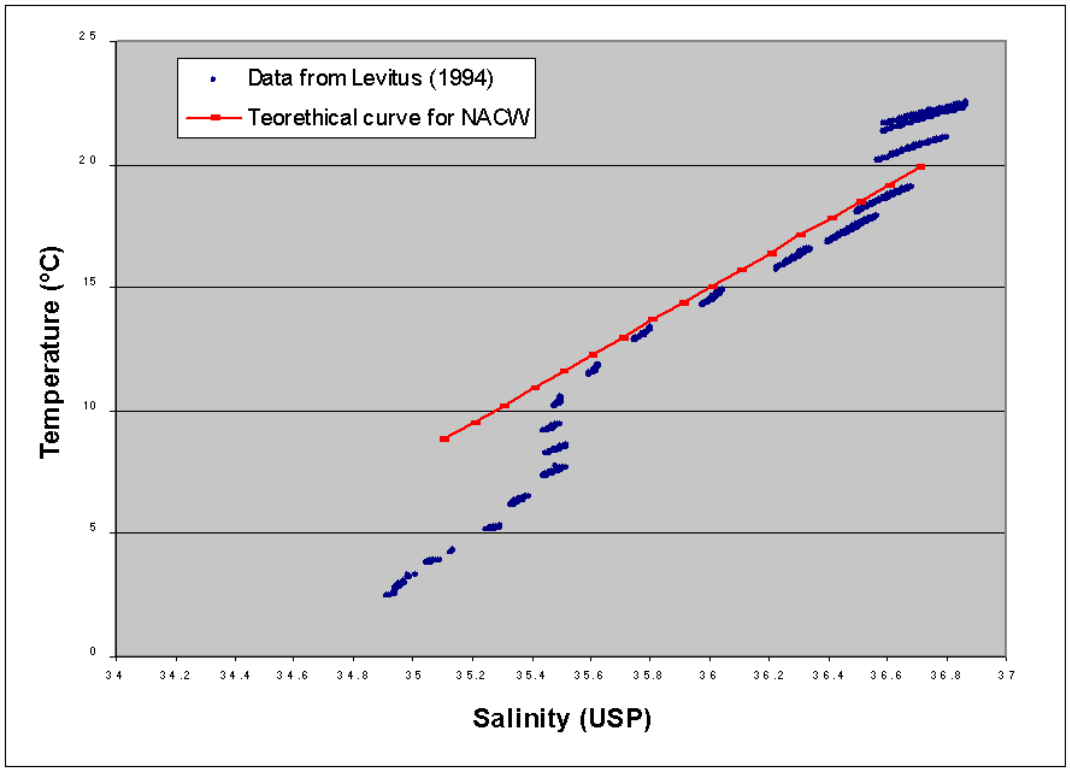


**Figure 6** – T-S Diagram for Madeira region.

### Canarias Current

The surface currents near Madeira Archipelago are part of the general circulation of the North Atlantic. Near Cape Hateras (in Florida) the Gulf Stream leaves the American coast and moves to the East. Southeast of the Grand Banks off Newfoundland, the Gulf Stream separates into two branches. The northern branch turns northeastward and becomes the North Atlantic Current. The southern branch, which becomes the Azores Current, heads southeastward across the Mid-Atlantic Ridge to the Azores, then flows

mainly eastward at a latitude of about 35ºN to the Gulf of Cadiz. The Azores Current is observed to be a meandering zonal jet 60-100 km wide with an eastward velocity of 25-50 $cms^{-1}$. The eastward flow is mostly in the upper few hundred meters but can reach as deep as 2000 m. The current carries a large fraction of the water entering the eastern recirculation flow of the Canary Basin. The other fraction of water entering the Canary Basin comes from the North and is the southern branch of the North Atlantic Current often called the Portugal Current (see Figure 7).

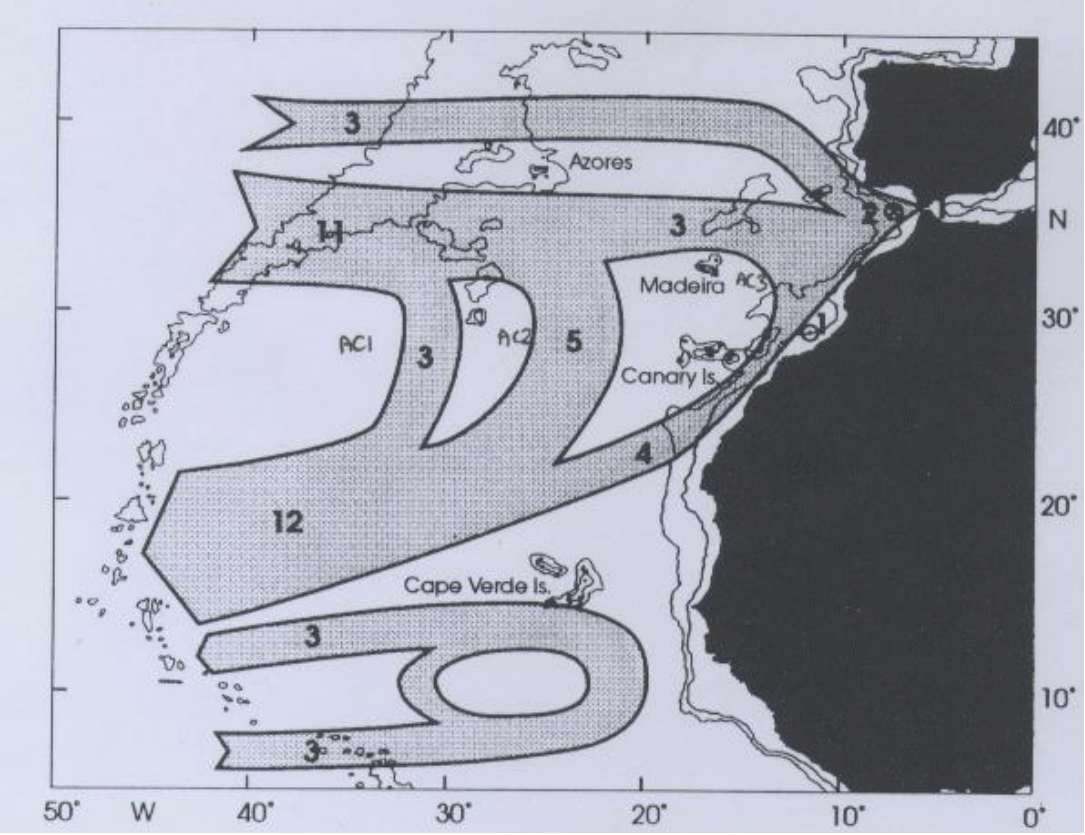


**Figure 7** - Schematic representation of the circulation in the NorthEast Atlantic. Numbers represent transports in Sv ($1Sv=10^6 m^3 s^{-1}$). Adapted from Siedler and Onken (1996).

In Figure 8, model results of the surface current field in the Northeast Atlantic are shown. It can be seen how the currents around Madeira are very weak with spatial variations in direction.

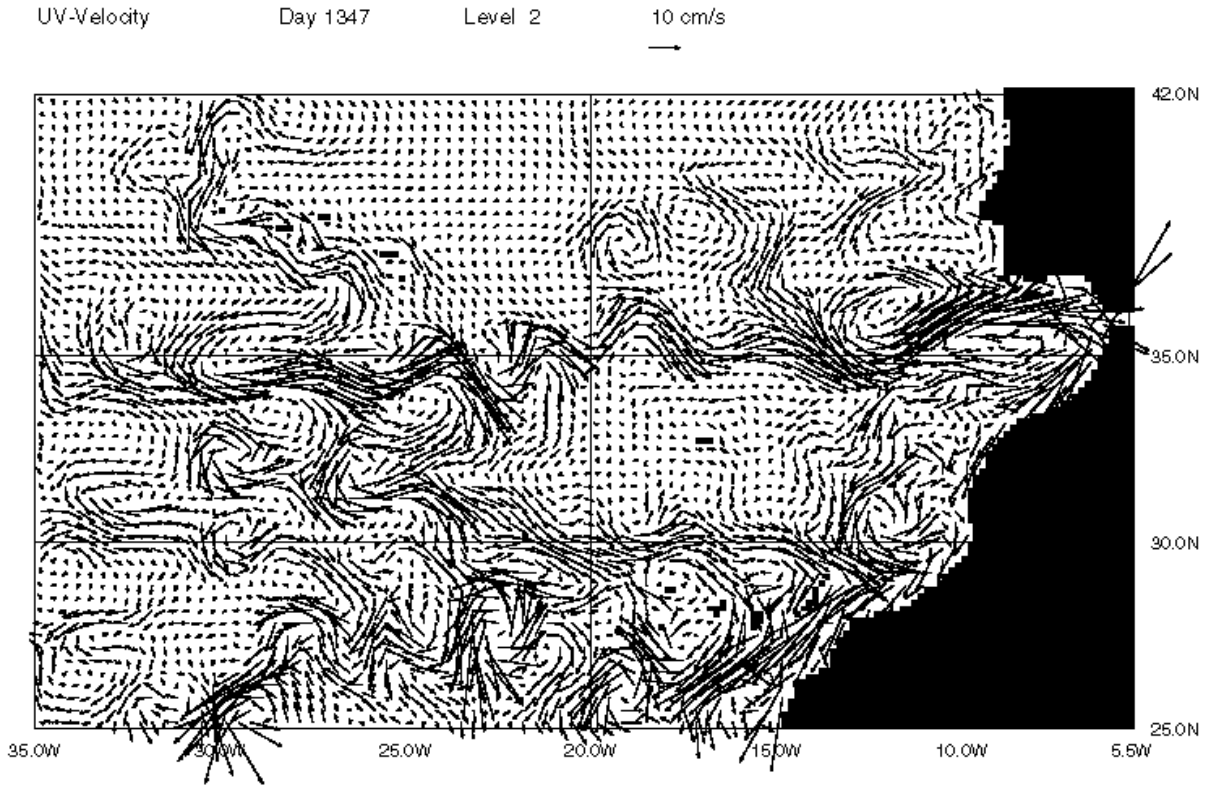


**Figure 8** – Velocity flow filed at 30 m depth an output of the model OCCAM obtain in the framework of the EU project CANIGO.

In Figure 9, the geostrophic circulation around Madeira is shown. Geostrophic circulation is a good estimate of large scale ocean currents. In this figure, it is possible to observe that, towards the East, the main flow changes from eastward to southeastward in agreement with what is known about the Canary Current in this area. Obviously this circulation pattern is also very dependent on the winds acting in the area.

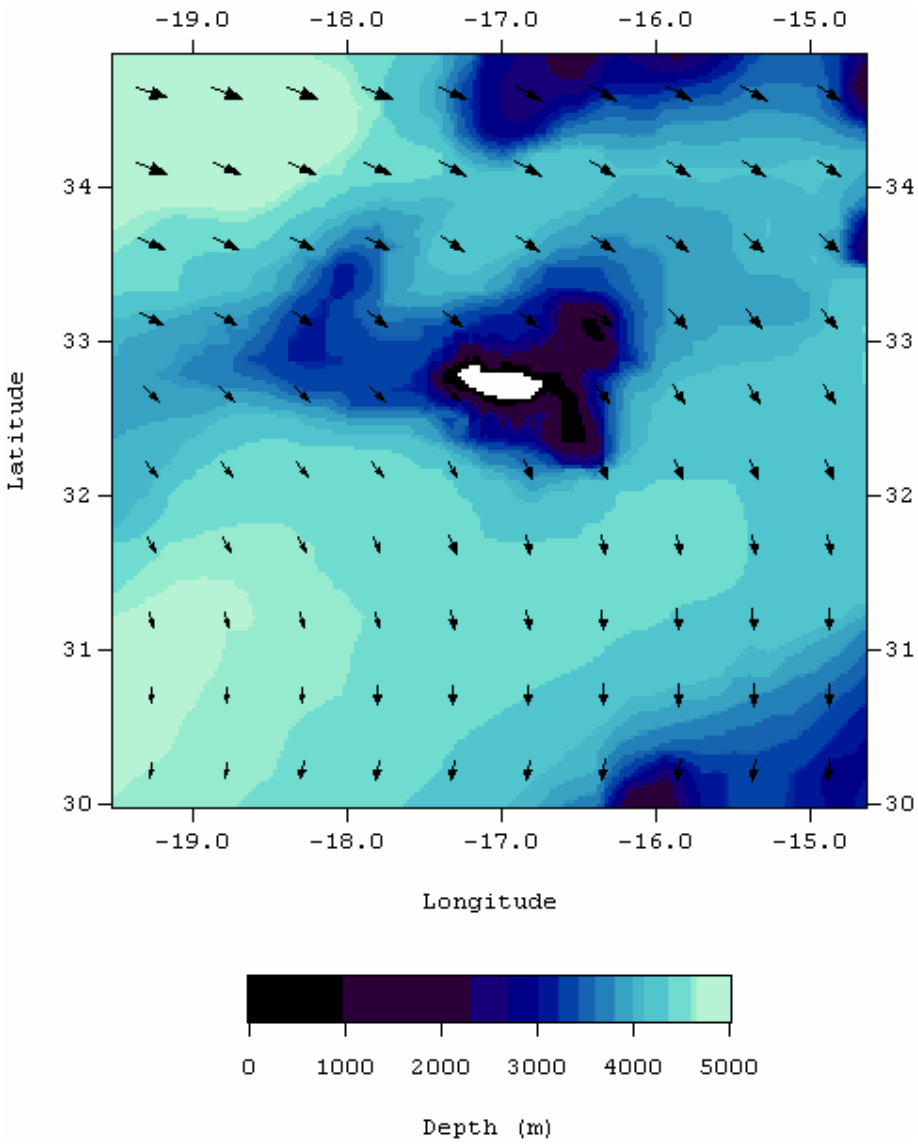


**Figure 9** – Surface geostrophic circulation around Madeira. Maximum velocity plotted is 5 cm $s^{-1}$.

## Tidal Wave

Tides in Madeira are dominated by the M2 semi-diurnal constituent and mainly modulated over a spring-neap cycle by the solar S2 semi-diurnal constituent. M2 amplitude is close to 0.7 m in the Funchal harbor. Along the study domain (30º-35º N, 19.5º-14.5º W) a small amplification from East to West can be observed (Figure 10). The tidal wave propagates from South to North, with a phase lag of M2 of about 50 minutes between South and North boundaries of the study domain. The amplification of the M2 amplitude between East and West boundaries is of approximately 20 cm. The amplitude of the highest astronomical tide in the Funchal harbor, which is the value

obtained by adding the amplitudes of all harmonic constituents, does not exceed 1.35 m see Table 3.

**Table 3** – Amplitudes and phases of tidal harmonic constituents in Funchal harbor (Direcção Geral de Portos).

| Constituent | Amplitude | Phase |
|---|---|---|
| $M_2$ | 0.71 | 9.9 |
| $S_2$ | 0.27 | 30.7 |
| $N_2$ | 0.14 | 354.4 |
| $K_2$ | 0.07 | 29.3 |
| $K_1$ | 0.06 | 29.3 |
| $O_1$ | 0.05 | 285.2 |
| $P_1$ | 0.02 | 16.2 |
| $M_4$ | 0.01 | 49.5 |

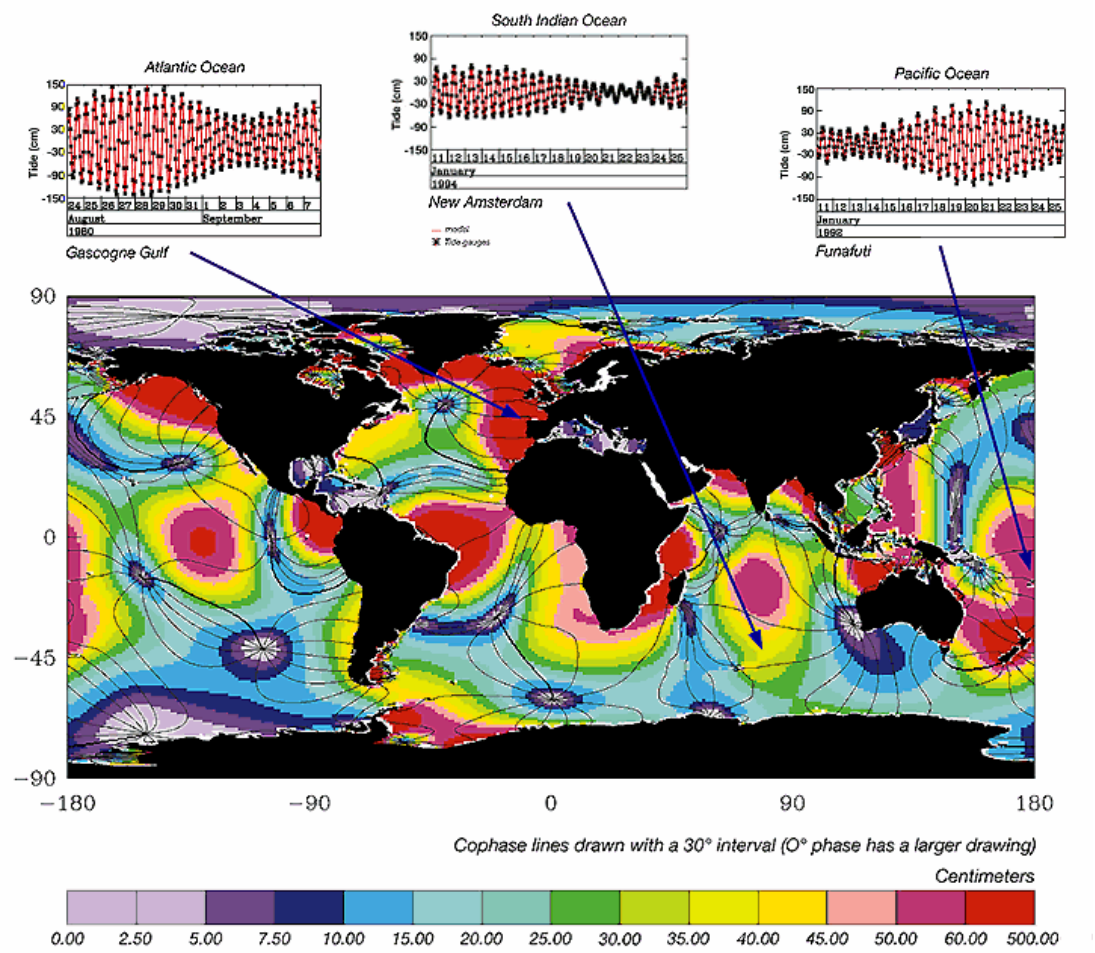


**Figure 10-** Amplitudes and phases of the major lunar tide M2 from Global Ocean Tides model FES95.2. This model predicts tidal sea level variations at any time and point in the deep ocean to within around 3 cm rms. Cophase lines are drawn with a 30° interval (0° phase has thicker lines) (Le Provost, 1998).

The tidal wave induces a surface level gradient that rotates anti-clockwise around the Madeira Island(Figure 11).

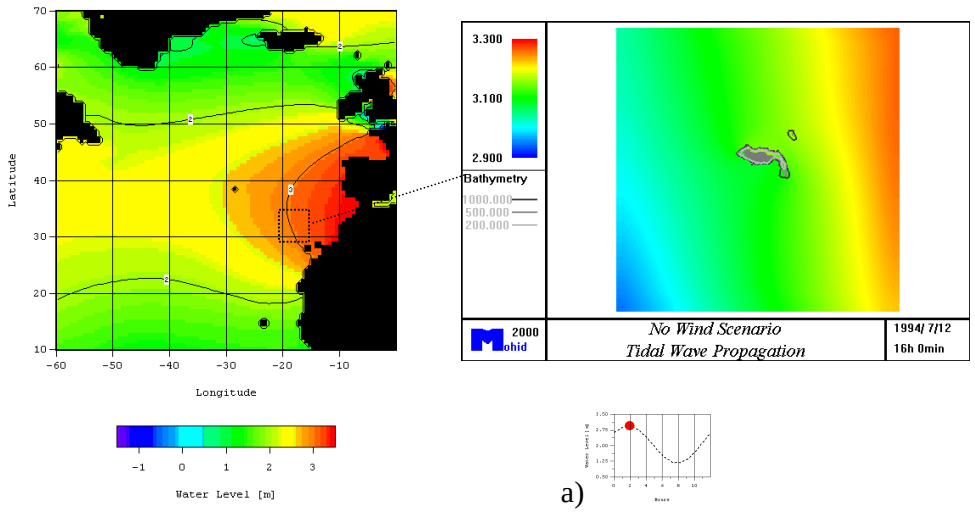
Latitude
Longitude
Water Level [m]
3.300
3.100
2.900
Bathymetry
1000.000
500.000
200.000
2000
ohid
No Wind Scenario
Tidal Wave Propagation
1994/ 7/12
16h 0min

a)

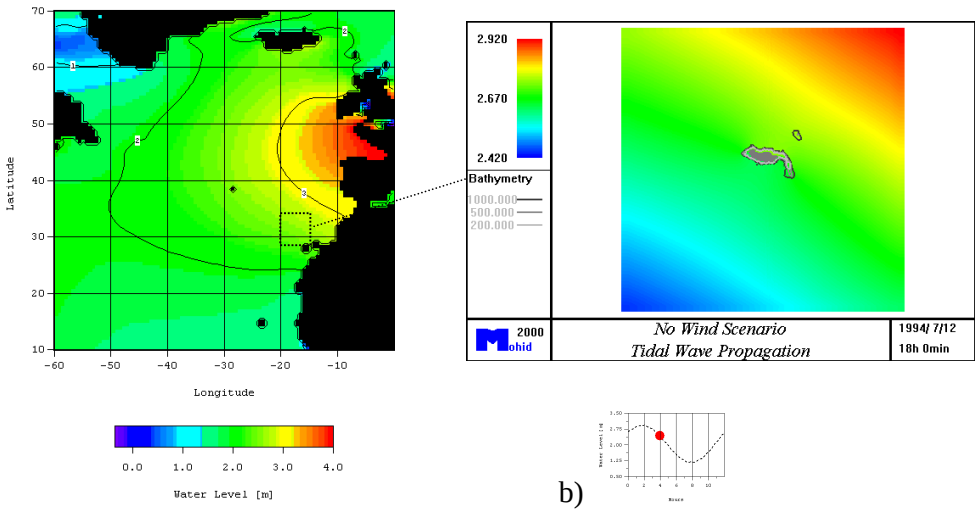
Latitude
Longitude
Water Level [m]
2.920
2.670
2.420
Bathymetry
1000.000
500.000
200.000
2000
ohid
No Wind Scenario
Tidal Wave Propagation
1994/ 7/12
18h 0min

b)

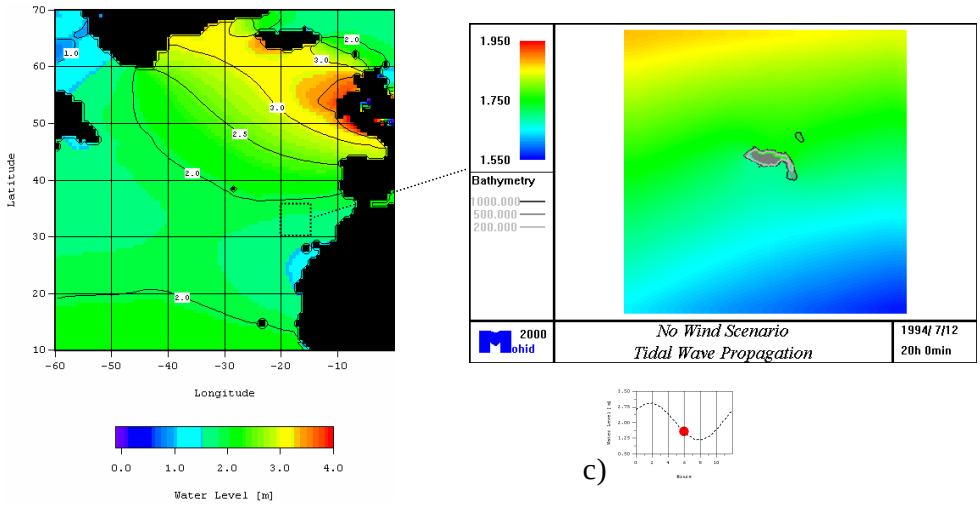
Latitude
Longitude
Water Level [m]
1.950
1.750
1.550
Bathymetry
1000.000
500.000
200.000
2000
ohid
No Wind Scenario
Tidal Wave Propagation
1994/ 7/12
20h 0min

c)

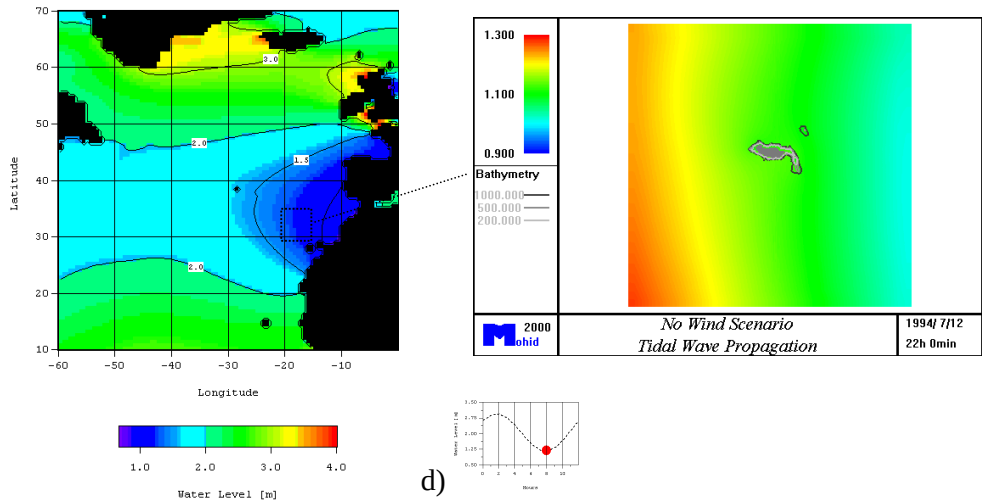


d)

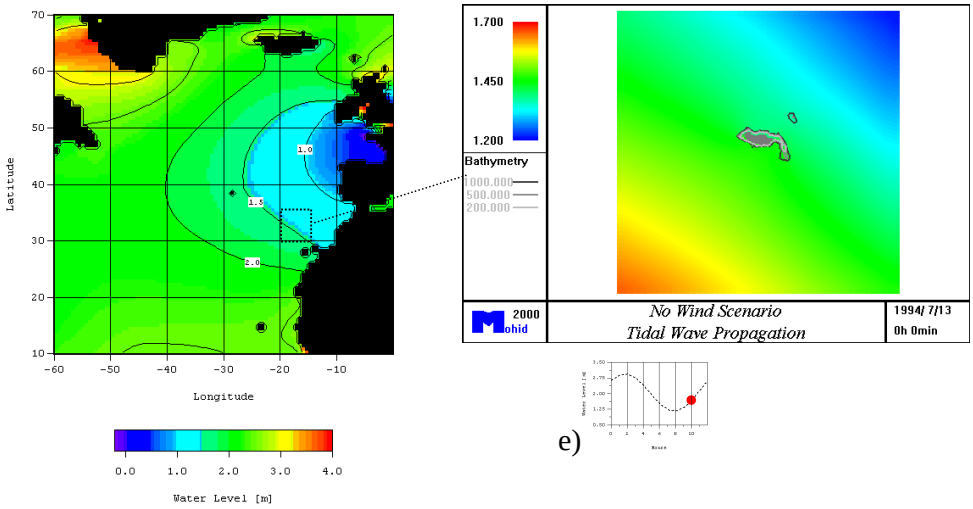


e)

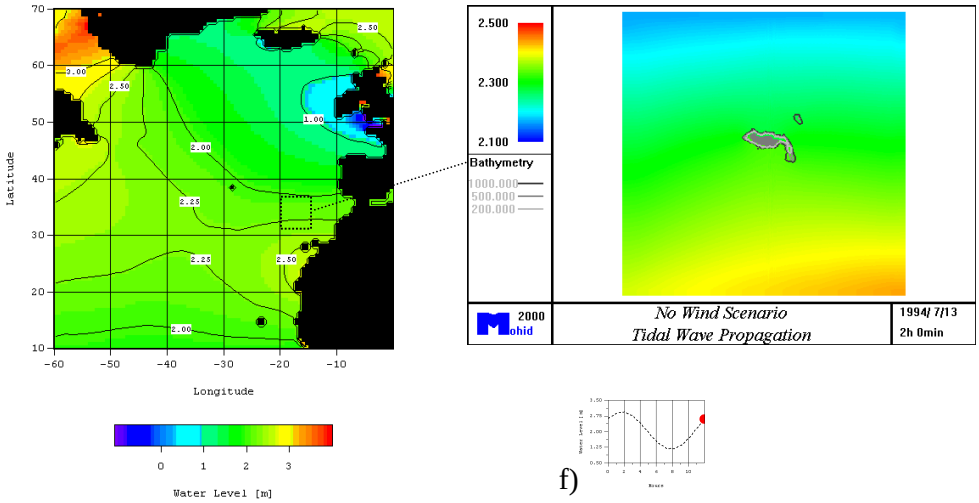


f)

**Figure 11 –** Tidal circulation in the North Atlantic during a spring tide: a) 0h after high tide, b) 2h after high tide, c) 4h after high tide, d) 6h after high tide, e) 8h after high tide, f) 10 after high tide.

## Local circulation

In a discussion of deep ocean dynamics, the effect of islands on the oceanic flow field is rarely considered. Most islands are part of the continents and therefore located on the continental shelf. The number of true deep ocean islands, like Madeira, is very small, and when compared to the size of the ocean basins, they are minuscule and of no consequence for the oceanic circulation. On the shelf, the impact of islands on currents and stratification can be considerable.

Before studying dispersion processes along Madeira coast we must first understand the local circulation. The Madeira Island together with the Desertas Islands can been seen as a "point" in the middle of the Atlantic Ocean where topography changes abruptly from approximately 4000 m below to 1500 above sea surface in less then 40 km. This "perturbation" will interact with the three main large-scale forcing mechanisms described in the General Circulation chapter: the Canary current (N-NE), the tidal wave and the Azores High (NE).

In the impact study of the submarine outfall by Drena (Drena, 1991), current meter information for 3 locations (F1, F2 and F4) in Funchal bay along 4 days (Figure 12) is presented. In the three locations, a current meter was moored at 15 meters from the bottom. In the F1 location also a current meter was moored at 10 meters from the surface. Depth at the mooring locations is: F1 – 55 m, F2 – 25 m and F4 – 75 m, so this means that the current meters in F4 and F2 are 60 and 10 meters respectively from surface.

Analysis of current meter records allows us to draw some information about local circulation. The current meter in F1 located 15 from surface (FU-1S) shows that x (WE) velocity component oscillates between W direction during floods and E direction during ebbs (Figure 14). The South-North component also oscillates between the two directions but in a irregular way. However, at the end of the second day, a tidal oscillation is present, although an East component dominates in the last 2 days. For the Y component the irregular variation is also present but always in the south direction. The bottom current meter at the same location (40 meters from surface) shows the same behaviour but only in the last day (Figure 14). The F2 current meter (Figure 15) reacts in the same way as the F1 surface current meter (FU-1S). On the other hand, the F4 current meter located 60 meters from surface does not show any reaction like the ones locate more near the surface (Figure 16).

In the impact study, a spectral analysis of the F2 current meter data (Figure 17) is also

presented. Spectral analysis is useful for identifying processes responsible for flow variability. The largest energy peak is associated to the semi-diurnal tidal frequency. Two other smaller peaks at frequencies of 48 and 23 hours can also be observed. The 48 h peak is probably due to wind variability and the last peak is due to the joint effect of diurnal tidal harmonics and inertial processes. For the latitude of Madeira, the inertial period is of 22 hours. We must remark that the analysed period was of 4 days, and consequently processes with large time scales like the oscillations of the subtropical Azores high pressure system can not be considered. At smaller time scales, tide dominates flow variability in the Funchal Bay.

In the study of the circulation in the outfall influence area, field data analysis is complemented with the use of a numerical hydrodynamic model. This numeric tool allows us to obtain spatially and time varying fields of flow properties compatible with the sparse field data. In a first step, the model is used to understand how large scale ocean currents can influence local circulation. Afterwards, a study of how the joint effect of ocean currents and large-scale wind circulation can influence circulation around Madeira in summer is carried out. Finally, tide-induced currents are modelled and described. In these simulations, the influence of large-scale processes over local currents is studied. In a second step, the turbulent local wind system associated with Madeira steep topography and its effect on local circulation is studied. Finally a sensibility analysis of wind effect over tidal currents is performed and special attention is given to the resulting residual currents.

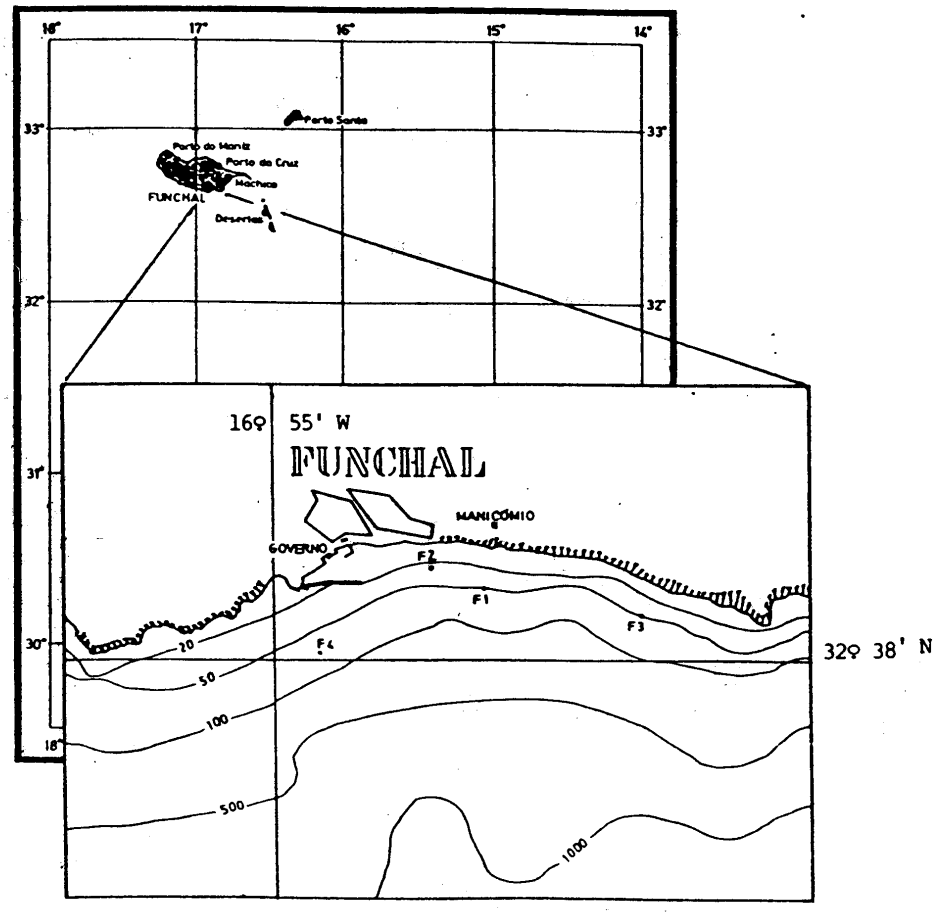


**Figure 12 –** Location of the current meters.

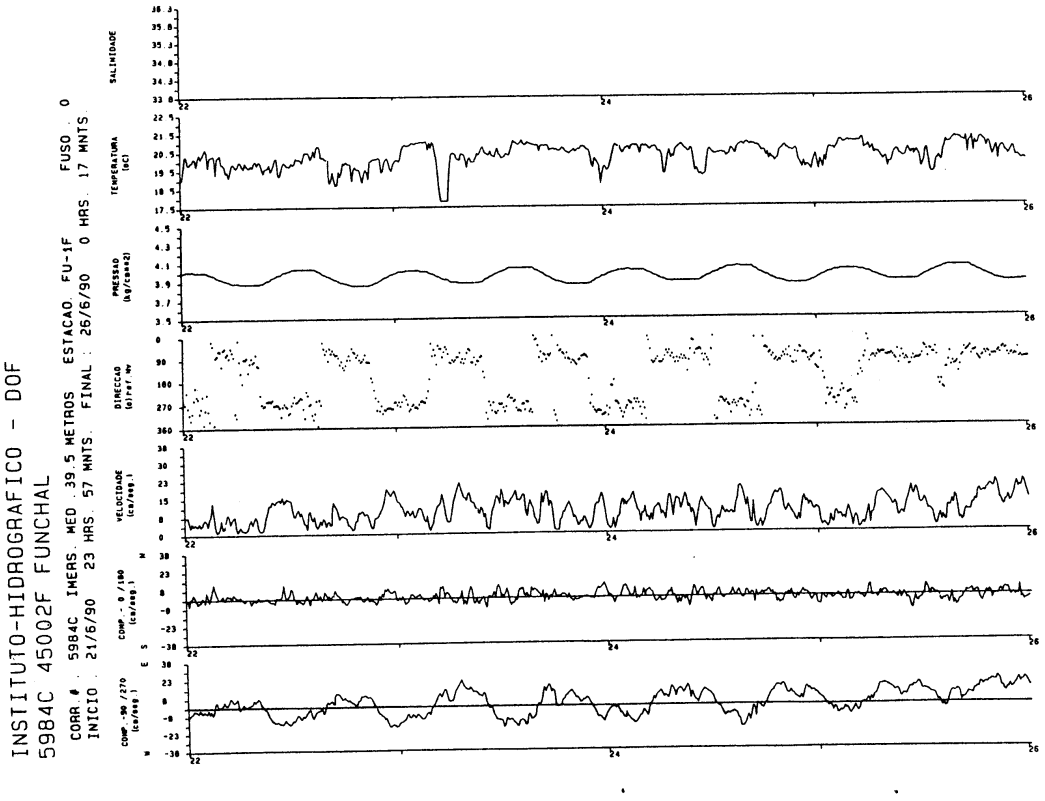


**Figure 13** – Current meter data for the F1 location at 15 meters from the bottom and 40 m from surface. The measurements were made along 4 days, between 21 and 26 of June of 1990 . The properties represent in each graphic form the top are: salinity, temperature, pressure, current direction, current absolute velocity, X (WE) velocity component and finally Y (SN) velocity component.

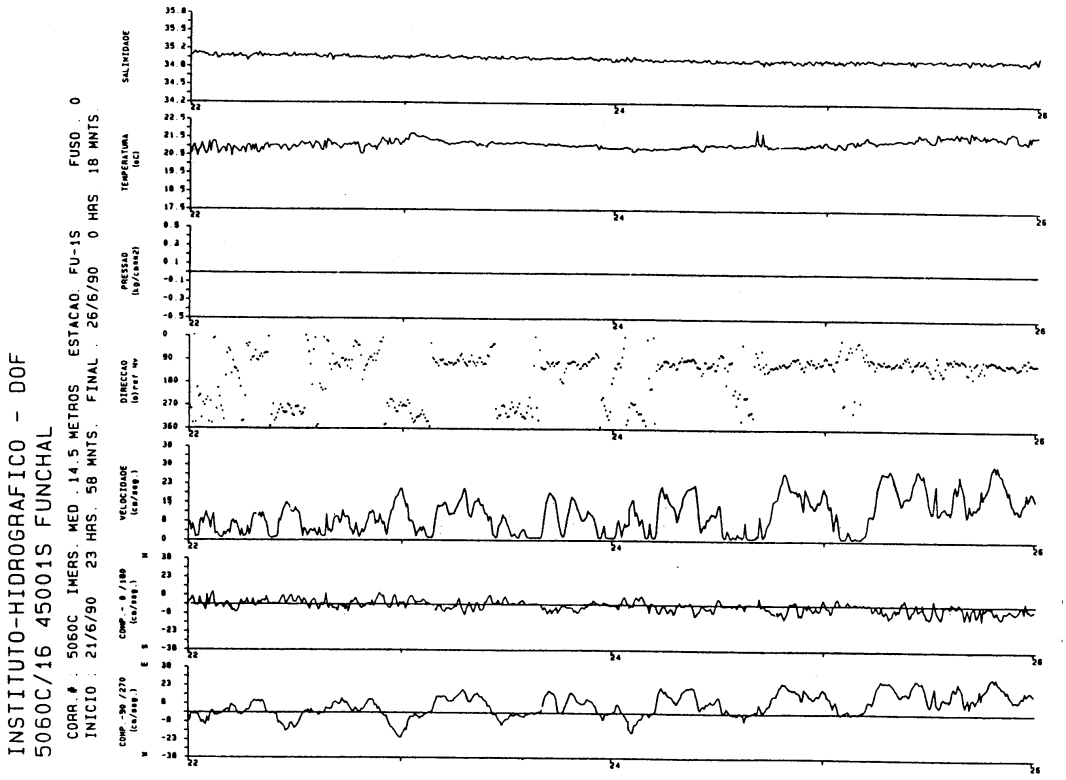


**Figure 14** – Current meter data for the F1 location at 40 meters from the bottom and 15 m from surface. The measurements were made along 4 days, between 21 and 26 of June of 1990 . The properties represented in each graphic starting from the top are: salinity, temperature, pressure, current direction, current absolute velocity, X (WE) velocity component and Y (SN) velocity component.

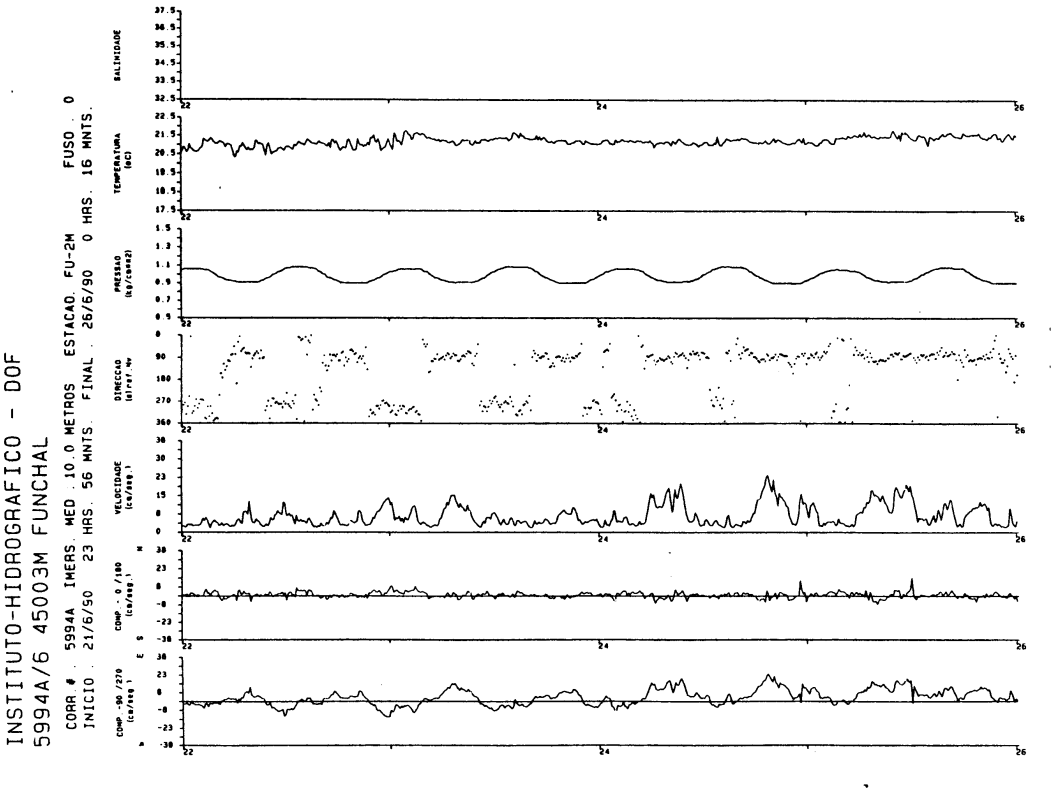


**Figure 15** – Current meter data for the F2 location at 15 meters from the bottom and 10 m from surface. The measurements were made along 4 days, between 21 and 26 of June of 1990 . The properties represent in each graphic starting from the top are: salinity, temperature, pressure, current direction, current absolute velocity, X (WE) velocity component and finally Y (SN) velocity component.

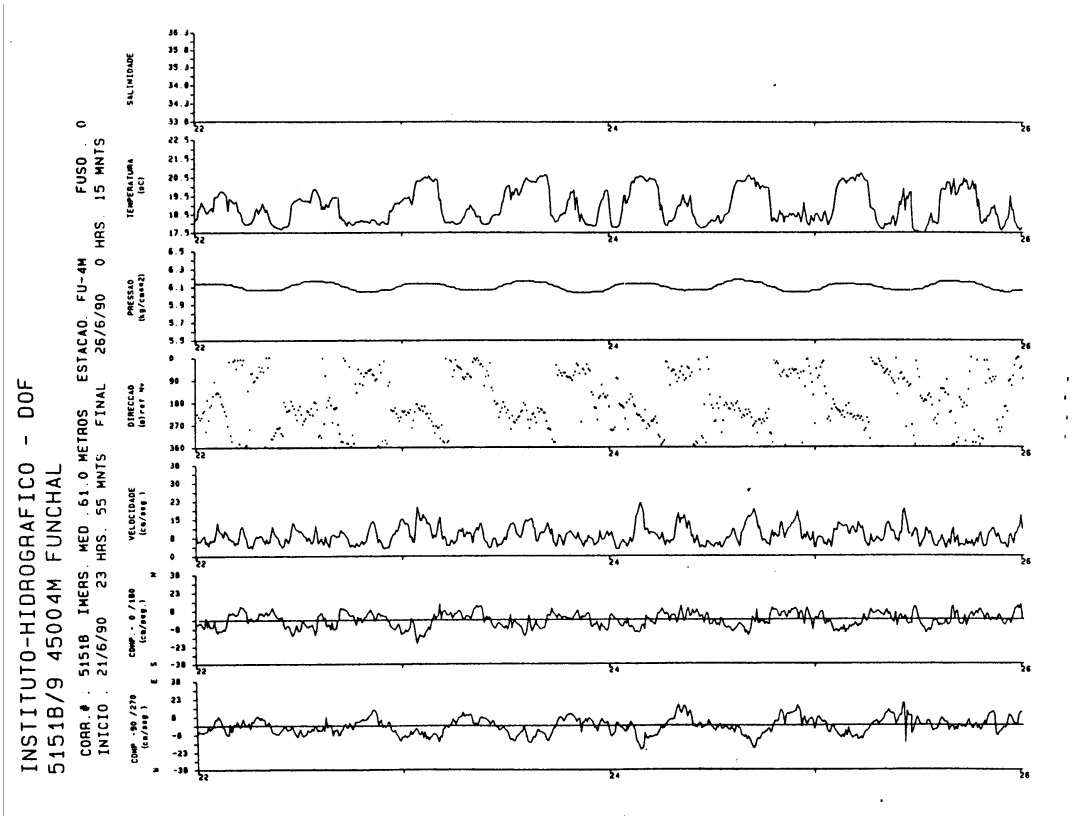


**Figure 16** – Current meter data for the F4 location at 15 meters from the bottom and 60 m from surface. The measurements were made along 4 days, between 21 and 26 of June of 1990 . The properties represent in each graphic form the top are: salinity, temperature, pressure, current direction, current absolute velocity, X (WE) velocity component and finally Y (SN) velocity component.

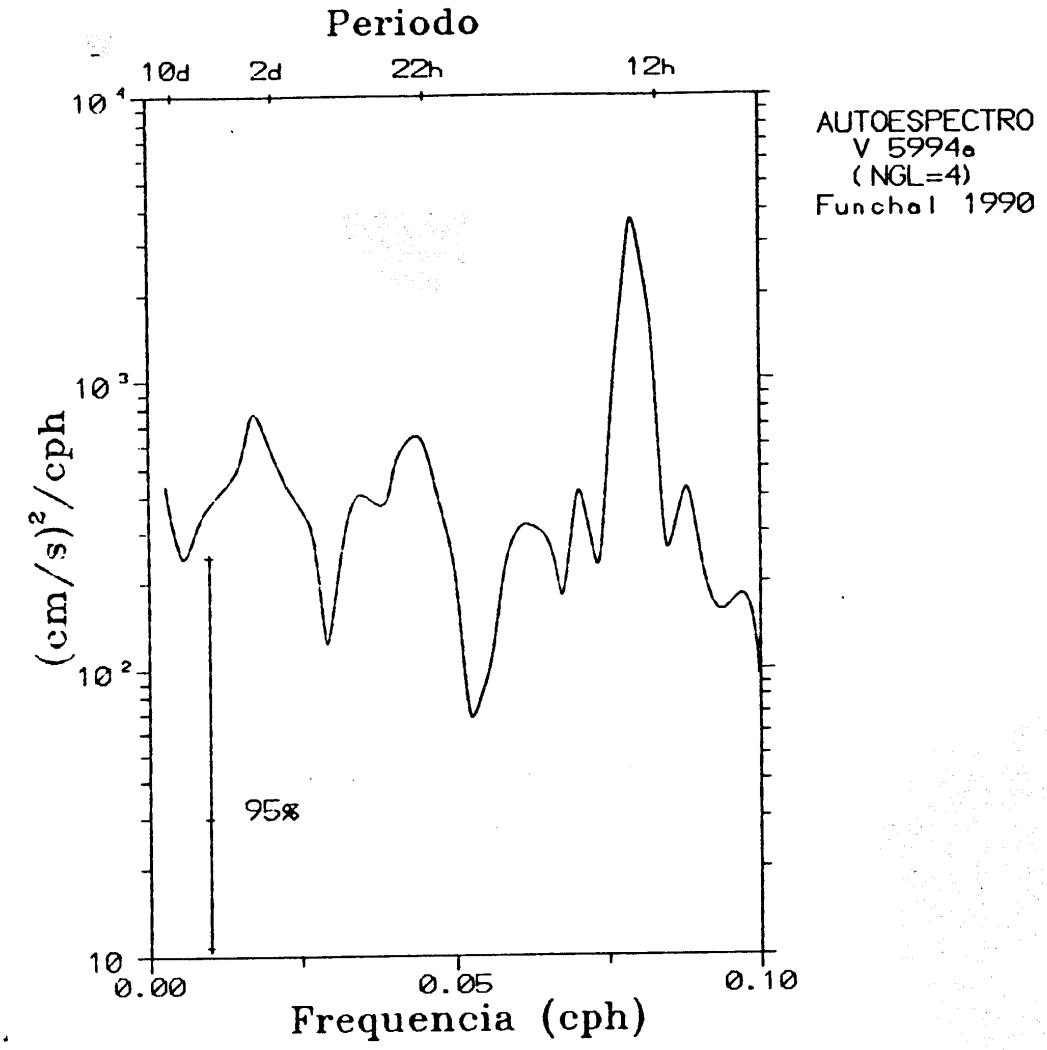


**Figure 17 –** Currentmeter data spectral analysis for the F2 location at 15 meters from the bottom and 10 m from surface. The measurements were made along 4 days, between 21 and 26 of June of 1990 .

## Model Implementation

The model used (MOHID2000) was originally developed by Santos (1995) at the Instituto Superior Técnico (IST). The first versions of MOHID2000 used sigma coordinates in the vertical. More recently, MOHID2000 evolved to a generic vertical coordinate model (Martins *et al.*, 1998; Martins *et al.*, in press). The model was used in several estuarine and oceanic applications (Cancino and Neves, 1998; Taboada *et al.* 1998; Martins *et al.*, 1999; Coelho *et al.*, 1999; Miranda *et al.*, 1999). MOHID2000 solves the three-dimensional primitive equations for incompressible flow in Cartesian coordinates. Hydrostatic equilibrium is assumed as well as Boussinesq approximation. The model is able to simulate the effects of density, tide and wind over the flow.

The study domain goes from 30º N to 35 º N and from –19.5ºW to –14.5ºW. The number of calculation points is 229,842 (113x133x18). The model runs were performed in a Pentium with two processors of 800 Mhz and with 525 MB of RAM memory. The horizontal grid spacing is variable and goes from 20 km to 500 m in both directions (Figure 18). The areas where the outfalls are located are the ones with greater horizontal discretization (Figure 18-c). A nautical chart from Instituto Hidrográfico (Portuguese Navy) was used to derive model bottom topography near Madeira coastline. The areas not covered by the nautical chart were derived from ETOPO5, a global topography database with a 5' precision. The model uses 18 vertical layers centred at constant z-levels at depths of 5, 20, 45, 80, 130, 200, 290, 400, 530, 680, 850, 1040, 1250, 1480, 1750, 2200, 3000, 4250 m. The bottom layer is represented using a shaved cell approach to avoid precision problems associated to the traditional steer case discretization (Visbeck et al., 1997). Turbulent viscosity in the vertical is computed using a mixing length parametrization (Nihoul, 1984) and in the horizontal, a Smagorinsky algorithm that considers viscosity dependent from the horizontal velocity gradient and the spatial step is used.

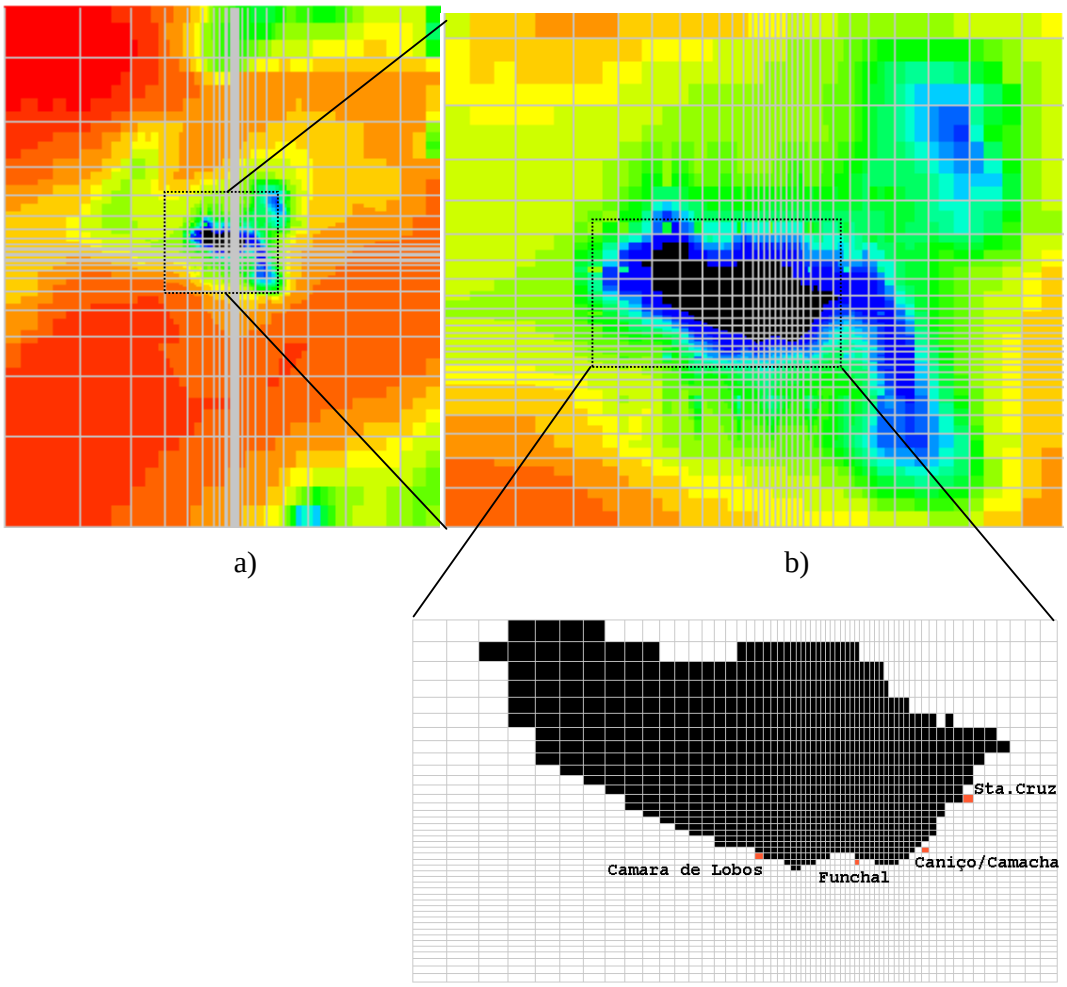


**Figure 18** – Hydrodynamic model grid: a) entire domain, b) zoom of the archipelago, c) zoom of the Madeira island.

## Density Driven Flow

The surface geostrophic circulation (density driven) presented in Figure 9 shows velocities of 2 cm/s to the south around Madeira Island. Current meters show values of an order of magnitude greater. The geostrophic circulation does not take in consideration non-linear effects produced by bottom topography and inertial oscillations. To understand the importance of these effects, the model was forced with a climatological summer density. The climatological temperature and salinity fields are extracted from Levitus and Boyer (1994) and Levitus *et al.* (1994) and are interpolated to the model grid and then smoothed using a simple cubic spline algorithm.

The model results are similar to the geostrophic (Figure 9) in almost the entire domain. However, this is not the case around Madeira, the presence of the island induces the flow to contour the coastline (Figure 19), with an increase of velocities along north and south coasts (Figure 20). Along the south coast, eastward residual velocities of 5 cm/s are observed (Figure 21). In the Funchal bay area, current intensity decreases with depth. In a horizontal section at 25 meters, residual velocities of 4 cm/s are still observed (Figure 22), while at 45 m (Figure 23) and 80 m (Figure 24), velocities are very small. These results also lead us to identify a permanent flow in the area of the outfalls induced by climatological conditions. In the Funchal bay where the current meters were moored, the intensity of the flow decreases very rapidly between the 25 and 45 meters. During the period 1990/6/21 and 1990/6/26, the wind in Funchal was negligeable. The absence of wind could explain the residual West current observed in the F1 and F2 current meters moored 40 m above bottom. This could also explain why no west component of residual current is observed in the F4 current meter at 60 meters depth.

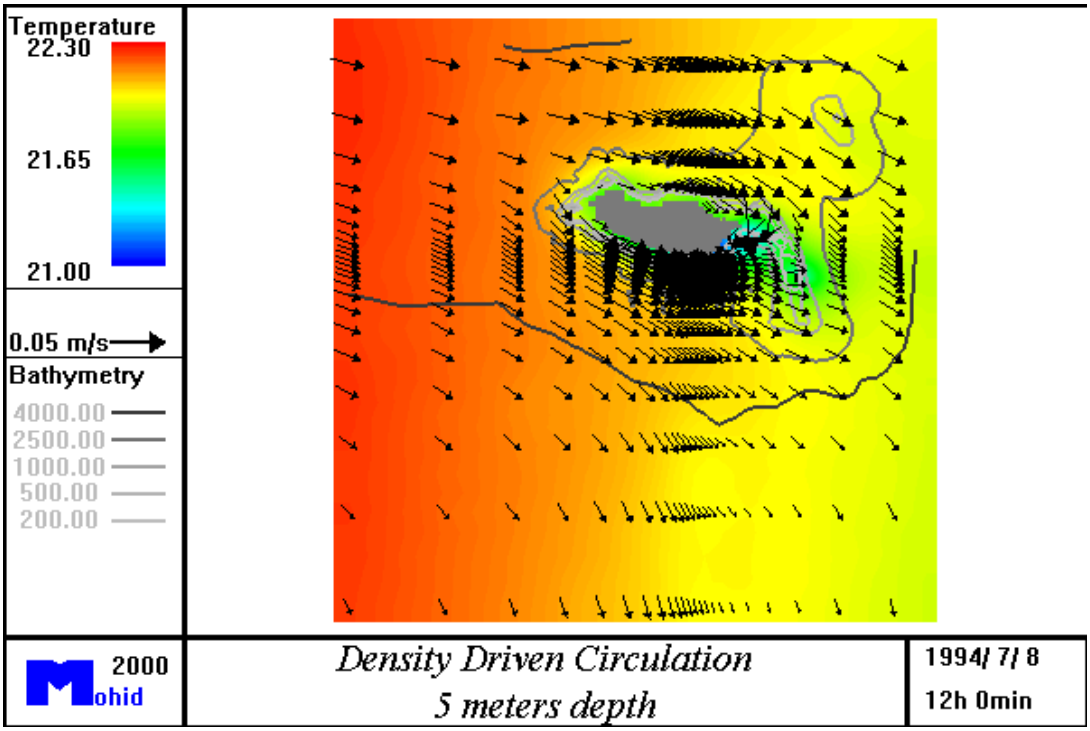


**Figure 19–** Surface residual circulation driven by summer climatological density at the Madeira archipelago scale. Colours represent temperature, isolines bathymetry and arrows velocity.

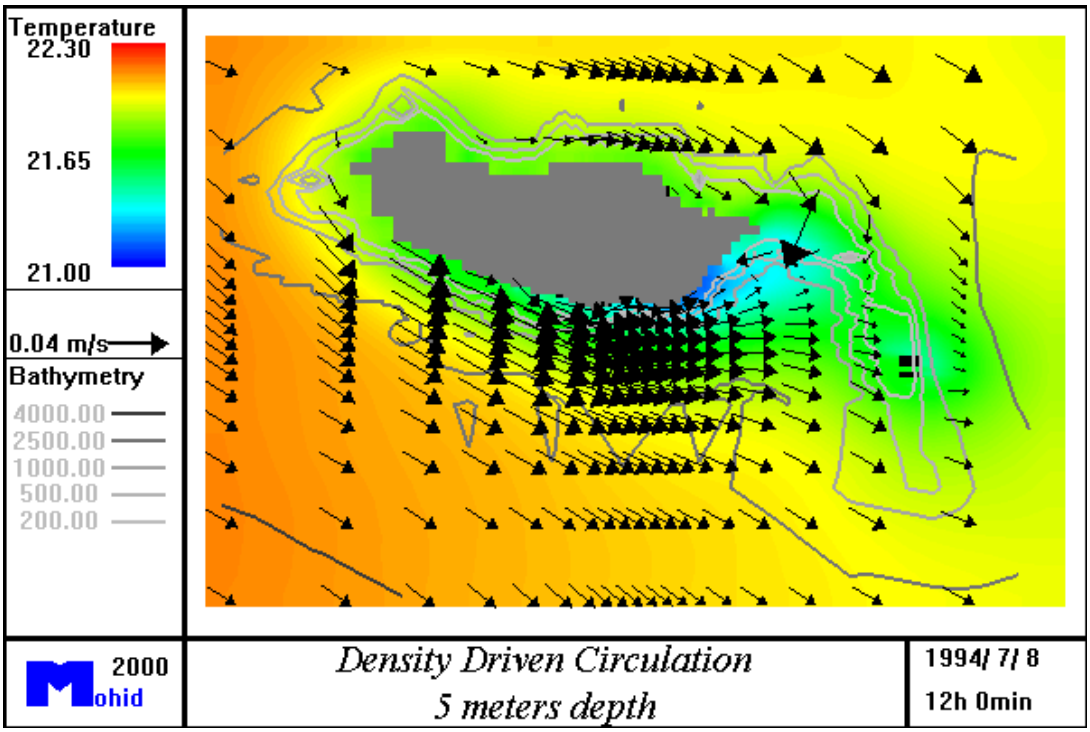


**Figure 20–** Surface residual circulation driven by summer climatologic density at the Madeira island scale. The colours represent temperature, the isolines bathymetry and the arrows velocity.

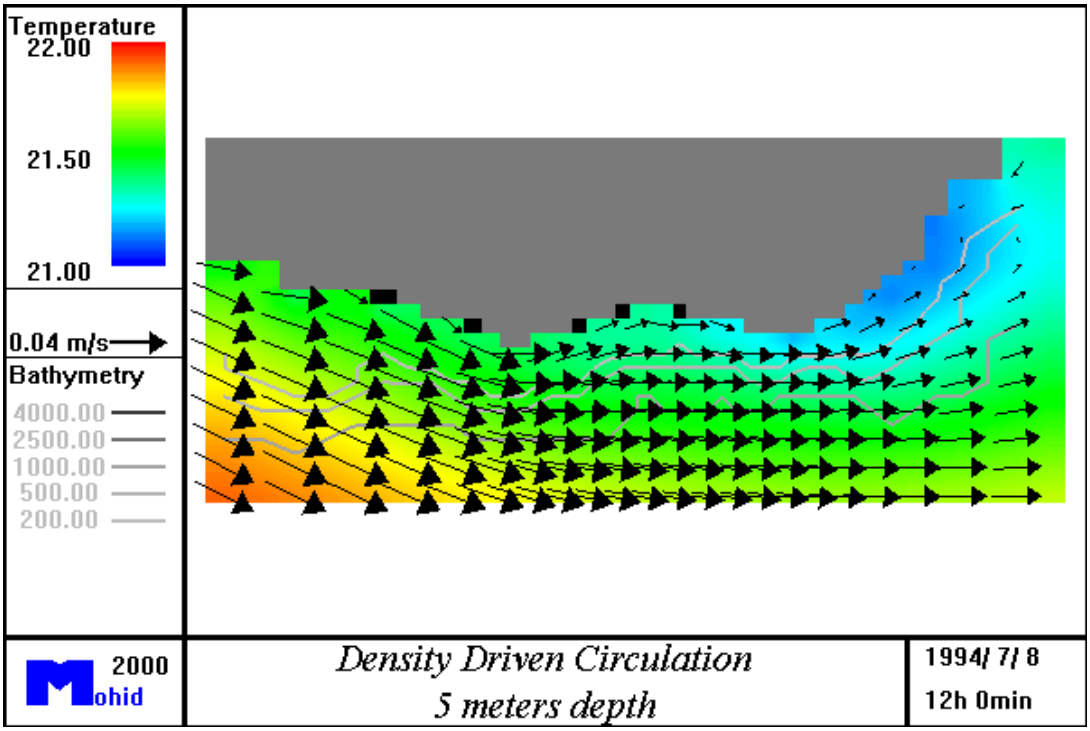


**Figure 21–** Surface residual circulation driven by summer climatologic density at the Funchal bay scale. The colours represent temperature, the isolines bathymetry and the arrows velocity.

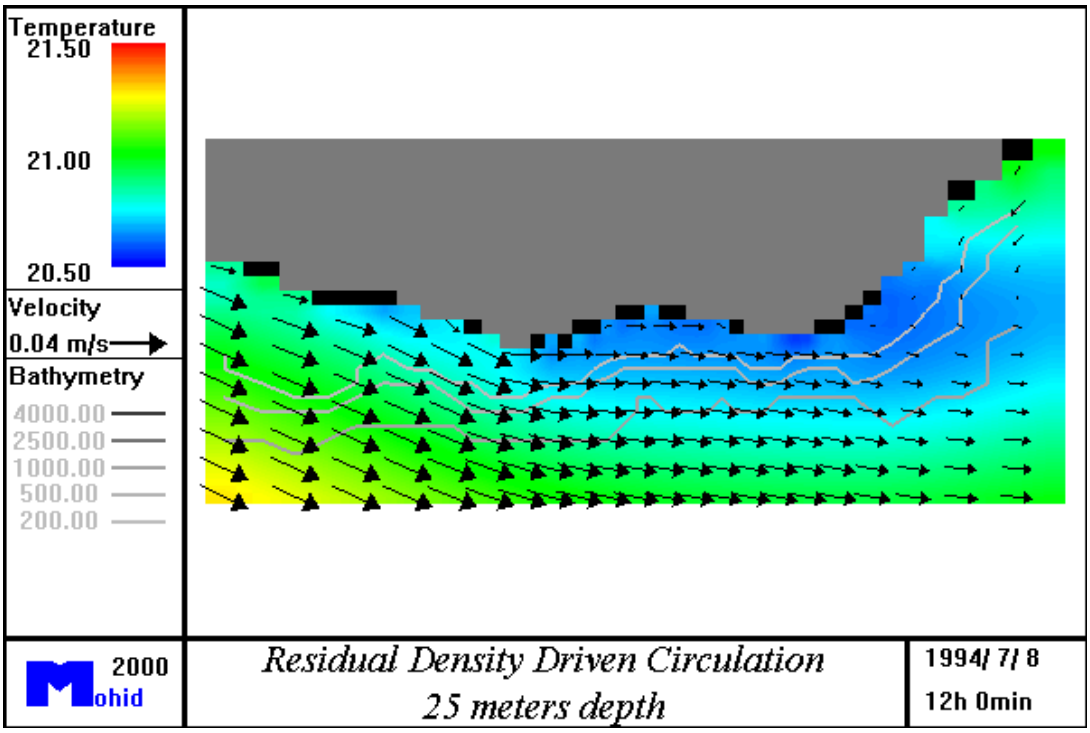


**Figure 22–** Residual circulation at 25 meters depth at the Funchal bay scale. The currents in this case are driven by summer climatologic density. The colours represent temperature, the isolines bathymetry and the arrows velocity.

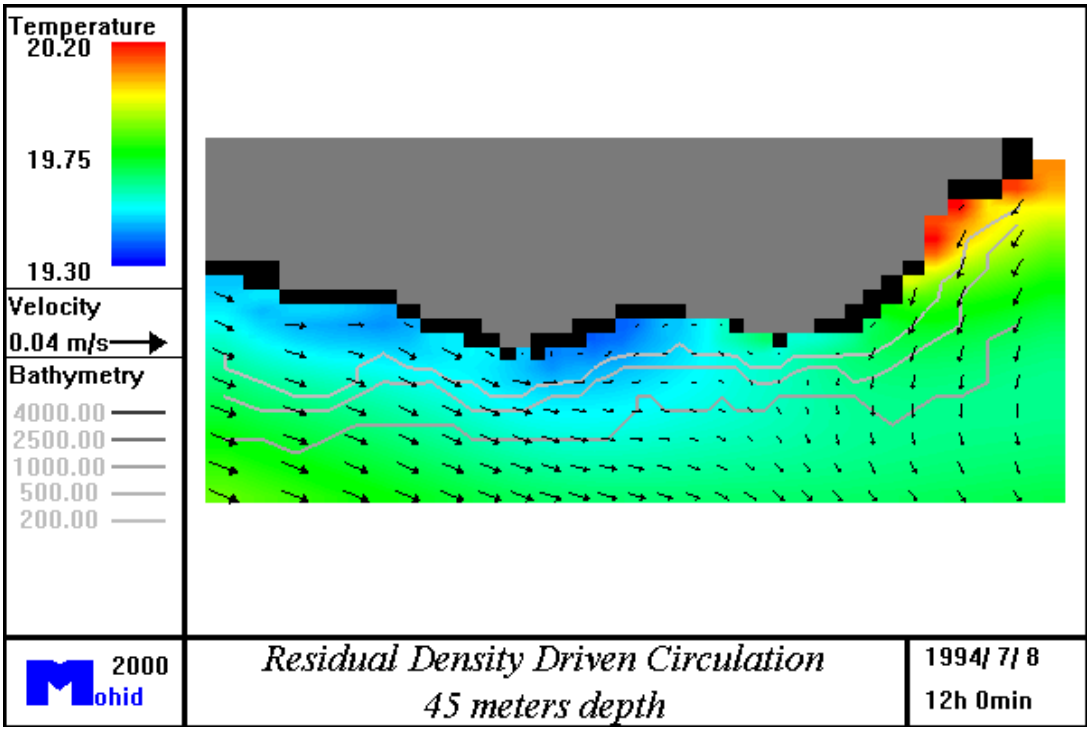


**Figure 23–** Residual circulation at 45 meters depth at the Funchal bay scale. The currents in this case are driven by summer climatologic density. The colours represent temperature, the isolines bathymetry and the arrows velocity.

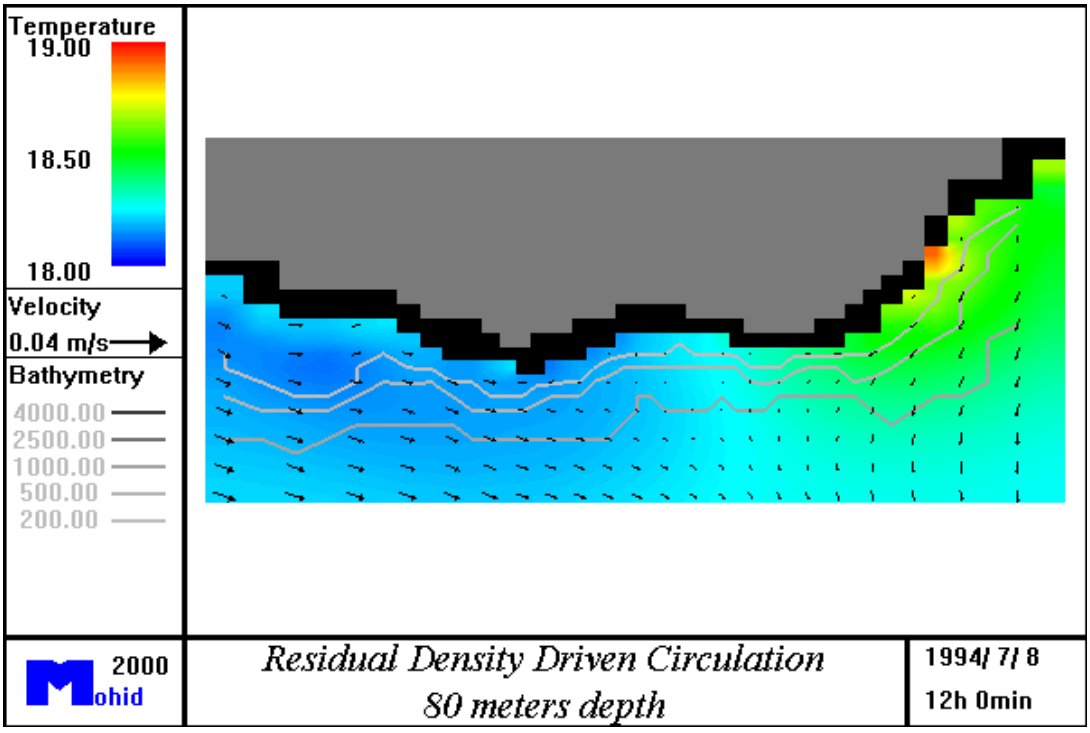


**Figure 24–** Residual circulation at 80 meters depth at the Funchal bay scale. The currents in this case are driven by summer climatologic density. The colours represent temperature, the isolines bathymetry and the arrows velocity.

An experience to understand how real atmospheric fluxes (heat and momentum) can

influence the density driven flow in the summer of 1994 was also performed. Surface momentum fluxes were derived from the near surface analyses of the European Center for Medium-Range Weather Forecasts ECMWF (Trenberth *et al.*, 1990) and they correspond to the period from 1 to 30 of July of 1994. Along this period, wind had always a dominant NE direction. The spatial resolution of the ECWMF fluxes was 0.5º by 0.5º. 0.5º are approximately 50 km at this latitude, so they do not consider the impact of the island topography over local wind circulation.

After 30 days of simulation, the presence of wind has significantly changed surface circulation around Madeira in comparison to the scenario forced by the climatologic density. In the density driven results, an eastward flow along North and South coasts and a significant velocity increase is obtained specially along the south coast (Figure 25). Wind forcing reversed current direction along the south coast and also reduced intensity (Figure 26). This effect is not only evident at the surface but also at a depth of 80 meters, although velocities are smaller (Figure 27).

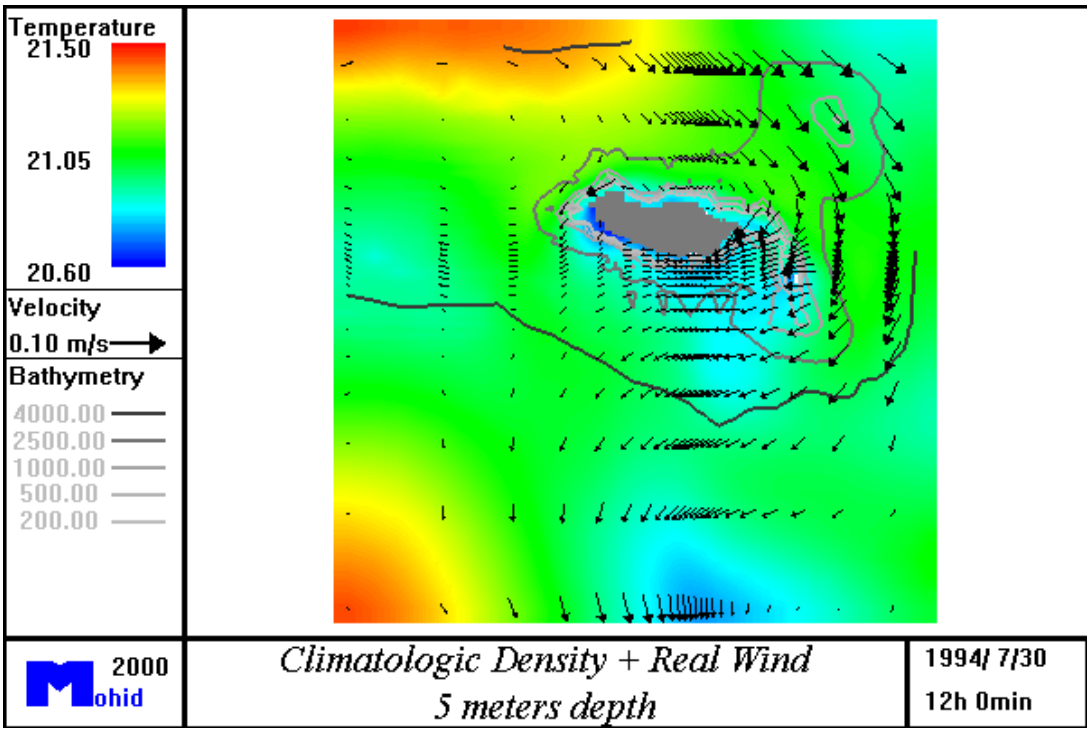


**Figure 25 –** Surface circulation driven by climatologic density and real wind at 5 meters depth at 30 of July of 1994 at the Madeira archipelago scale. The colours represent temperature, the isolines bathymetry and the arrows velocity.

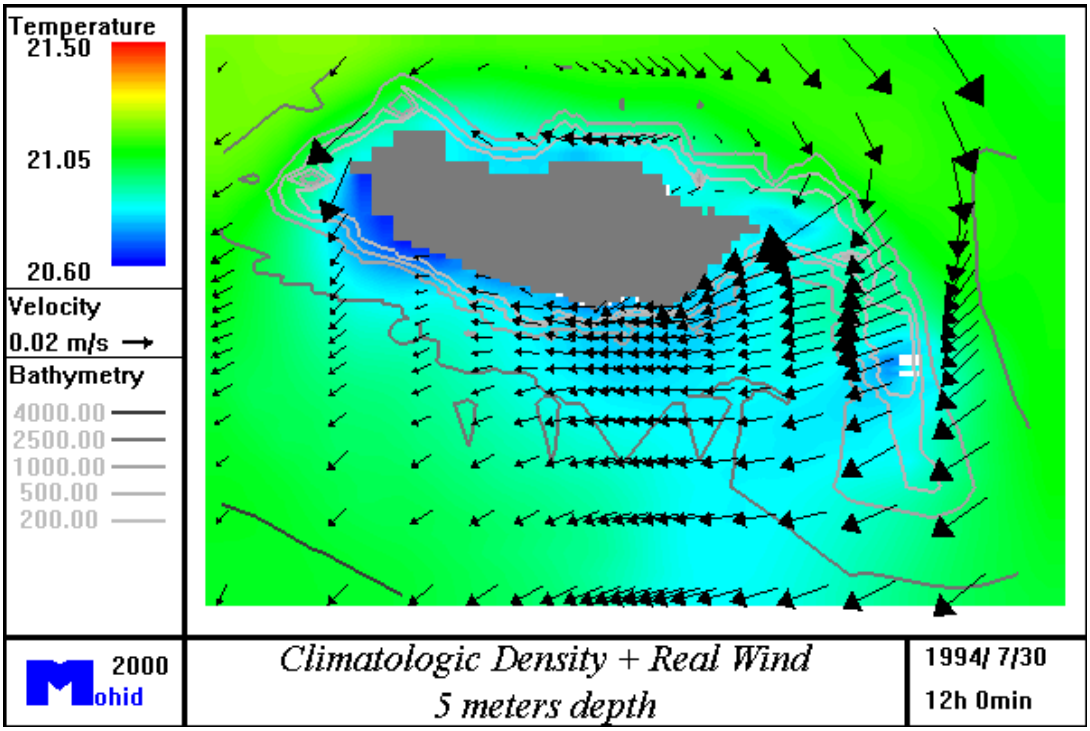


**Figure 26 –** Surface circulation driven by climatologic density and real wind at 5 meters depth at 30 of July of 1994 at the Madeira island scale. The colours represent temperature, the isolines bathymetry and the arrows velocity.

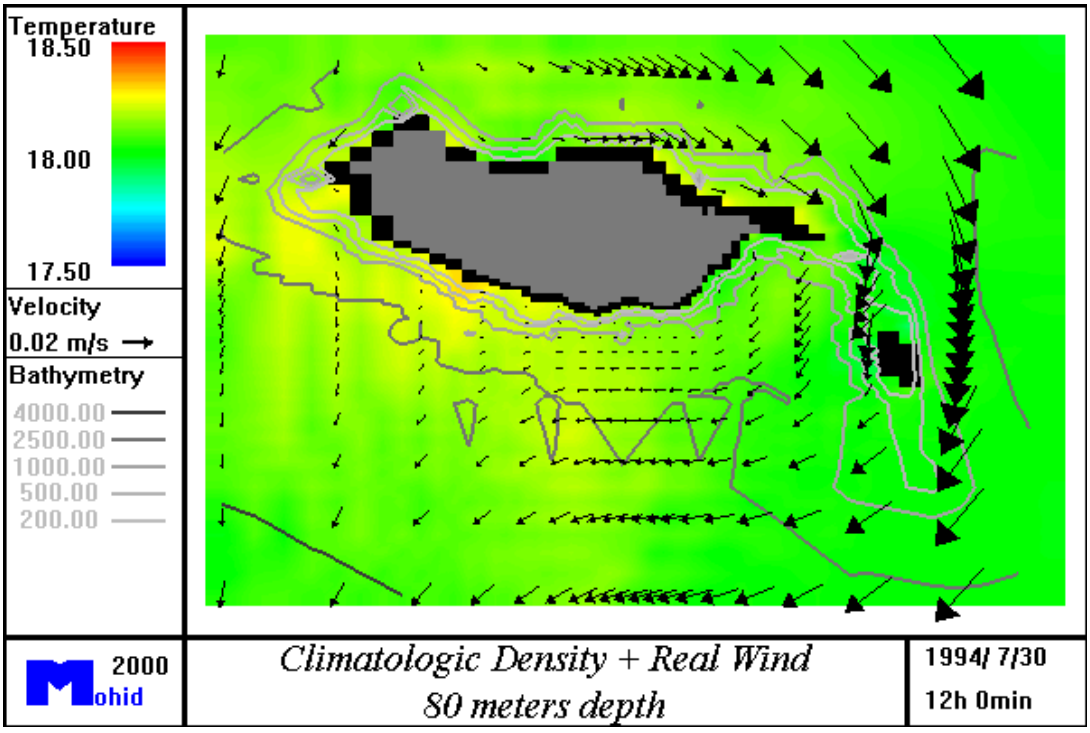


**Figure 27 –** Surface circulation driven by climatologic density and real wind at 80 meters depth at 30 of July of 1994 at the Madeira island scale. The colours represent temperature, the isolines bathymetry and the arrows velocity.

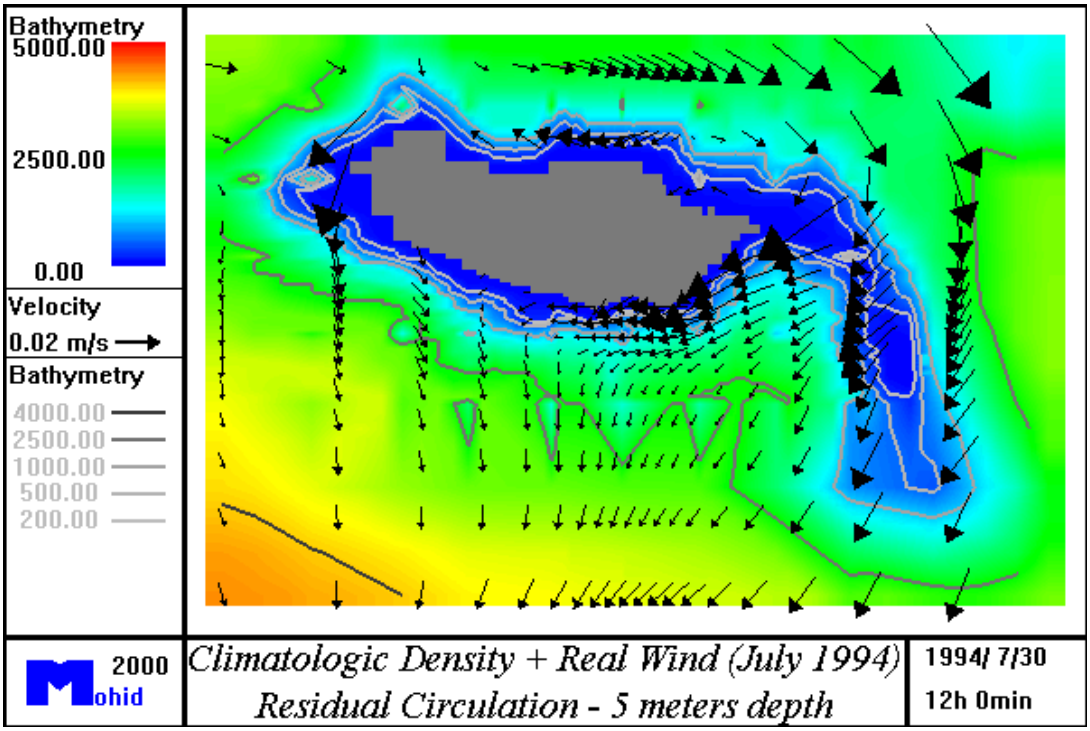


**Figure 28** – Residual surface circulation driven by climatologic density and real wind for along a 30 days period (July of 1994) at the Island scale at 5 meters depth. The colours and the isolines represent bathymetry and the arrows velocity.

## Tidal circulation

After studying the importance of density gradients in the local circulation, the tidal forcing was analysed. Once again the MOHID2000 model with the same grid describe above is used. Open boundary conditions were derived from the global tidal model FES95.2 (Le Provost et al., 1998).

The main characteristics of FES95.2 are: a finite-element spatial discretization and data assimilation in areas where field data is available (mainly in the Atlantic, Indian and Pacific oceans). Data assimilation is made using the empirical model CSR2.0 from Texas University. The reason pointed out for errors in the previous version of this model, FES94.1 (Le Provost et al., 1994), was the poor quality of the bathymetric information in some areas of the globe. This is the reason why a data assimilation module was added in the last version.

The FES95.2 model results can be accessed via WWW (ftp://spike.cst.cnes.fr/pub/techine/tide/fes95.2.1). The available model results are 26 tidal components for the entire world in a 0.5º degree grid. The model computes 8 main constituents, K1, O1, Q1, M2, S2, N2, K2 e 2N2, using data assimilation to correct the first six. The other 18 constituents are derived by admittance. Among them are $\mu_2$, $\nu_2$,

$L_2$, $T_2$, $M_1$, $P_1$, $J_1$ and $OO_1$. The quality of the solution is evaluated by reference to a standard real sea data set of 95 stations. Quality is significantly improved after the assimilation process is applied: the root-sum-square (RSS) of the differences between solutions and observations, for the eight major constituents, is reduced from 3.8 cm for FES94.1 to 2.8 cm for FES95.2.

The period simulated was from the 5 to the 13 of July of 1994. This is a period of 8 days along which is possible to see model performance in spring and also in neap tide situations. The model water level results agree very well with the data from Funchal tidal gauge (Figure 29). No significant phase and amplitude errors are observed and quality of the results is the same along the entire simulated period.

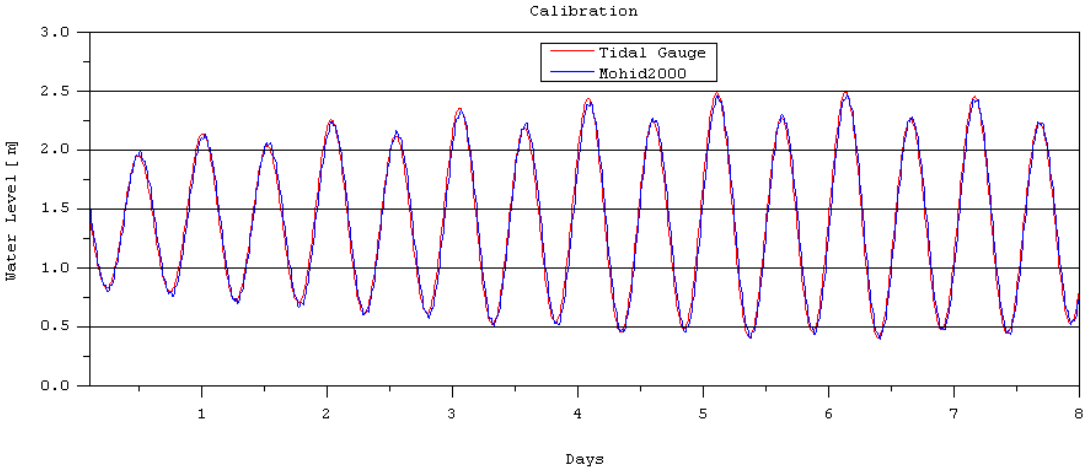


**Figure 29 –** Comparison between Funchal tidal gauge and model results along 8 days.

In principle, it would be very useful to calibrate velocities because they are responsible for transport. However, there is not sufficient field data available to compare with model results. Long periods of current meters data are necessary (more then 1 month), if possible harmonic analysed, to identify the contribution of tide. The data available are only 4 day long and for the Funchal bay. Despite the lack of information, the presented water level calibration gives a good indication of model accuracy.

The model results along a spring tidal cycle show a strong water level difference between North and South coast of approximately 15 cm. During the ebb period, Madeira is an obstacle to a large-scale flow with a South direction and a water piling can be observed in the North coast. In the flood period the opposite effect happens. This piling of water generates a strong water level gradient along the coast, forcing strong currents in the East and West coasts in both periods that can reach 50 cm/s.

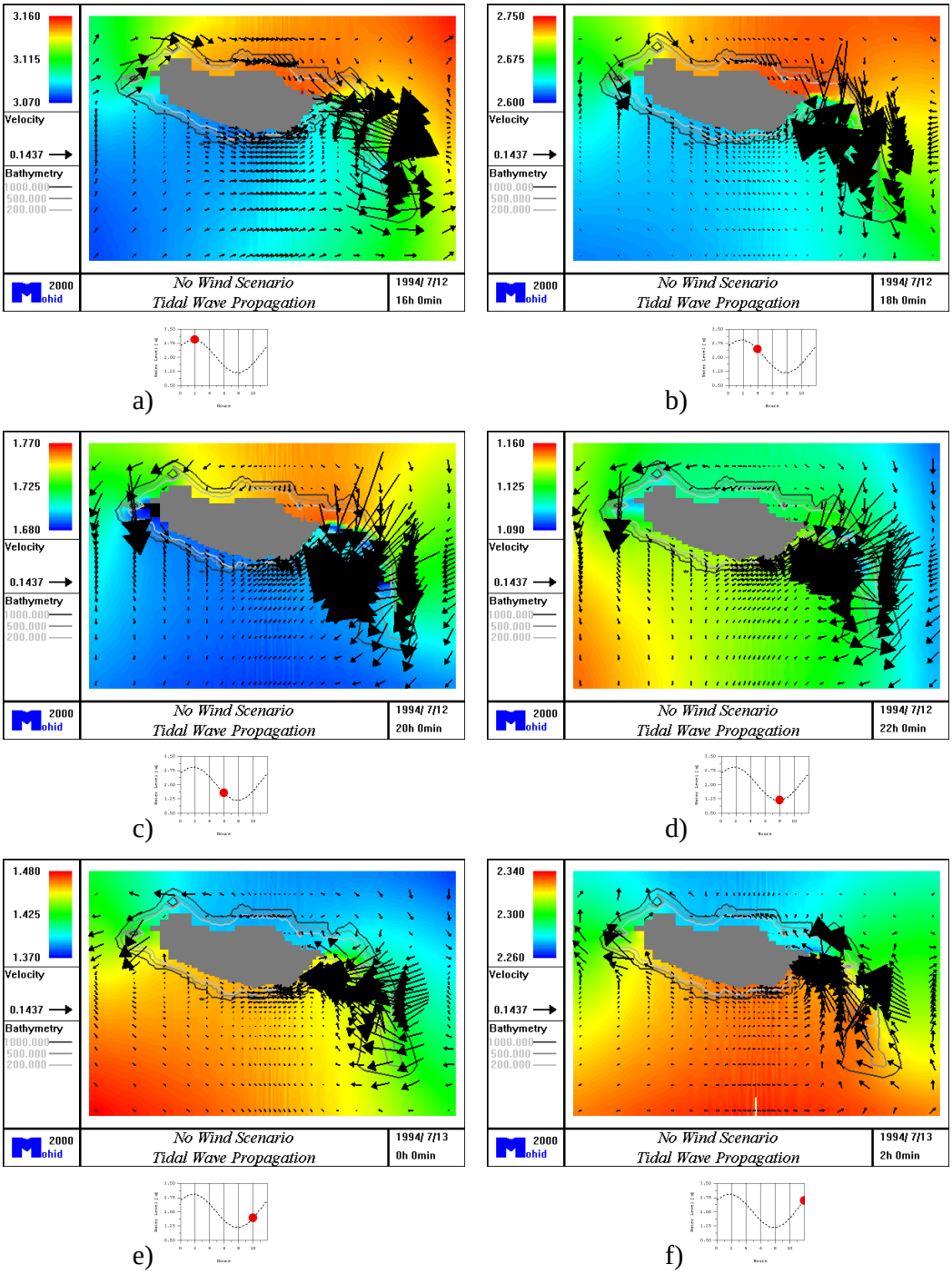


**Figure 30 –** Tidal circulation along a spring tidal cycle with compute by the Mohid2000 model. The grey solid lines represent the bathymetry and the colours the water level: a) 0h after high tide, b) 2 after high tide, c) 4h after high tide, d) 6h after high tide, e) 8h after high tide, f) 10h after high tide.

Below are presented model results of surface velocity evolution along an 8 days period where there is current meter data available (stations F1, F2 and F4 - Figure 12). Only velocities with west-east direction are presented. The south-north velocities are negligble because the flow is approximately parallel to the coast. The water level

asymmetry between two consecutive tidal cycles can be also observed in the velocities. In all stations, as expected, the minimum velocities occur during neap tides (≅0.5 cm/s) and the maximum ones in spring tides ((≅5 cm/s). In all stations the residual velocity is negative, i.e. with a west direction. The F4 station is the one with larger velocities several times along the entire period the 5 cm/s maximum is achieved. In contrast the F2 station the velocities are never larger then 2.5 cm/s.

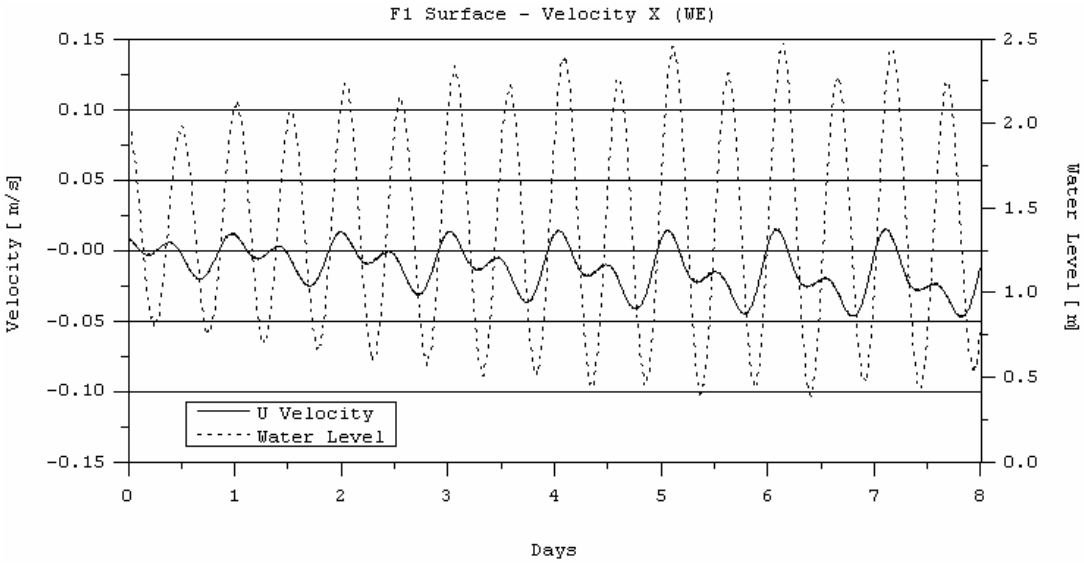


**Figure 31** – Model water level and X velocity (WE) results for station F1. The velocity is compute 5 meters from surface.

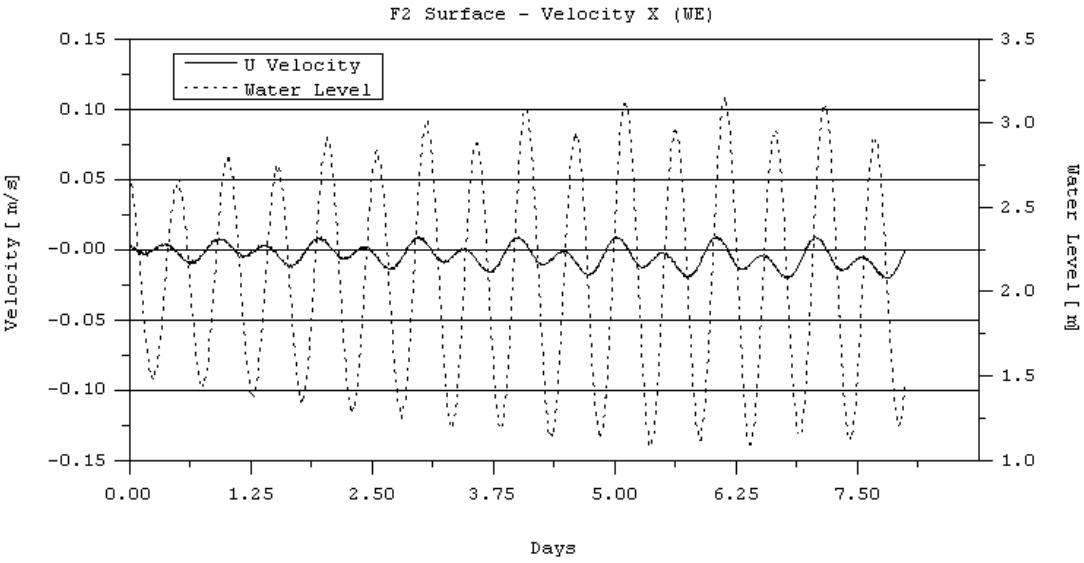


**Figure 32 –**Model water level and X velocity (WE) results for station F2. The velocity is compute 5 meters from surface.

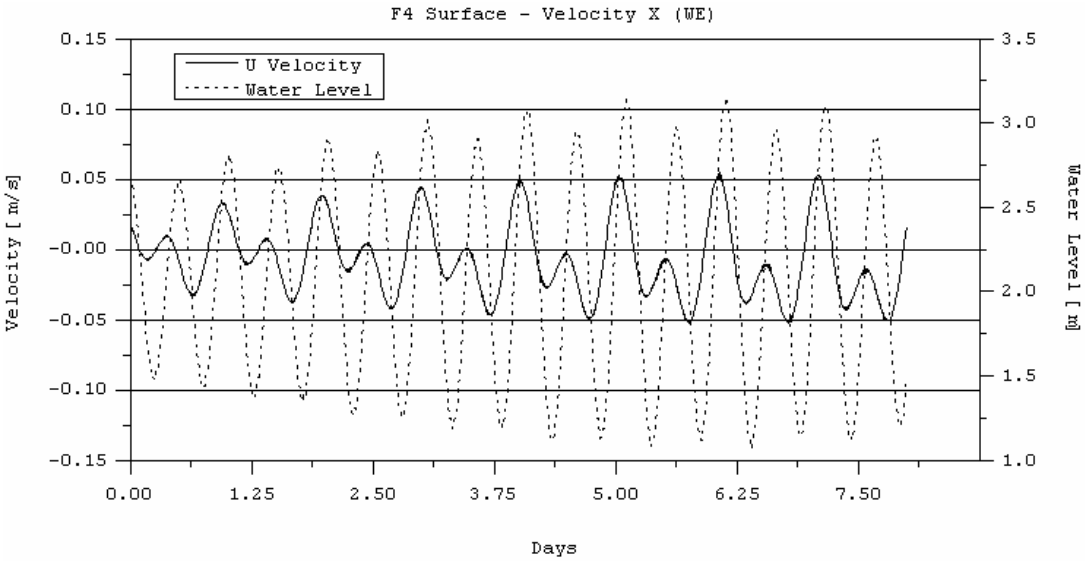


**Figure 33** – Model water level and X velocity (WE) results for station F4. The velocites is compute 5 meters from surface.

## Local Wind Variability

Before analysing the model results is necessary to understand the complex wind system associated with the coastline protected from the NE dominant winds. The topography above the sea level can have an indirect impact on local hydrodynamics. Madeira Island is an obstacle to wind propagation in the middle of the Atlantic. The steep topography and the NE wind dominant direction makes the south coast an area protected from strong winds. This is due to the formation of a wake structure in the protected side.

The effect of an obstacle on uniform flow under different Reynolds numbers can easily be investigated in a towing tank. It is found that four different types of flow are observed, depending on the value of Re in the experiment. At very small Reynolds number the flow around the obstacle is controlled by friction; it occurs entirely within the frictional boundary layer and is laminar and symmetric (Figure 34). At slightly larger Reynolds numbers the boundary layer separates behind the obstacle, creating a vortex pair with opposite rotation and central return flow (Figure 35).

Moderately high Reynolds numbers lead to the formation of a wake, which exhibits wave disturbances or instabilities at its interface with the undisturbed current (Figure 36).

Very high Reynolds numbers produce the separation of the vortices from the obstacle; vortices separate in turn from either side and drift away with 80% of the background velocity u, forming a downstream sequence of vortices with alternate sense of rotation known as a von Karman vortex street (Figure 37). Table 4 lists typical values found for

a flat plate oriented perpendicular to the flow. Other obstacle shapes produce the same transition from laminar boundary layer flow to vortex pair, wake with wave disturbances and von Karman vortex street; but the change from one type of flow to another occurs at somewhat different Re values. Table 4 gives a range of Reynolds numbers observed for a large variety of obstacle shapes.

**Table 4 -** Typical values found for a flat plate oriented perpendicular to the flow, other shapes are also consider.

| Flat plate | Other shapes | Type of flow |
|---|---|---|
| Re < 1 | Re < 0.5 | Laminar flow, no separation |
| Re>= 1 | Re > 2 - 30 | vortex pair with central return flow |
| Re >= 10 | Re > 40 - 70 | wake formation with wave disturbances |
| Re >> 10 | Re > 60 - 90 | von Karman vortex street |

Eddies dissipate energy, and wakes behind obstacles are regions of intense energy dissipation. The energy is withdrawn from the mean flow and has to be replaced if the situation is to remain in a steady state. The laboratory experiment from which the values in Table 4 were derived were all done by towing an obstacle through a tank with fluid at rest, so the energy dissipated in the wake is provided by the action of towing the obstacle through quiescent water. In the ocean the wind field, an internal pressure gradient or the tides can supply it.

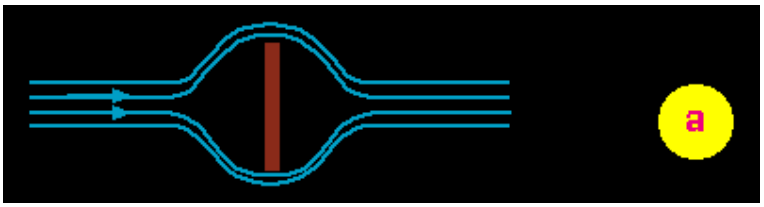


**Figure 34 -** No separation, laminar boundary layer


**Figure 35 –** Vortex pair with central return flow.

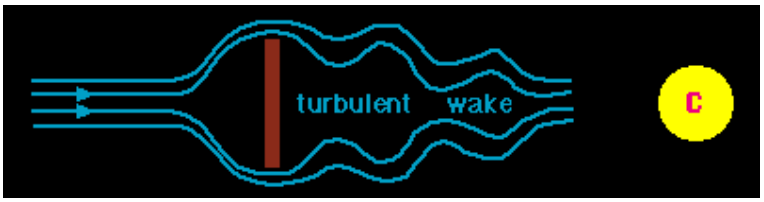


**Figure 36 -** wake formation with wave disturbances along the current/wake interface.


**Figure 37 -** von Karman vortex street.

Barkley (1972) described the wake system formation behind Madeira. If the incident wind flow is strong enough a vortex street could be formed like the one presented in Figure 38. The wake formation process has been observed via satellite in many places and is common to islands like the Grand Canaria (Barton et al, 2000), an island situated only 4 degrees south of Madeira. Low wind velocities can be associated to a wake but also strong direction variability. This is the reason why in Funchal harbour there is no dominant wind direction (Drena, 1991, anexo 2).


**Figure 38 -** Examples of vortex streets behind an island observed in the atmosphere. The island of Guadelupe is seen to produce a von Karman vortex street. Two vortices are visible in the first image, the vortices on the other side of the vortex street cannot be seen because of a break in the cloud cover; the image is adapted from NASA (1968).

## Transport Scenarios

The model when forced by climatologic density and large-scale real wind summer fields together and in separate generate superficial currents offshore in the south Madeira

coast. In the outfalls implementation areas this two forcing mechanisms when consider together produce a superficial south offshore current. When density is consider as the only forcing mechanism also an offshore superficial current is generate but now with an east direction.

For simplicity reasons the transport modelling was performed considering only tide and local wind effects. This approach is a conservative one because the currents forced by climatologic density (Figure 20) and large-scale wind dominant circulation (Figure 28) will tend to transport offshore the outfall plume. Basically not considering these effects will increase the retention time in the outfalls area.

In spite of large-scale wind processes are not considered the effect of local wind condition by Madeira steep topography is study. Due to the strong local wind direction variability a sensitiveness analysis was performed to understand the wind influence over the local circulation. Several scenarios were simulated using typical wind velocities (7 m/s). Five different scenarios with wind constant in time were simulated: constant wind in space with west, east, north and south direction and a variable in space schematic wind pattern representing a wake. In the wake case, a NE wind of 7 m/s is imposed in all domain except in a square (50 km x 50 km) south of Madeira where a SW wind with 3.5 m/s velocity is admitted. This schematic wind was inspired in the field measurements made by Barton et al. (2000) in the Gran Canaria. This island is under the influence of the same large-scale wind circulation. The model was also forced with tide to understand how these two mechanisms interact. Vertical density gradients were consider to simulate well vertical turbulent processes in other words to estimate accurately the wind effect over the flow.

The model results at 5 meters depth for the stations F1 and F4 where current velocities were measured are presented below (Figure 12). For the F1 station, located over the Funchal outfall, it is possible to see a strong response of the model x (WE) velocity component to West and East winds (Figure 39). Under the influence of a west wind in both stations, surface current has a strong east residual direction. In the case of F1 station the flow along the entire 8 days period has always the east direction. The F4 station does not have the same strong reaction because in this case the velocities generated by tides are larger (Figure 41). The same differences can be observed in the east wind situation, but in this case currents have a strong residual west direction. A

south wind only changes significantly the Y velocity component and some differences are observed for both components at station F1 and at station F4. The changes in the Y component for both stations indicate that south winds will generate a small north transport in the area, indicating a near downwelling situation (Figure 40, Figure 42). The east wind produces similar changes, while the north and west winds have the opposite effect (upwelling).

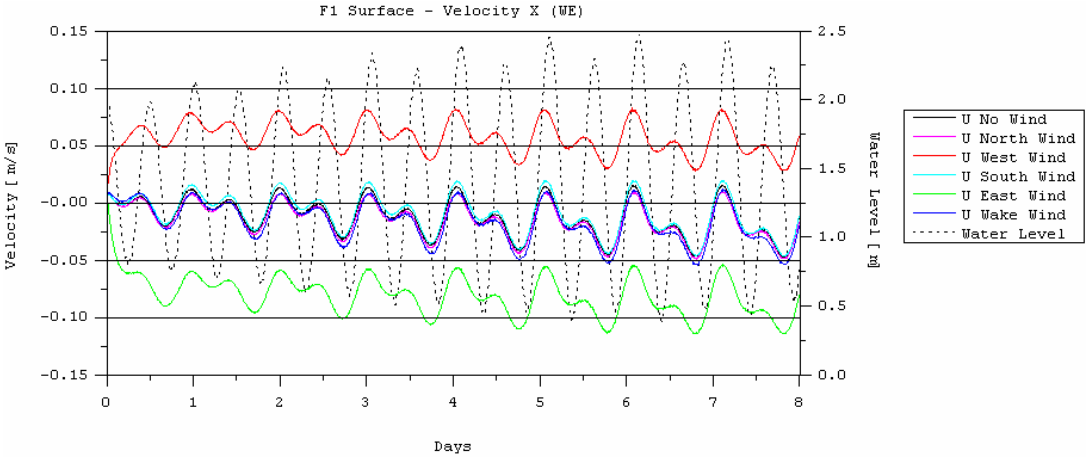


**Figure 39** – Model X velocity at 5 meters depth at F1 station evolution a long a period of 8 days for several scenarios: No wind, west wind, east wind, north wind, south wind and schematic wake wind.

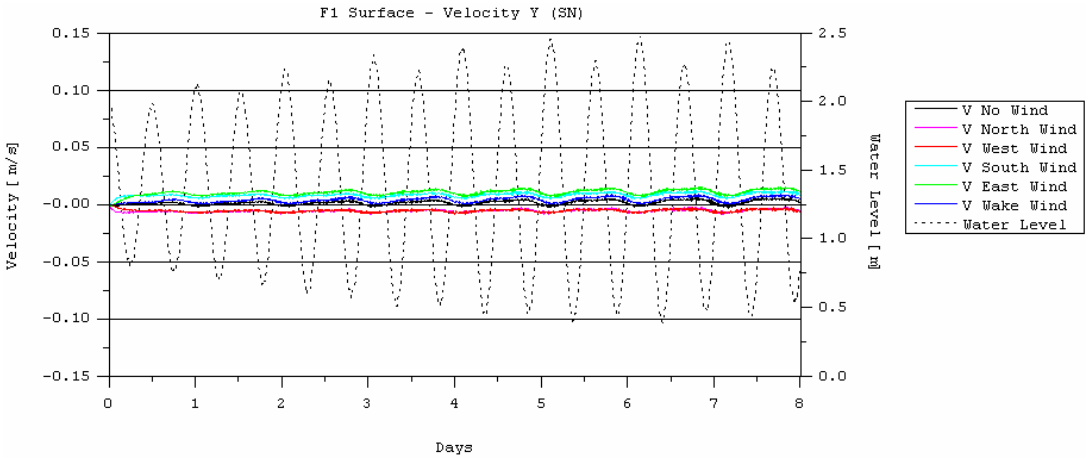


**Figure 40** – Model Y velocity at 5 meters depth at F1 station evolution a long a period of 8 days for several scenarios: No wind, west wind, east wind, north wind, south wind and schematic wake wind.

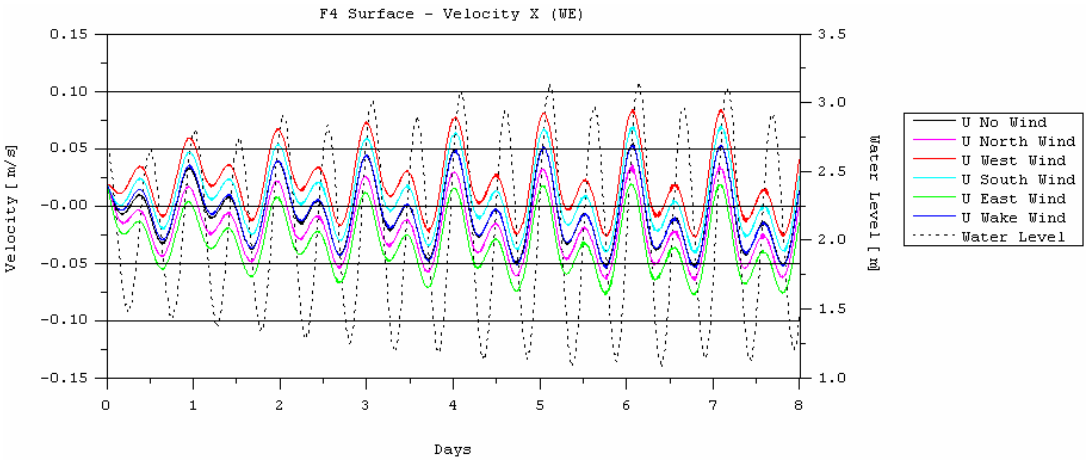


**Figure 41** – Model X velocity at 5 meters depth at F4 station evolution a long a period of 8 days for several scenarios: No wind, west wind, east wind, north wind, south wind and schematic wake wind.

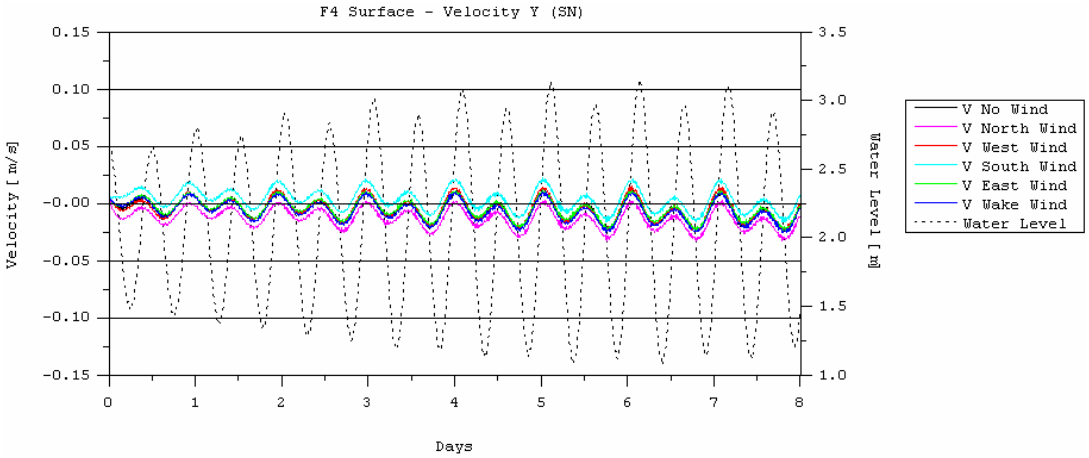


**Figure 42** – Model Y velocity at 5 meters depth at F4 station evolution a long a period of 8 days for several scenarios: No wind, west wind, east wind, north wind, south wind and schematic wake wind.

## Residual circulation

To begin the study of the residual circulation, we will consider a current of constant speed and direction flowing past an idealized island with vertical coasts and we will consider a zero Coriolis force. Islands are obstacles to the flow; they force water particles to depart from the straight path, which they would follow in the absence of the island. By deviating from its intended path the particles experience an acceleration perpendicular to their original direction. At the same time, the particles experience friction as they try to pass around the island. The path of an individual particle around an island will thus be determined by the balance of two forces, the force associated with

the acceleration that causes its departure from a straight path, known as the inertial force, and the frictional force associated with the frictional boundary layer around the island (Figure 43).

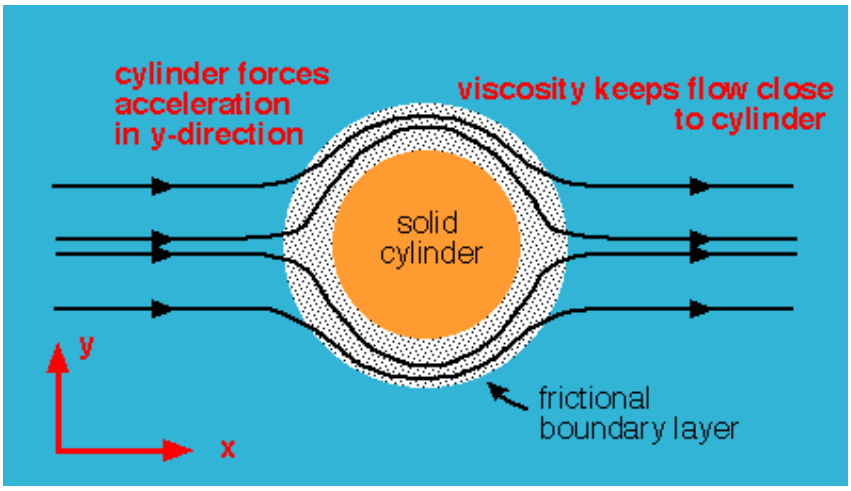


**Figure 43 -** Sketch of the flow field around a cylinder (circular island), showing the frictional boundary layer and the forces experienced by a water particle as it moves along a streamline (Tomczak, 1996).

Now we add the Coriolis force effect to the process described above. Considering that in the open ocean the pressure and Coriolis forces transversal to the trajectory are in balance, an obstacle like Madeira Island will tend to reduce the velocity component perpendicular to it and consequently the Coriolis force. Instead of a symmetric flow like the one presented in Figure 43, the left branch that contours the island will have larger velocities. Basically an open sea current with variable direction that intersects an Island will tend to produce a clockwise residual flow around it. The interaction between the tidal wave and the bottom will also increase the wave amplitude. The main consequence of this is stronger sea level gradients parallel to the coastline and consequently stronger current velocities.

The clockwise residual circulation tide induce is reproduce by the model around Madeira (Figure 44) and Desertas Islands (Figure 45). This circulation has residual currents more intense around Desertas Islands, in the west and east (outfalls area) coasts of Madeira Island. In the outfalls area residual tide currents are parallel to the coast and with a west direction. In the the residual currents intensity is approximately 1 cm/s while in the *Caniço/Camacha and S$^{ta}$ Cruz* are the double (Figure 47). The main effect of the North wind is the increase of currents intensity to the double. The only effect over the currents direction is near *Câmara de Lobos* and *Funchal* outfalls where an offshore current is observed. This residual upwelling effect was already foreseen in the model time series analysis presented earlier (Figure 40 and Figure 42). In the South wind

scenario the residual currents have an onshore direction in the *Câmara de Lobos* and *Funchal* outfalls (Figure 48). Once more this was foreseen in the time series analysis presented above. In the other outfalls area the flow is parallel to the coast and with a NE direction. The currents intensity is around 2 cm/s but in the middle of Funchal Bay lower values are observed. This indicates high residence times in this area. At 20 meters depth in Funchal bay an offshore residual current is observed to compensate the strong superficial onshore transport (Figure 49). The West wind produces a residual current with an east direction and 4 cm/s of intensity near the coast line between *Câmara de Lobos* and *Funchal* outfalls. Near the first one the current have small offshore component. At larger depths and in the other outfalls the current have a south direction and intensities between 1 and 2 cm/s. The east wind produces a current with a west direction in all outfalls. Near the coast the current intensity is of 6 cm/s while at depths greater than 500 m this value decrease to 2 cm/s. Finally the schematic wake wind generate a residual circulation similar to the North wind scenario but in the *Câmara de Lobos* and *Funchal* outfalls area the currents intensity is much lower with out offshore component.

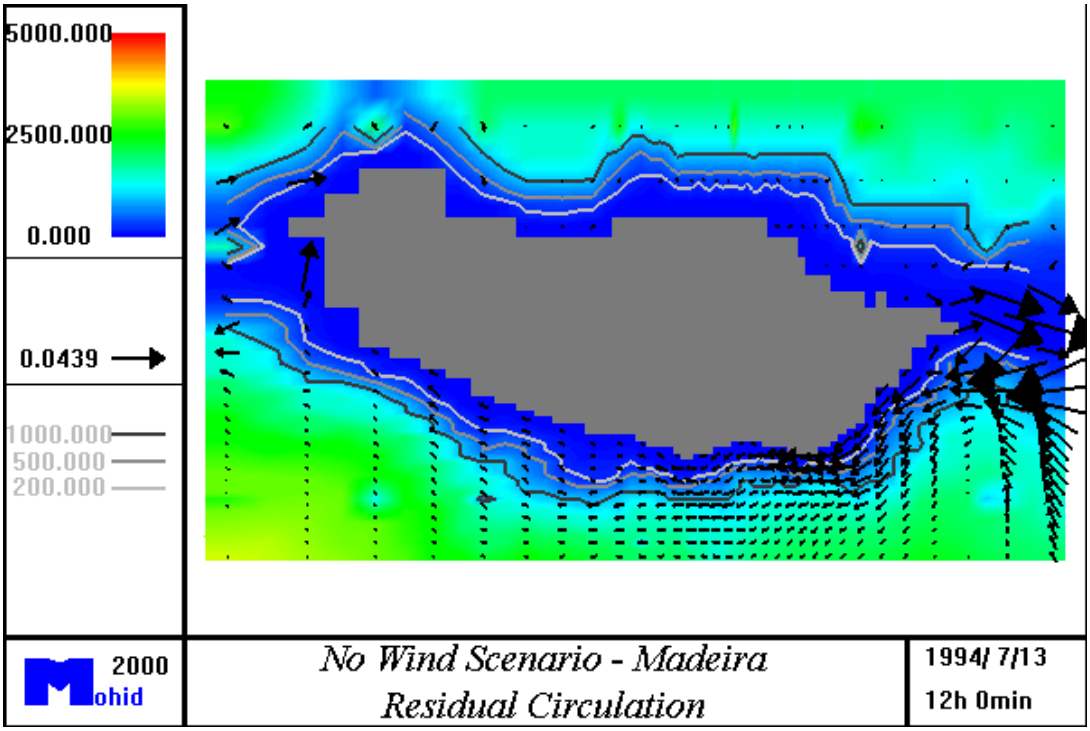


**Figure 44 –** Surface residual circulation forced by tide for a period of 8 days along the Madeira coast line.

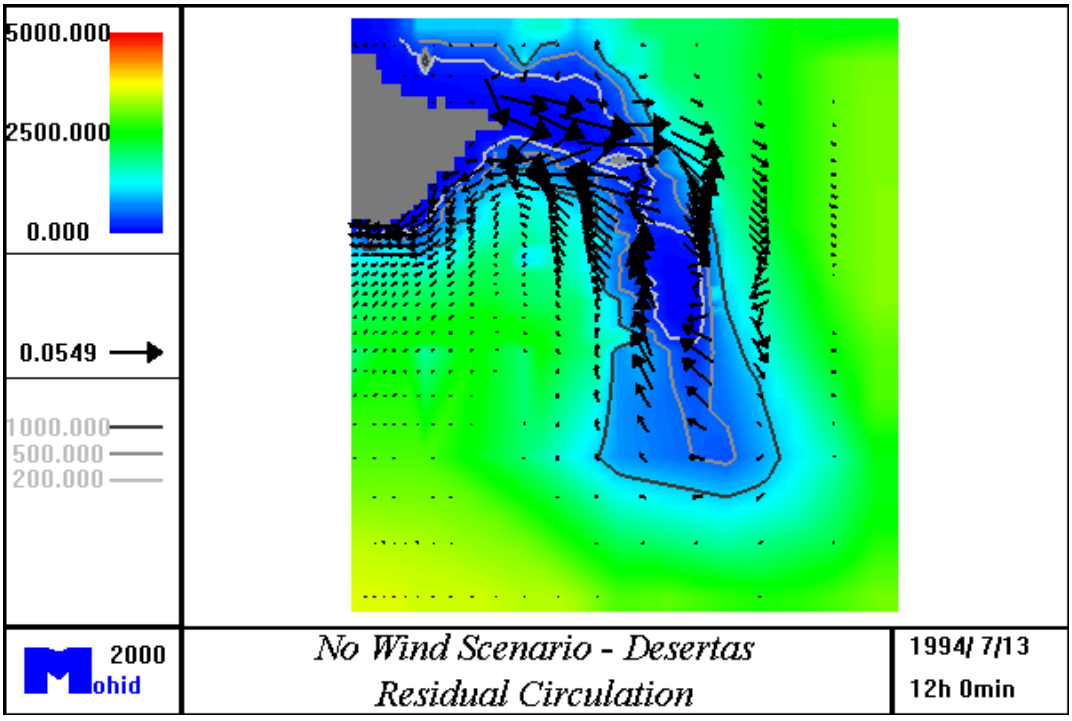


**Figure 45 -** Surface residual circulation forced by tide for a period of 8 days in the Desertas islands.

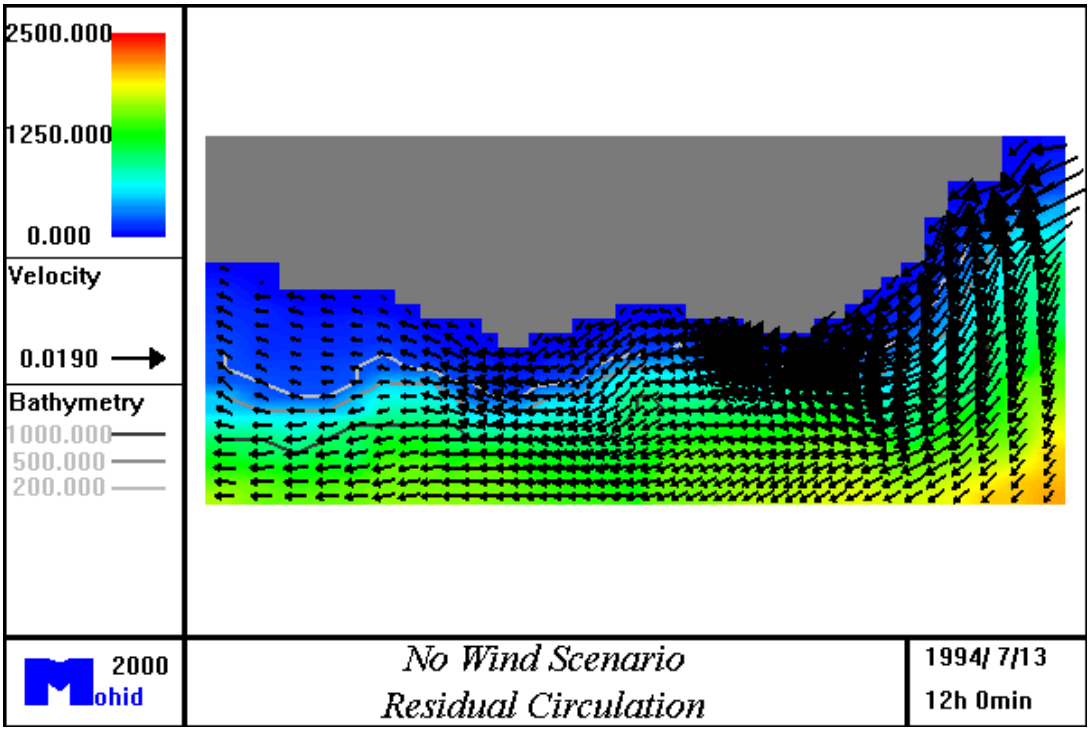


**Figure 46 –** Surface residual circulation forced by tide for a period of 8 days along Madeira south coast .

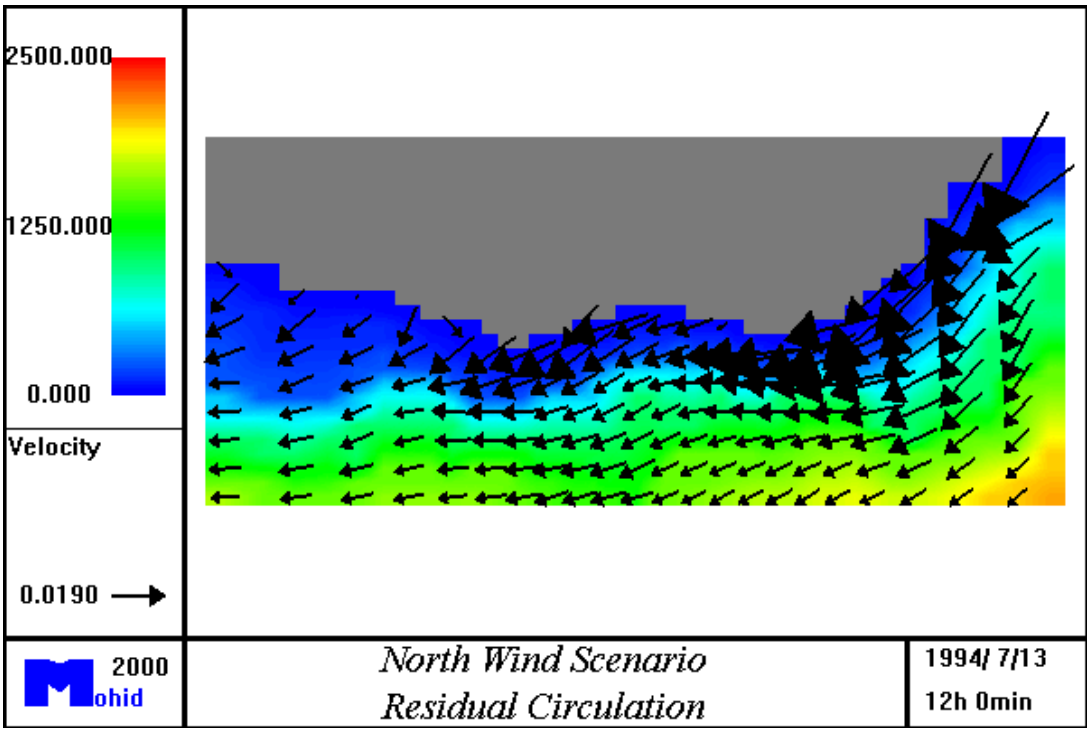


**Figure 47** – Surface residual circulation forced by tide and north wind for a period of 8 days along Madeira south coast .

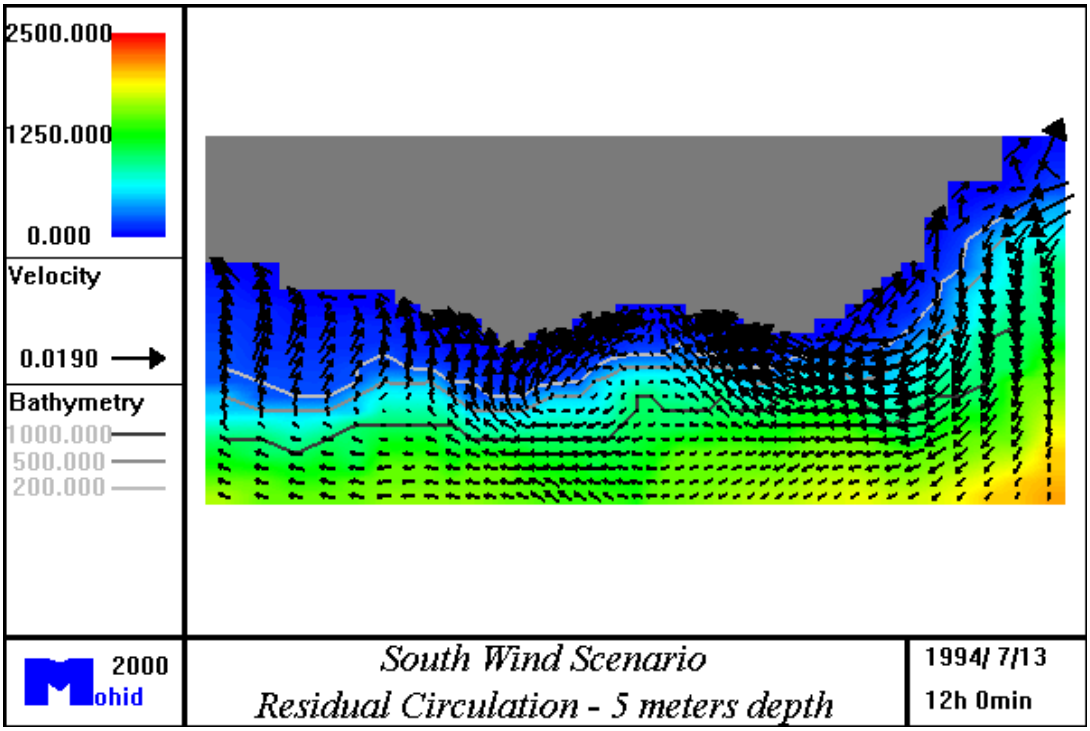


**Figure 48 –** Surface residual circulation forced by tide and south wind for a period of 8 days along Madeira south coast .

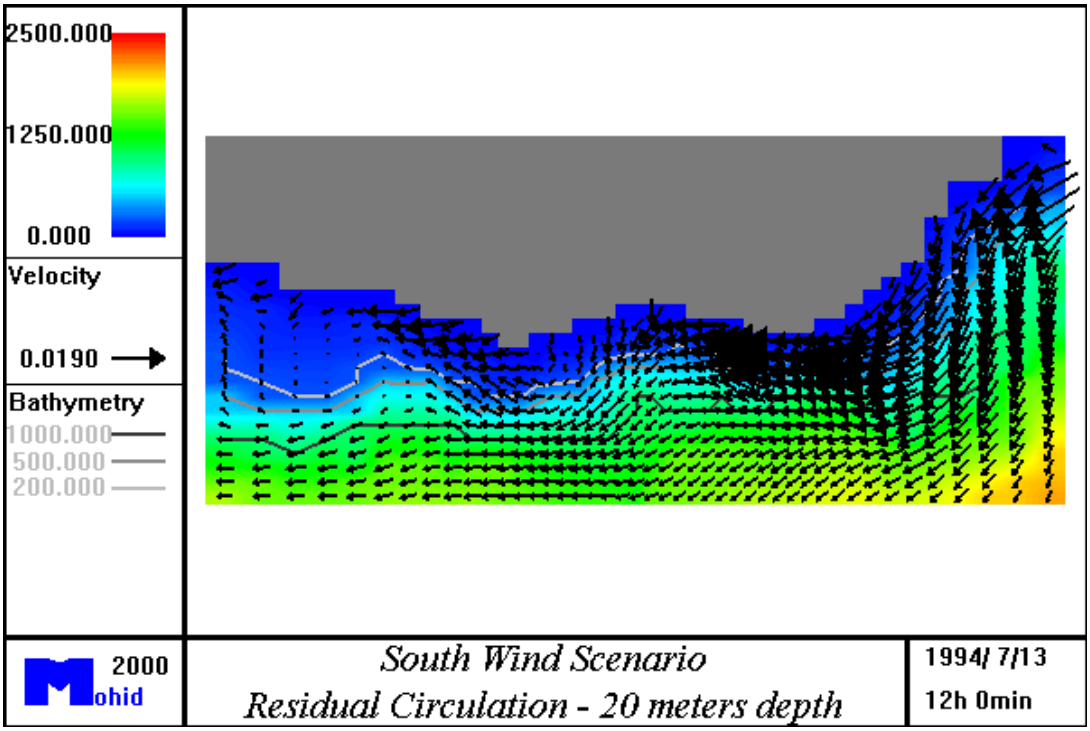


**Figure 49** –Residual circulation at 20 meters depth forced by tide and south wind for a period of 8 days

along Madeira south coast .

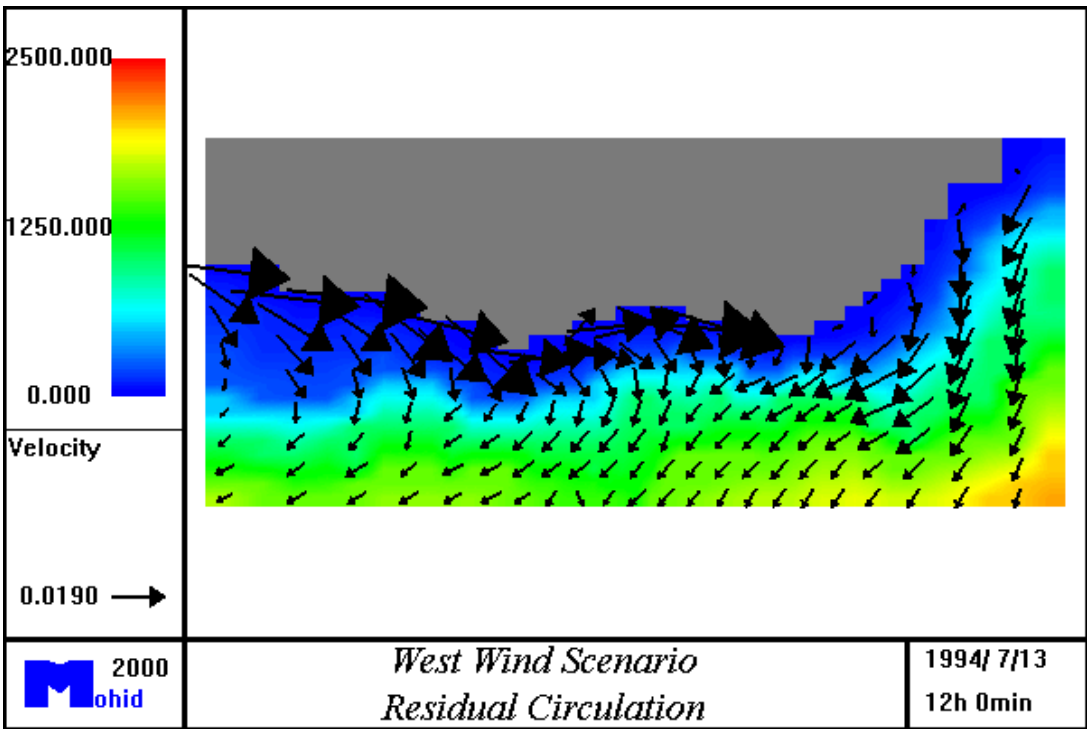


**Figure 50**– Surface residual circulation forced by tide and west wind for a period of 8 days along Madeira south coast .

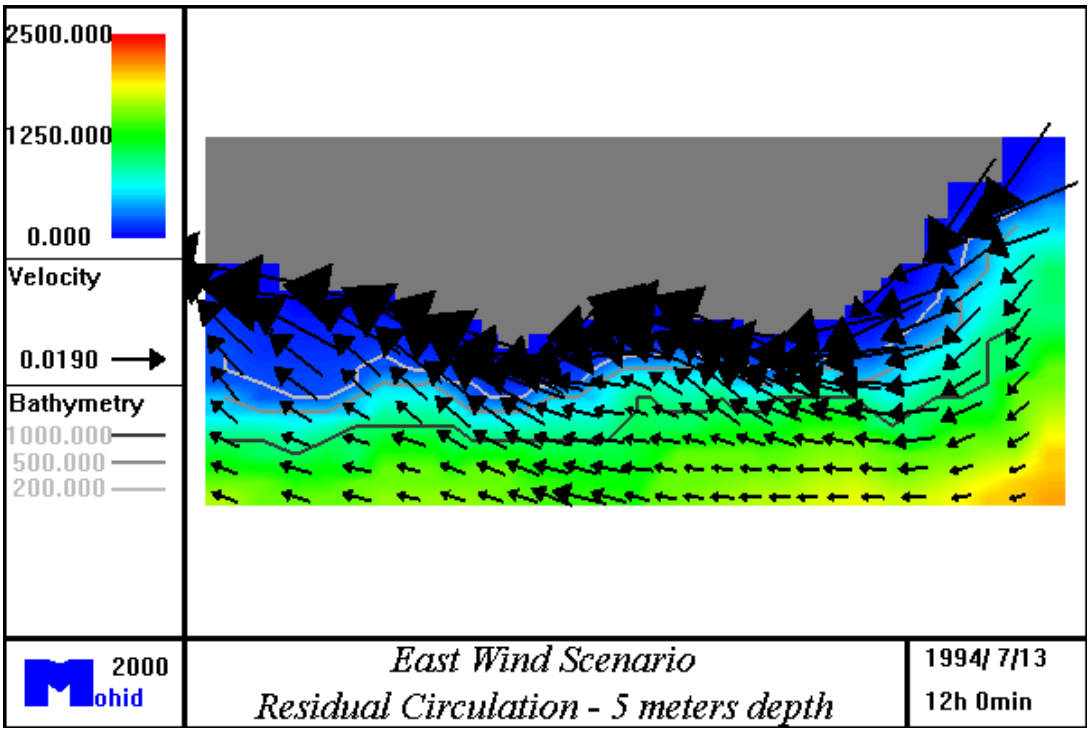


**Figure 51** – Surface residual circulation forced by tide and east wind for a period of 8 days along Madeira south coast .

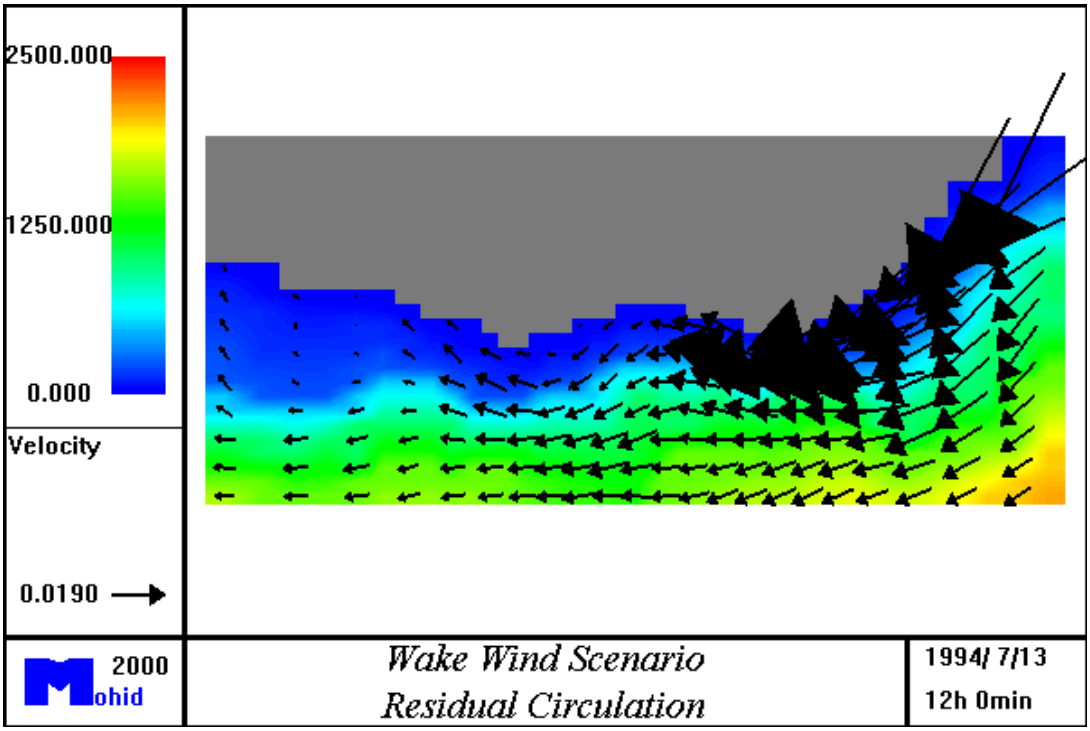


**Figure 52** – Surface residual circulation forced by tide and schematic wake wind for a period of 8 days along Madeira south coast .

## Avaliation of the effects in the receptor mean

### Description and Microbiological Characterization of Beaches

In result of its volcanic origin, the coastal edge of Madeira Island is composite mainly for great basaltic tablets having, only, some rolled pebble of average dimensions (about 20 cm) beaches. In the influence zone of Funchal submarine outfall exists only one beach, known as the Barreirinha beach, while in the influence zone of Câmara do Lobos submarine outfall there are none.

Similarly to most island beaches, Barreirinha's beach is a rolled pebble beach. The water quality in this beach is monitorised periodically by two different entities: the Public Health Regional Direction (PHRD) and the entity responsible for the Funchal wastewater treatment plant (ETAR).

Figure 53, Figure 54 and Figure 55 presents, respectively, the distribution of total coliforms, fecal coliforms and fecal streptococci in Barreirinha beach, between 1993 and 2000. The results presented in these figures are in logarithmic scale.

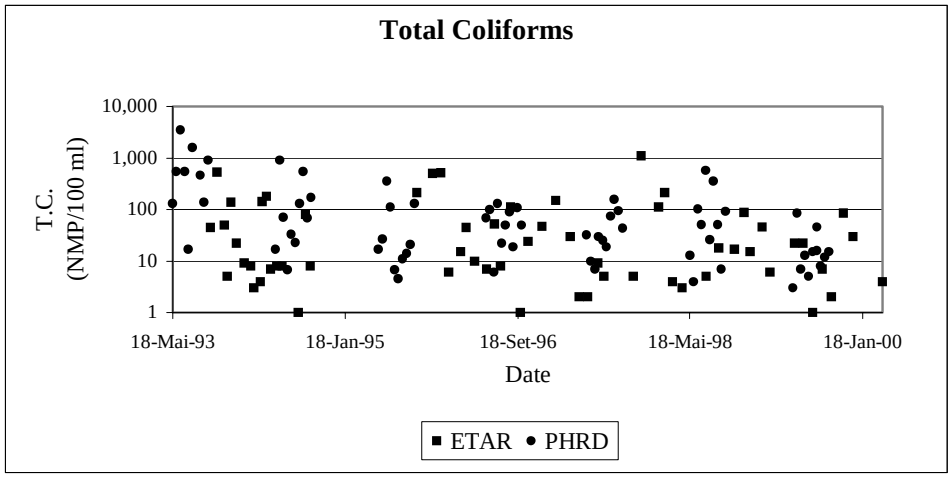


**Figure 53 - Distribution of total coliforms (NMP/100 ml) in Barreirinha beach**

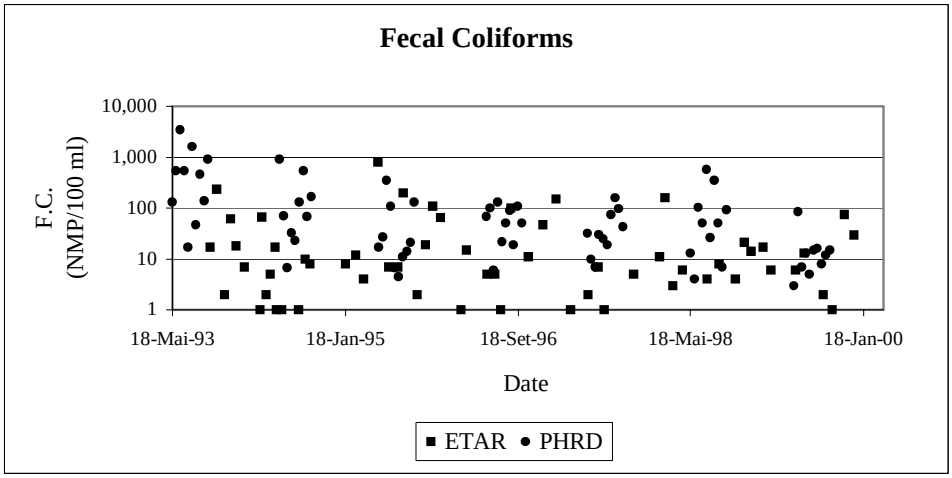


**Figure 54- Distribution of fecal coliforms (NMP/100 ml) in Barreirinha beach**

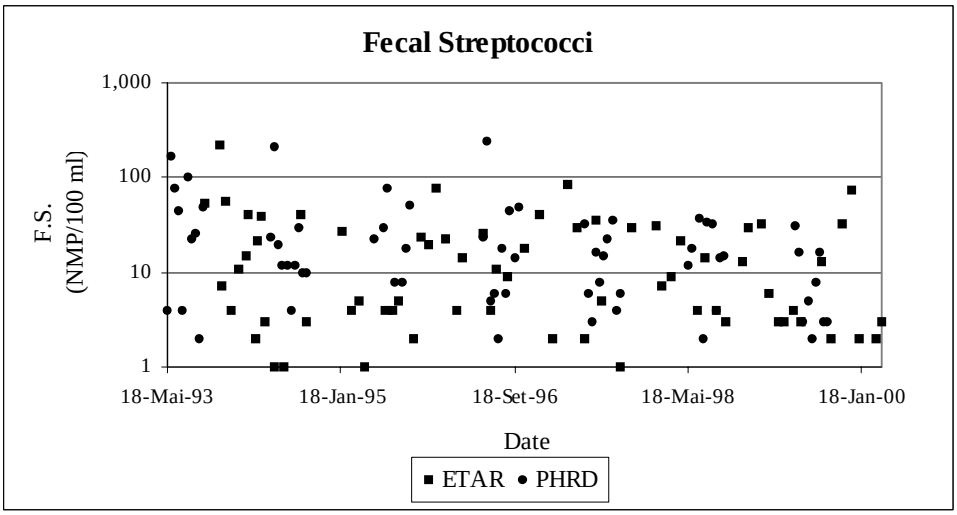


**Figure 55 - Distribution of fecal streptococci (NMP/100 ml) in Barreirinha beach**

The water quality in Barreirinha's beach has always been acceptable. However, it can

be detected an improvement in this quality since 1994, in terms of total coliforms and fecal coliforms. During the monitoring campaing carried out between 1993 and 2000, only one sample exceed the maximum value allowed in terms of fecal coliforms (in the 14$^{th}$ of June, 1993), coinciding with the starting month of the Funchal wastewater system. The remaining results are smaller than the maximum value allowed. Since 1998 the water quality was always been good. The samples never exceed the recommendable maximum values of Council Diretive 76/160/EEC – Bathing Waters.

The results obtained confirm the good quality of beach waters, which is always compatible with direct contact leisure. However, this quality has suffered a significant improvement since 1998 and now it can be considered good.

## Primary Production in Madeira Coastal Areas

The superficial layer of the ocean near the Madeira Island coast, which develops between 0 and 100 meters, is characterized by being a region in constant changing, which reflects permanently dispersion. The changing of the environment conditions that this dispersion reflects results of a set of time and space variations that occurs, such as air temperature variations, interaction between the sea surface and the atmosphere (evaporation and conduction) and processes of vertical mixture.

In accordance with Decree Law 152/97, of 19 June 1997, the south coast of Madeira Island is classified as a **less sensitive zone**. This situation is essentially the result of the location of the island (in the meddle of the Atlantic Ocean), its high coastal edges slopes and high transparency deeps.

Next presents a summary analysis of the main features of the ocean in the study zone, in terms of the parameters mentioned in INAG, 1998: nitrates, chlorophyll-a, dissolved oxygen and transparency and, also, an analysis of the enteric pollution.

### Nitrates

The coastal band of Madeira Island is a region with oligotrophic characteristics, which means that in here the ocean has small concentrations of the essential nutrients (nitrogen, phosphorus and iron).

In October 1998, the dissolve nitrate concentration at sea surface of Madeira's south coast was measured. The sampling stations chosen were situated near Funchal and Câmara de Lobos outfalls and in four other points situated at a distance of 300 m of the shoreline, between the two outfalls. The sampling stations are presented in Figure 56.

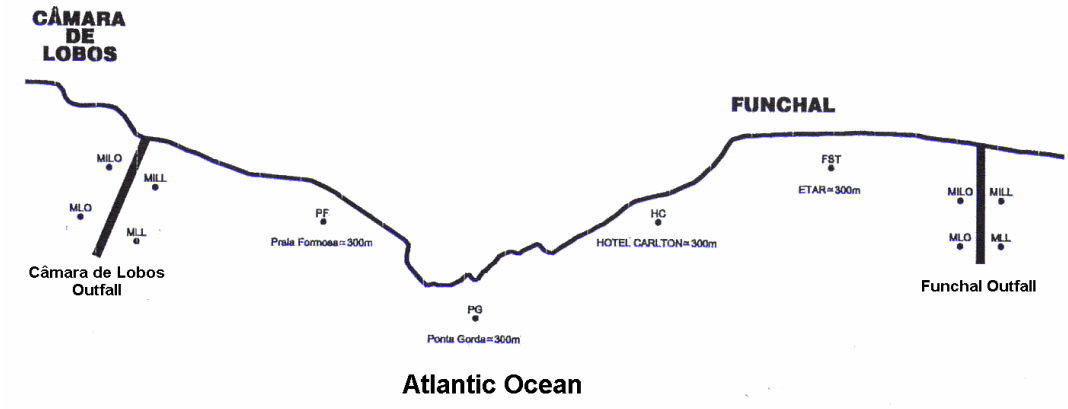


**Figure 56 – Squematic presentation of the sampling stations**

The dissolved nitrate concentration levels are always below maximum limit of 15.0 µmol/l presented in INAG, 1998. This values present good agreement with the oligotrophic characteristics of the study zone.

## Chlorophyll-a

Figure 57 presents the space variation of chlorophyll-a at sea surface in October 1998 in some sampling stations near Funchal e Câmara de Lobos submarine outfalls, as well as in coastal waters between the two outfalls.

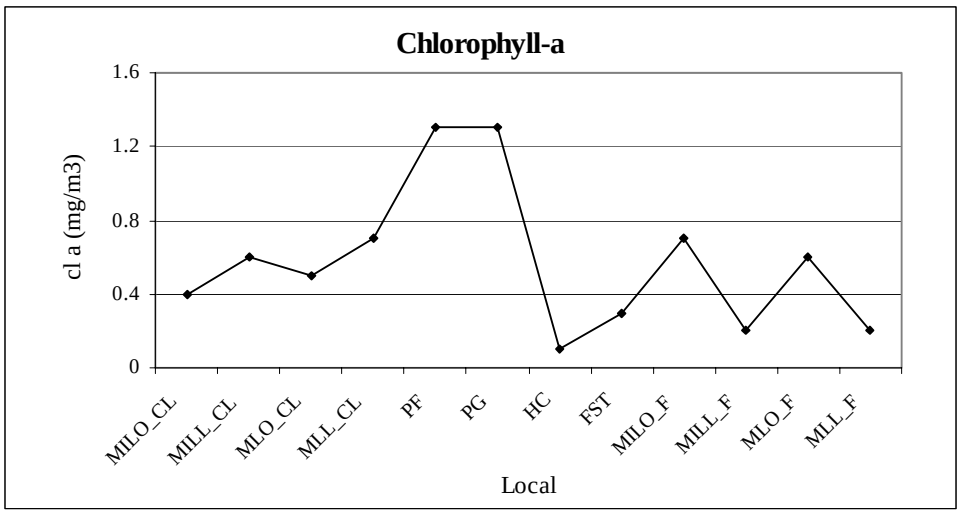


**Figure 57 - Space variation of the concentration of Chlorophyll-a in October 1998**

In the surface, the chlorophyll-a concentrations remain very low, with values smallest than 2.0 mg/m$^3$, clearly below the limit of 10 mg/m$^3$ presented in INAG, 1998. These values suggest the presence of a small phytoplanktonic biomass and, consequently, a low potential for primary production.

## Transparency

The coastal waters of Madeira Island present high transparency depths (of about 30 meters in depth) associated with blue watercolor characteristic of poor productive oceanic areas.

In October 1998, the surface water transparency was measured in the represented sampling stations. This parameter was measured with a Secchi disk. The transparency values had been always greater than 4 meters in depth.

The measured data of transparency parameter near Funchal's coast shows that the transparency levels in the sea are always high (equal or greater than the minimum limit established of 2 meters).

The results in terms of transparency suggests that the suspended solid concentration in the sea is not significant and that the particulate material unloaded by the outfalls does not magnify the suspended solid concentration in a visible form.

## Dissolved oxygen

The dissolved oxygen concentration in water depends on the atmospheric reaeration, photosyntetic oxygen production and local oxygen consumption (use of oxygen for respiration by aquatic plants and oxidation of the organic waste material). The oxygen production is limited by the concentration of nutrients, such as nitrogen and phosphorus. Figure 58 presents space variation of the dissolved oxygen concentration in October of 1998 in some sampling stations located near Funchal and Câmara de Lobos outfalls, as well as in coastal waters between the two outfalls.

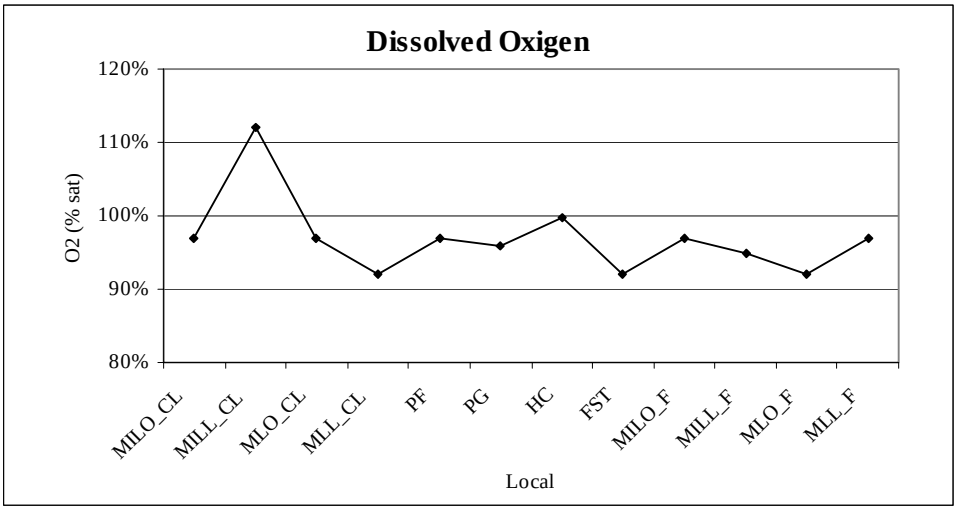


**Figure 58 – Spacial variation of dissolved oxigen concentration in October 1998**

These values reveals that the dissolved oxygen concentration is always closed to the

saturation value and that it does not vary significantly in the stations next to the diffuser, where the effluent is discharge to the receptor mean.

The high transparency that occurs suggests low concentration of organic substance and small consumptions of dissolved oxygen. The mixture induced by the wind contributes to magnify the reaeration between the water and the atmosphere.

## Indicator Bacteria

Figure 56 presents the schematic location of the sampling stations in the sea near Funchal and Câmara de Lobos submarine outfalls. Figure 59, Figure 60 and Figure 61 presents the concentrations of total coliforms, fecal coliforms and fecal estreptococcis at sea surface near the two submarine outfalls. The scale used in the graphical representation is the logarithmic scale.

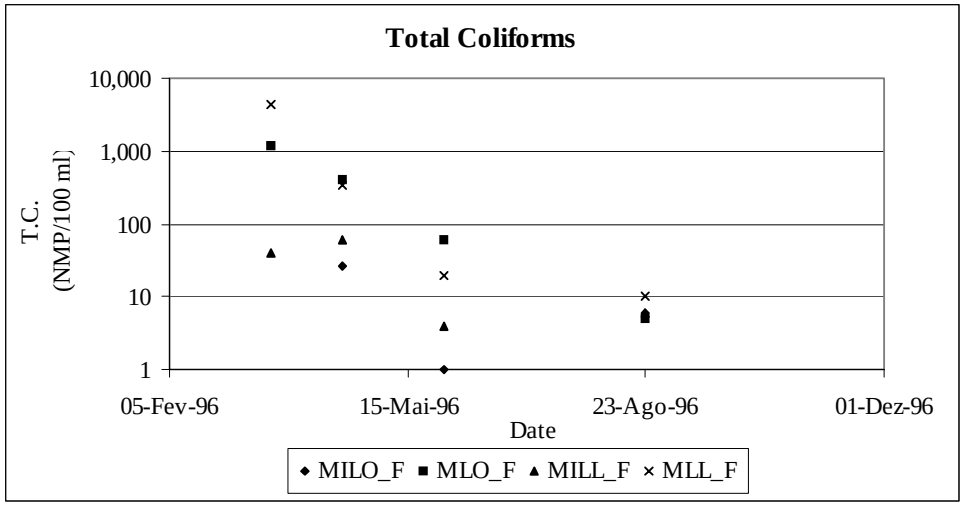


**Figure 59 – Distribution of total coliforms near the Funchal outfall**

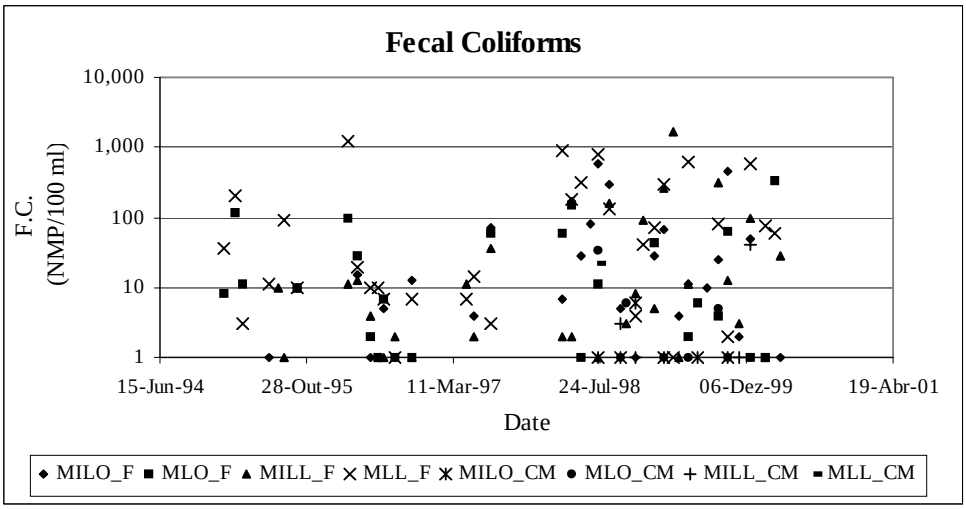


**Figure 60 – Distribution of fecal coliforms near the Funchal and Câmara de Lobos outfall**

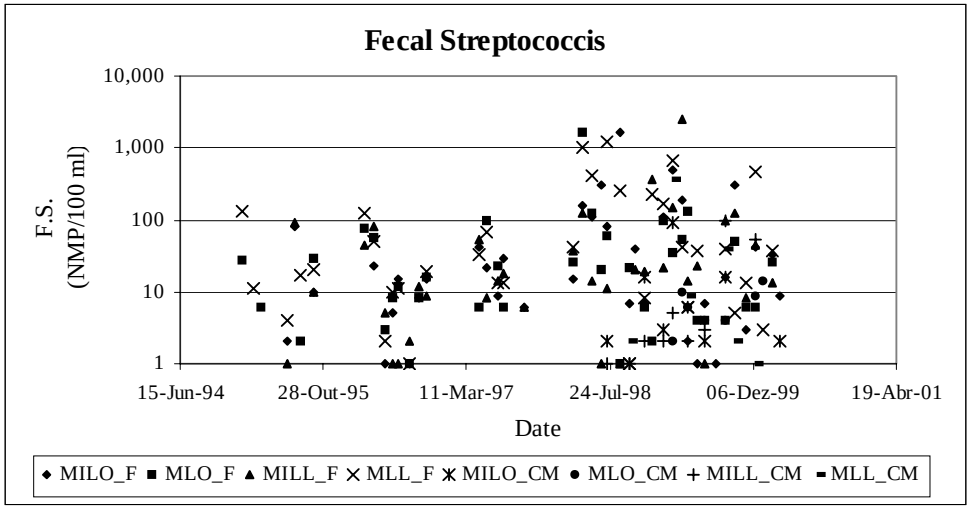


**Figure 61 – Distribution of fecal streptococcis near the Funchal and Câmara de Lobos outfall**

The results confirm the high values of initial dilution that occurs near the submarine outfalls. As it can be observed, the values of concentrations of total coliform bacteria group, fecal coliform and fecal streptococci on the water surface, exactly in the neighborhood of the diffusers, are very low, with concentrations smaller than $2{,}5x10^3$ NMP/100 ml.

These results demonstrate that concentration levels of enteric pollution are very low (generally smaller than the permissible maximum values) even in the diffusers neighborhood, next to the discharges point at a distance greater than 500 meters of shoreline and at a distance of 2,000 m of the only beach located near these outfalls (Barreirinha beach).

## ASSESSMENT OF THE EFFECTS ON THE RECEIVING WATERS

The effects of ocean waste disposal are the result of a complex relation between two variables, concentration and time. The effect of the oceanic environment on the effluent is of critical significance. After discharge to the ocean, the effluent experiences changes in its physical and microbiological properties, which vary at each point as a function of time. The discharge of any potential pollutant to the sea requires justification, particularly when the general public regards any such discharge as cumulative dumping. The outfall discharge directly influences the bottom of the food chain, which in consequence can affect higher tropic levels. We are interested in the lower end of this cycle where biological processes return waste matter back into the food chain. For this process to function the marine environment requires a good supply of oxygenated water, light, and a balanced bacterial and faunal population both in the water column and on

the sea bed. Far from being delicate, the marine living environment is highly adaptable to variations of waste input, whether it is from natural or man-made sources. However at least two conditions are necessary: That the receiving waters and sea bed are in a sufficiently “healthy” condition to receive and treat the effluent; That the effluent discharge is of such a quantity and character that the receiving waters can accept and treat the additional load. Thus the discharge of domestic and other biodegradable effluents to the sea may be seen as part of the natural cycle of life and decay. It follows that the marine environment can legitimately be utilised, where appropriate, for the treatment of such sewage effluents.

The quality of the environment is typically defined on the basis of a series of biophysical and chemical parameters. The relative health of that environment is related directly to any deviation from some specified norm. Modelling can be a fruitful way to assess marine environmental impacts caused by outfalls by simulating the physical and biological processes and determining if the recycling capability of the receiving waters is overstepped causing a deviation from the biophysical and chemical typical parameters.

## Simulation data

The simulations were carried out, considering the following average flows to each outfall.

Table 5 – Flow in each outfall

| ***Location*** | ***Flow*** $(m^3/s)$ |
|---|---|
| ***Funchal*** | 0.255 |
| ***Camâra de Lobos*** | 0.05 |
| ***Camacha/Caniço*** | 0.056 |
| ***Sta. Cruz*** | 0.033 |

Table 6 presents the concentrations of wastewater at the entrance to the Treatment Station, and which serves as a basis for the simulations carried out.

Table 6– Characterisation of affluent at the ETAR

| ***Parameters*** | ***Concentration (mg/l)*** |
|---|---|
| ***Particulate nitrogen (mgN/l)*** | 0.05 |
| ***Nitrates (mgN/l)*** | 2.0 |
| ***Nitrites (mgN/l)*** | 0.02 |
| ***Ammonia (mgN/l)*** | 38.0 |
| ***$BOD_5$ ($mgO_2$/l)*** | 350 |
| ***Dissolved oxygen ($mgO_2$/l)*** | 0 |
| ***Faecal Coliforms (units/100 ml)*** | $10^7$ |

Table 7 presents the reduction provided for in the pollutant load deriving from the adoption of primary treatment at the ETAR.

Table 7 - Reduction of pollutant loads in accordance primary treatment

| *Parameters* | *Primary treatment (%)* |
|---|---|
| ***$BOD_5$ ($mgO_2$/l)*** | 20 |
| ***Suspended Solids (mg/l)*** | 50 |
| ***Nitrogen (mgN/l)*** | 10 |
| ***Faecal Coliforms (units/100 ml)*** | 50 a 90 |

The environmental conditions of the sea water considered for the purpose of simulation are presented in Table 8. Seawater properties were specified using data collected by INIP (Instituto Nacional de Investigação das Pescas) during cruises of a support program to fishery from 1980 to 1984 Table 8lists the values used that represent the results integrated over the first 60 meters depth of the field stations located near the Madeira Island.

Table 8 - Seawater ambient conditions.

| ***Property*** | ***Concentration*** |
|---|---|
| ***Phytoplankton (mgC/l)*** | 0.003245 |
| ***Zooplankton (mgC/l)*** | 0.0003245* |
| ***Particulate Nitrogen (mgN/l)*** | 0.0001* |
| ***Refractory Dissolved Nitrogen (mgN/l)*** | 0 * |
| ***Labile Dissolved Nitrogen (mgN/l)*** | 0.00001* |
| ***Nitrate (mgN/l)*** | 0.0045* |
| ***Nitrite (mgN/l)*** | 0.00021 |
| ***Ammonia (mgN/l)*** | 0.00133* |
| ***Biological Oxygen Demand ($mgO_2$/l)*** | 0 |
| ***Dissolved Oxygen ($mgO_2$/l)*** | 7.64 |
| ***Temperature (ºC)*** | Data series |
| ***Salinity (ppm)*** | Data series |
| ***Extinction Coefficient ($m^{-1}$)*** | 0.057 |

* Estimated values.

## Available light assessment

Selective absorption and scattering due to the seawater itself, and dissolved and suspended matter in the water reduce light penetrating into the water. The reduction of light in the water column can be expressed in terms of the vertical extinction coefficient

k, generally defined as $m^{-1}$:

$$I_d = I_o \exp(-kz)$$

where $I_0$ is the incoming light intensity, $I_d$ the light intensity travelling a distance of (z). The value of k can be estimated from Secchi measurements using the empiric relation:

$$k = \frac{1.7}{D_s}$$

where $D_s$ stands for the Secchi disk reading (Parsons et al. 1984). Table 8 presents the value of extinction coefficient used in the simulation based on the measurement with Secchi disk from INIP cruises.

# ASSESSMENT OF THE BEHAVIOUR OF INITIAL DILUTION

## General considerations

### Physical considerations

Before the horizontal mixing and dispersion phase, the buoyant effluent must rise towards the sea surface form its seabed discharge point. The dilution of a buoyant rising plume, or multiple plumes rising from a sea bed outfall to the sea surface is a function of discharge rate and efflux velocity, diameter of exit port, depth of water and fluid density difference. Another environmental parameter relevant to initial dispersion is the velocity of current in the receiving waters. The influence of velocity is revealed at two levels: it increases local turbulence and reduces residence time. Turbulence of the water column promotes the mixing of the discharged effluent with salt water existing in the receiving waters. Corresponding to the reduction in residence time in the diffuser zone, and for the same interval of time, there is an increase in the volume of water where the effluent is subject to dispersion, and a corresponding reduction in concentrations of discharged substances.

### Biological considerations

Changes in the concentration of pollutant substances discharged by the submarine outfall depend on the respective interaction with the receiving waters. The greater the initial dispersion (or dilution), the faster the biological activity (mineralisation of organic material and consumption of nutrients) due to the greater transport of

phytoplankton and microorganisms. Not necessarily: low dilution can lead to high nutrients, eutrophication and rapid mineralisation locally – the price is the loss of system equilibrium. Also, which phytoplankton gets transported? Not from the effluent, where it does not exist, so presumably this refers to locally produced phytoplankton, which implies a high local production due to localised nutrient enrichment (=low dilution) – these statements appear contradictory. A high dilution also contributes to an increase in light penetration and oxygen interaction with the atmosphere, due to the greater plume surface, which may also contribute to an increase in biological activity.

### Methodology for simulation with CORMIX

For the estimate of initial dispersion, simulations were carried out, using the CORMIX model ("CORnell MIXing System"), developed at the University of Cornell, USA, for the environmental conditions observed in the field (current velocities and temperatures). By the time of this preliminary report was finished not all data necessary was available. So a first study was carried out for the Funchal outfall with the conditions presented in Table 9

| Table 9 - Parameters used for simulation of the initial dispersion, in stratification conditions | ***Stratified water column*** |
|---|---|
| **Parameters** | |
| ***Effluent flow (m$^3$/s)*** | 0.255 |
| ***Concentration of faecal coliforms (*CF/100 ml)** | 7x10$^6$ |
| ***Temperature (º*C)** | 20 |
| ***Equivalent length of diffuser (*m)** | 140 |
| ***Number of diffuser orifices*** | 60 |
| ***Diameter of diffuser orifices (*cm)** | 10 |
| ***Depth of thermocline (*m)** | 15 |
| ***Density of upper layer (-)*** | 1.024 |
| ***Density of lower layer (-)*** | 1.026 |
| ***Depth of discharge (*m)** | 52 |
| ***Velocity of current (*m/s)** | 0.1 |

It can be stated that the exceptional conditions of the receiving waters (in terms of restoration capacity and current velocities in particular), allied to the conditions in which the discharge of effluent is processed in terms of depth led to the obtaining of an extremely high initial dispersion ratio of 2000. Nevertheless some technical details were estimated (flow orientation in relation to outfall location, water densities, location of orifices and other) so our option in this matter is to use a dilution rate "less optimistic" (r = 1000) that was computed for the Guia outfall with some similarities to this one.

## Results of the Discharge Effects Simulation

During the ascension of the plume, there is high initial dispersion. The degree of dispersion depends on the geometry of the diffuser, on the discharge of effluent, on the velocity of the currents in the environment and the structure of the density profile of the water column.

In the model, the plume in each outfall was simulated emitting tracers along a line, at the depth given by the automatic calculation programme. Six points were considered to each outfall to represent the linear shape of the plume.

The concentration of each pollutant, after the initial mixing, is given by the following expression:

$$C_{initial,i} = (Idr * C_{effluent,i} + (1-Idr) * C_{environment,i})$$

with

$C_{initial,i}$ – *initial concentration of the pollutant i,*

*Idr –initial dispersion rate,*

$C_{effluent,i}$ - *concentration of pollutant i in the effluent (after treatment),*

$C_{environment,i}$ - *environmental concentration of the pollutant i.*

The concentrations obtained, are presented respectively in Table 10. This table present the concentrations of substances in the receiving waters for two distinct scenarios: with primary treatment and with secondary treatment. The concentrations of phytoplankton and dissolved oxygen were considered zero in the effluent of the ETAR but, after the initial dispersion, they practically equalled the values of the concentration present in the environment.

Table 10– Concentrations obtained after initial dispersion

| ***Parameters*** | ***Primary Treatment*** |
|---|---|
| ***Phytoplankton (mgC/l)*** | 0.003245 |
| ***Particulate nitrogen (mgN/l)*** | 0.010 |
| ***Nitrates (mgN/l)*** | 0.037 |
| ***Nitrites (mgN/l)*** | 0.020 |
| ***Ammonia (mgN/l)*** | 0.058 |
| ***$BOD_5$ ($mgO_2$/l)*** | 0.28 |
| ***Dissolved oxygen ($mgO_2$/l)*** | 7.642 |
| ***Faecal Coliforms (units/100ml)*** | 100 |

# SYSTEM ASSESSMENT: EFFECTS ON THE RECEIVING WATERS

## Introduction

For the mathematical simulations the MOHID modelling system was used.

The MOHID mathematical model system has been developed at the Instituto Superior

Técnico since 1986, as part of national and international research projects. The system includes hydrodynamic models of estuary and oceanic circulation, models for wave propagation, sediment transport dispersion and water/ecology quality.

The MOHID system is used at the University of the Algarve, the University of Santiago de Compostela, the Free University of Brussels, at the CIOO (Holland), at the Federal University of Rio de Janeiro and at UNISANTA, also in Brazil.

In Portugal, the system has been implemented in the main estuaries. The system has also been applied to the main rias in Galicia, the Escalda estuary (Holland/Belgium), the Gironde estuary (France), in Carlingford Lough (Ireland), in the Bay of Mussulo (Angola), in Macao and in the estuaries of Santos and Paraíba (Brazil). In the Northeast Atlantic, the system has been applied in several different locations, especially in the region between the Canaries and the north of Scotland.

MOHID applications have been carried out for a variety of projects, validation of the results being based on fieldwork carried out by all the partners involved in these projects.

The model is currently being applied to several projects financed by the European Commission.

### Eutrophication assessment

The simulation of the water quality processes is developed with the following considerations. Autotrophic producers (phytoplankton) consume inorganic nutrients and depend on both their availability and sunlight as a source of energy for photosynthesis. Nitrate and ammonia are the inorganic nitrogen forms that primary producers consume. The Primary and Secondary producer's excretions are considered, acting as source for the nitrogen cycle. Primary producers are consumed by secondary producers, which in turn are consumed by higher trophic levels.

During the winter period, biological activity is reduced and regeneration increases the concentration of nutrients.

In the spring, biological activity is revitalised by the growing levels of luminosity, the concentration of phytoplankton increases and the concentration of nutrients diminishes duo to heavy consumption. The zooplankton grows and feeds on the phytoplankton. In this way, in summer the phytoplankton concentration is reduced due to the low concentration of nutrients and the high consumption by the zooplankton.

Usually a second production peak occurs in autumn results from the new increase in the concentration of nutrients, which can have two different origins: regeneration and

upwelling of deep water.

Oxygen enters this complex cycle in two adjacent processes, consumption by microorganisms that perform the degradation of organic matter. This process accomplishes conversion of the discharged organic waste to its basic mineral compounds, which consequently will be consumed by primary producers. The second process consists in the inorganic nitrogen oxidation performed by nitrifying bacteria that captures oxygen to convert nitrogen release in the surrounding water as ammonia to nitrate in a process known as nitrification. To predict the extend of oxygen depletion it is necessary to know how much waste is being discharged and how much oxygen will be required to degrade the waste. However, because oxygen is continuously being replenished from the atmosphere, as well as being consumed by organisms, the concentration of oxygen in water is determined by the relative rates of these competing processes.

### Methodology Used

A Lagrangian water quality model was used. The model considers the plume to be composed of small masses of water (tracers), simulating the transformations of substances transported by that water.

The concentrations dissolved oxygen, ammonia, nitrates, phytoplankton, CBO5 and coliforms were calculated for primary treatment level.

The simulations were carried out allowing for action of tides and the absence or presence four wind regimes, North, South, West and East during for 8 days.

In the far field, the plume of each outfall is submitted essentially to dispersion and to degradation processes of biological origin. Dispersion was simulated using a three-dimensional model of the particle location. Degradation of materials was simulated using a water quality model independent of the number of dimensions and of the advection - diffusion algorithm.

The hydrodynamic model uses a variable mesh to calculate pollutant concentrations. In the proximity of each diffuser, a 500-metre mesh was used. the temporal step is 1200 seconds. The velocities calculated by the hydrodynamic model are used to simulate the movement of the tracers. The small-scale processes, not resolved by the hydrodynamic model, create a variability that is not represented by this velocity, the respective effects being quantified in two ways: random displacement of the tracer and increase in its volume.

### Water quality simulation results

Next figures show the results from the four outfalls, for the situations of north, south, east, west and no wind. They show as expected that the established limits to discharge are well above the results obtained. The values of nitrate, chlorophyll-a and oxygen saturation**,** are always below the maximum surface limit referred to in INAG, 1998 respectively 0.21 mg N/l, 0.6 mg C/L e oxygen saturation>90%. This circumstance contributes to confirming that the local hydrodynamic conditions due to action of the tides, constitutes an important mechanism for dispersion of pollutants in the area and there are no risks of eutrophication, in this area.

North wind simulation

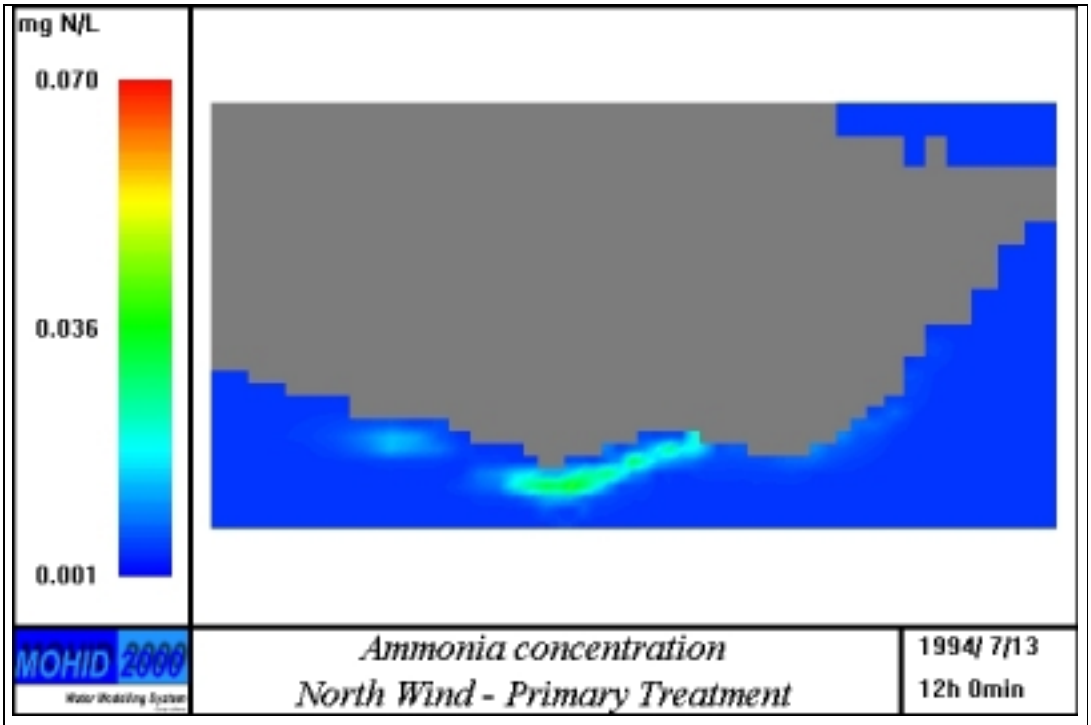


**Figure 62 Simulation with North wind. Increase ammonia concentration caused by wastewater discharge after primary treatment.**

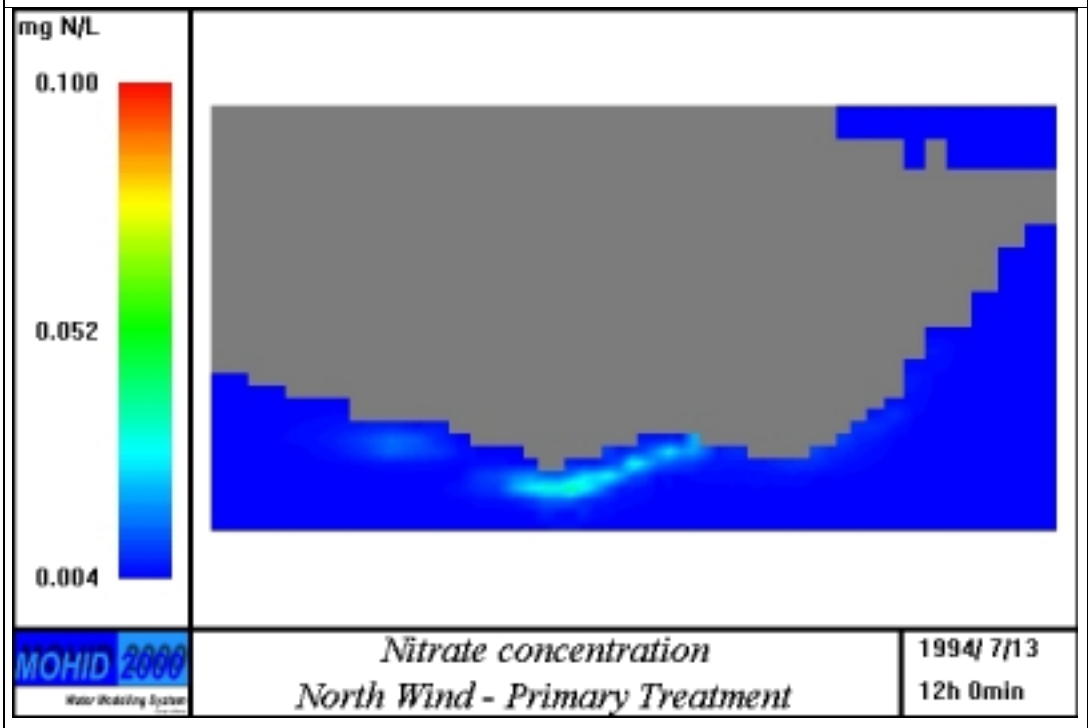


**Figure 63 Simulation with North wind. Increase nitrate concentration caused by wastewater discharge after primary treatment.**

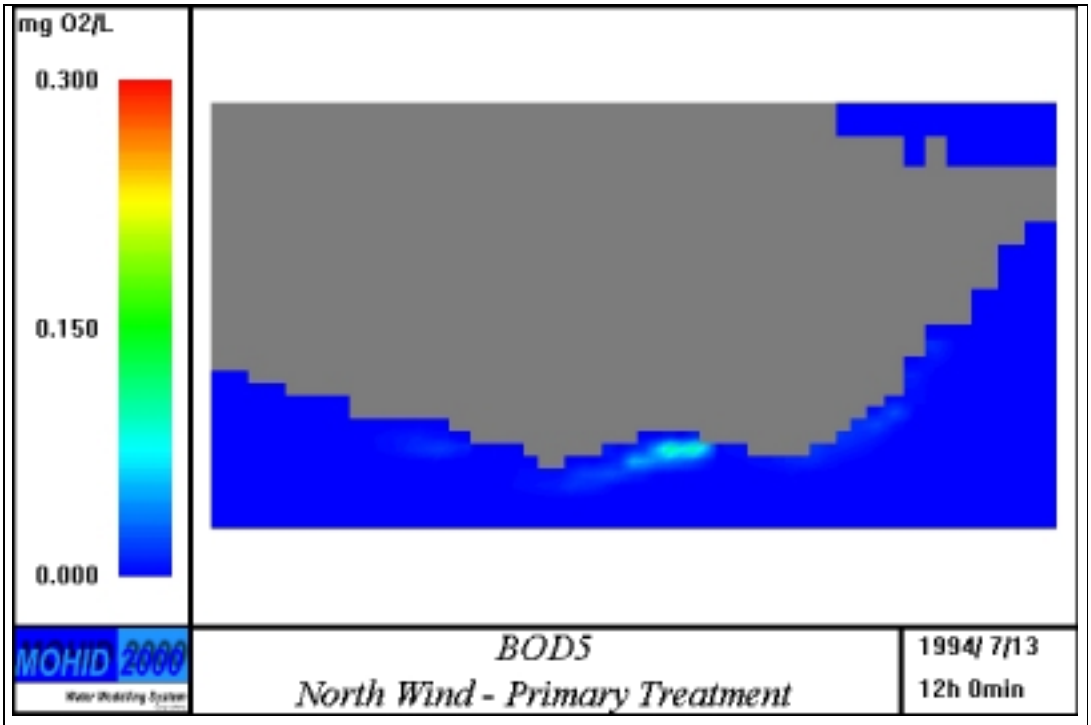


**Figure 64 Simulation with North wind. Increase $BOD_5$ concentration caused by wastewater discharge after primary treatment.**

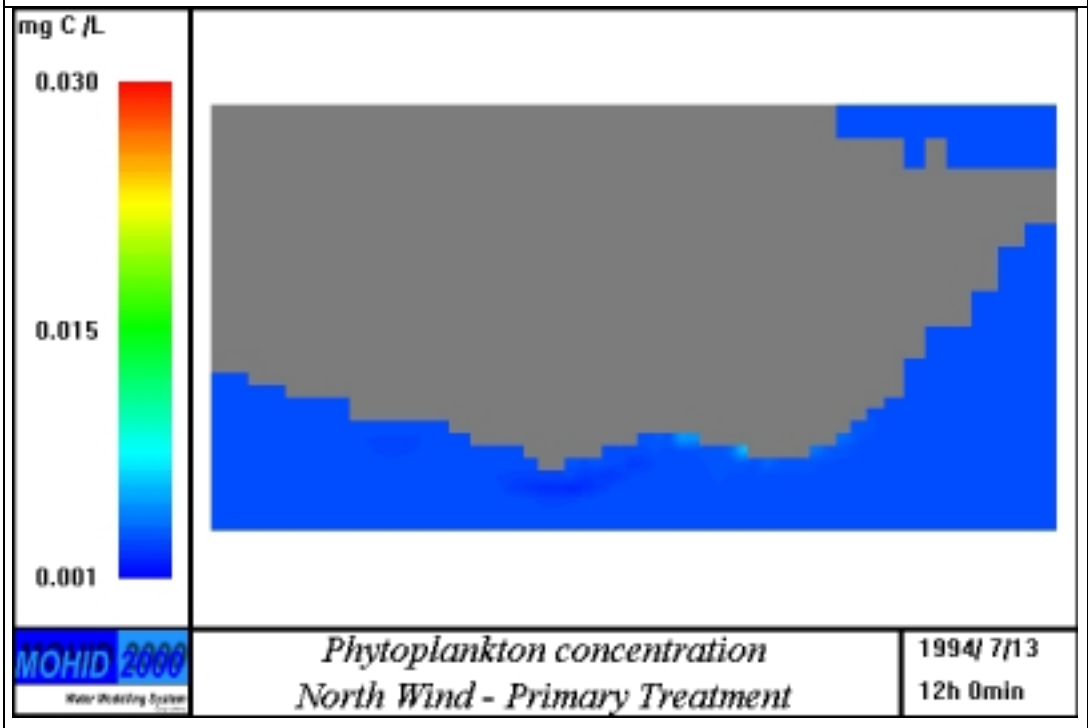


**Figure 65 Simulation with North wind. Increase phytoplankton concentration caused by wastewater discharge after primary treatment.**

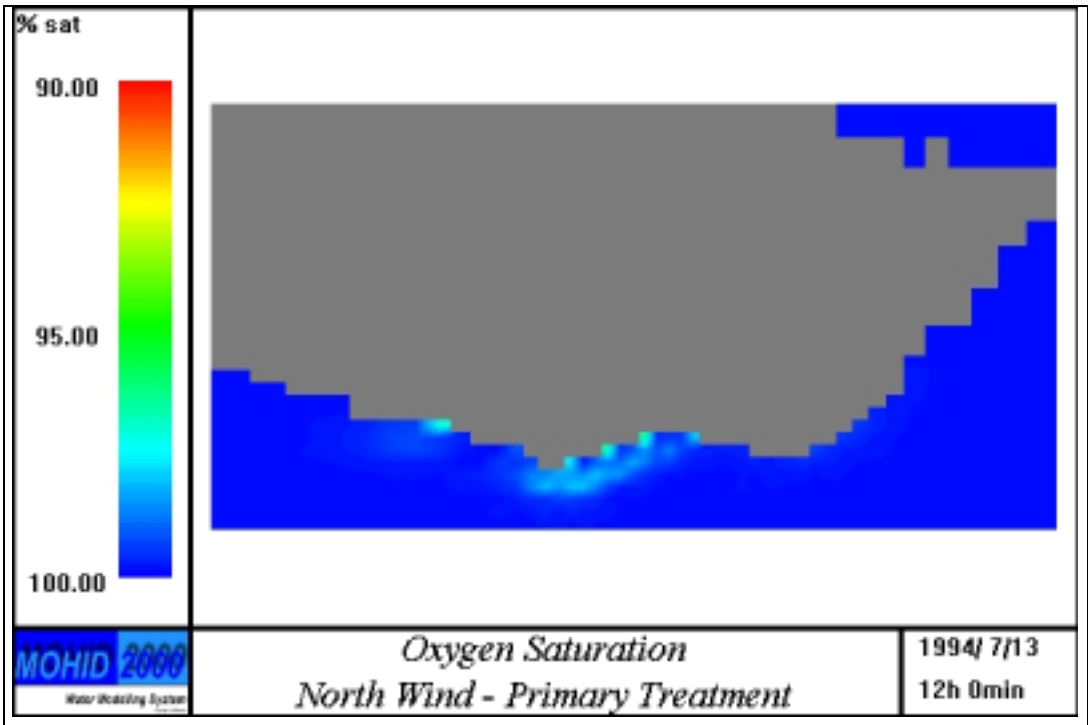


**Figure 66 Simulation with North wind. Decrease oxygen (percentage) caused by wastewater discharge after primary treatment.**

South wind simulation

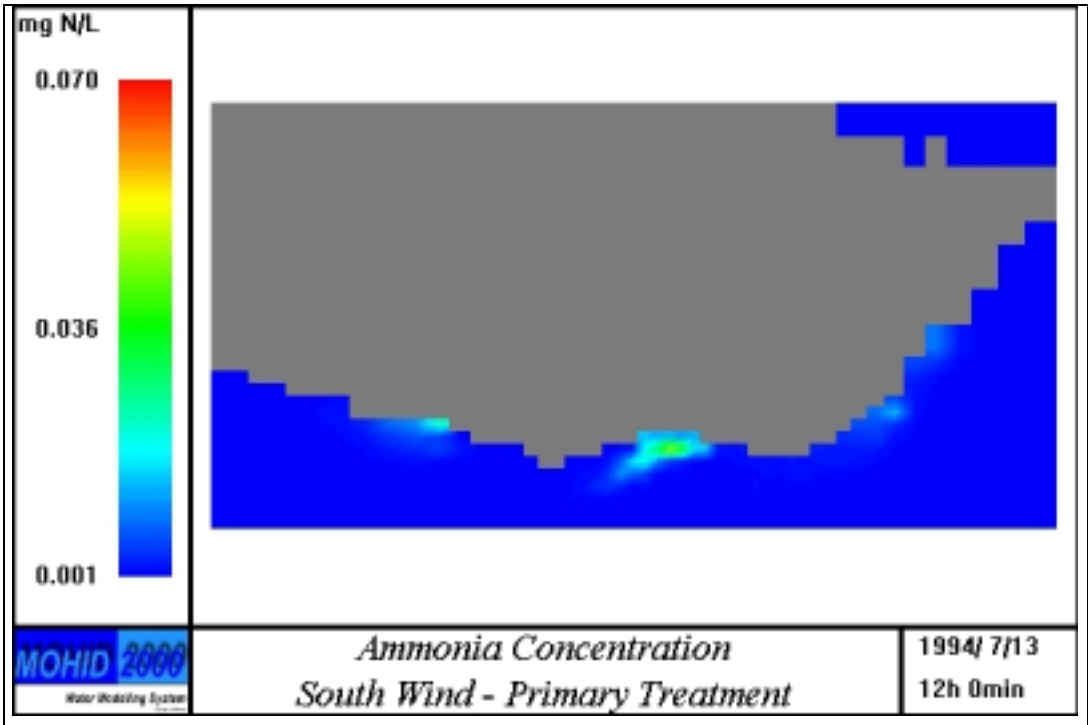


**Figure 67- Simulation with South wind. Increase ammonia concentration caused by wastewater discharge after primary treatment.**

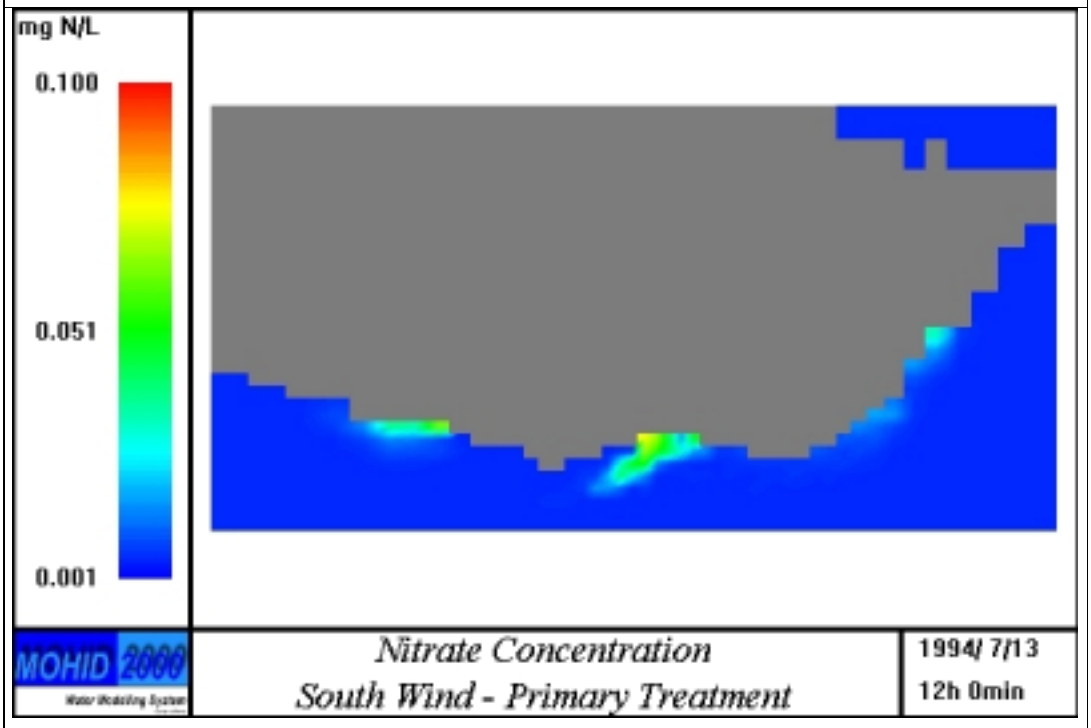


**Figure 68 Simulation with South wind. Increase nitrate concentration caused by wastewater discharge after primary treatment.**

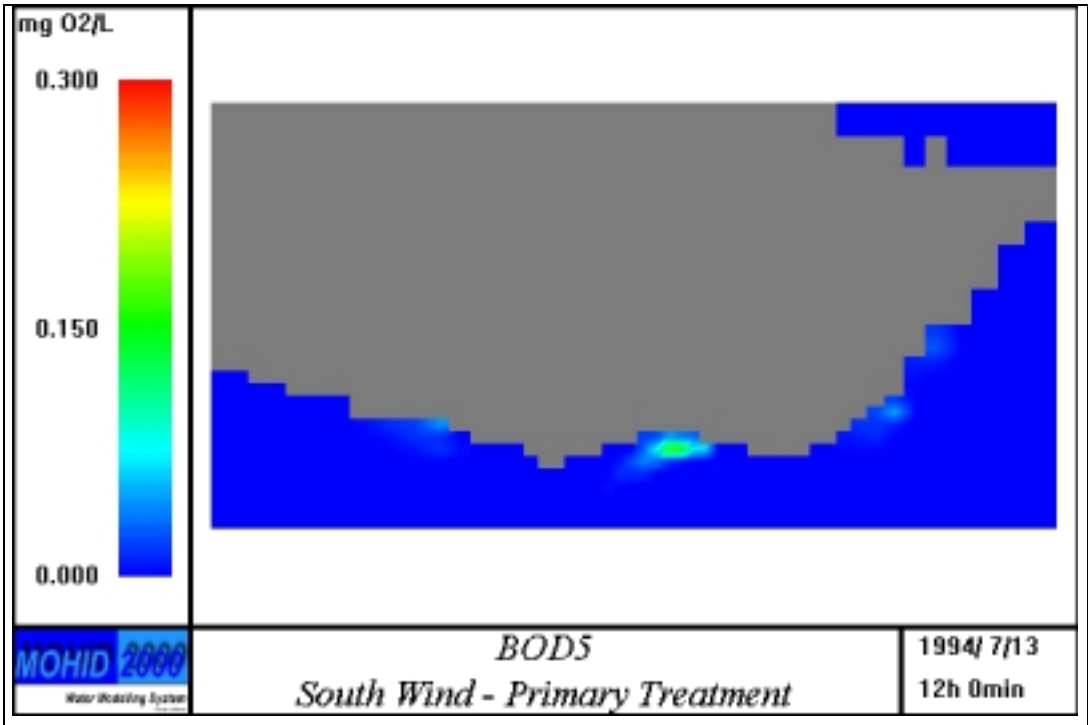


**Figure 69 Simulation with South wind. Increase $BOD_5$ concentration caused by wastewater discharge after primary treatment.**

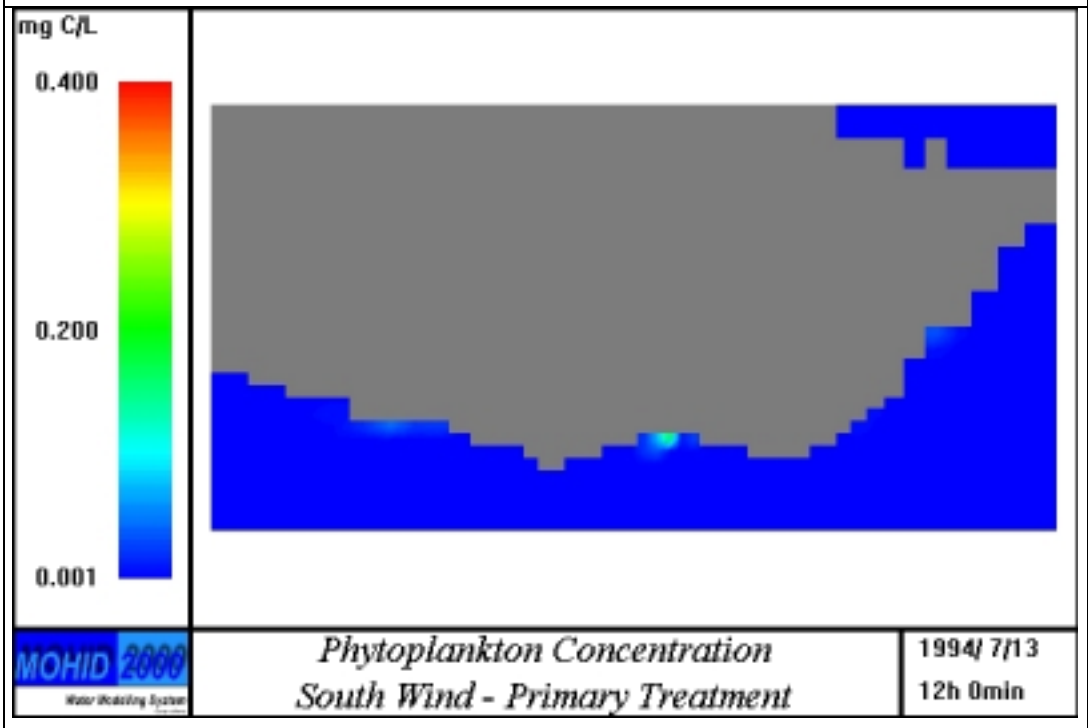


**Figure 70 Simulation with South wind. Increase phytoplankton concentration caused by wastewater discharge after primary treatment.**

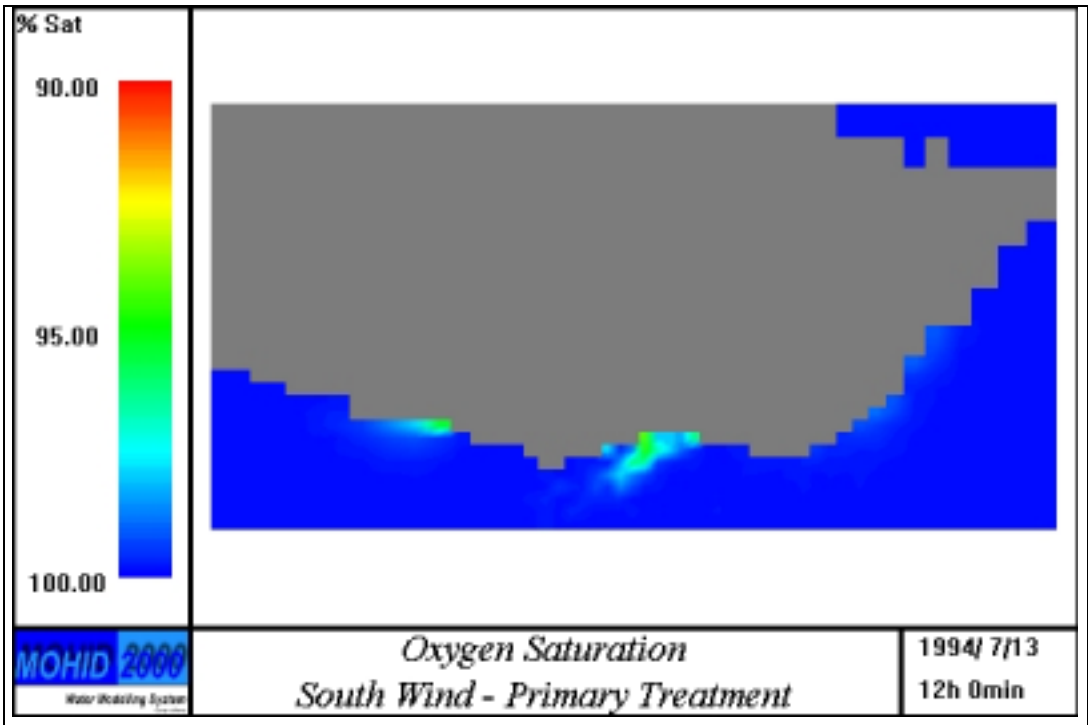


**Figure 71 Simulation with South wind. Decrease oxygen (percentage) caused by wastewater discharge after primary treatment.**

West wind simulation

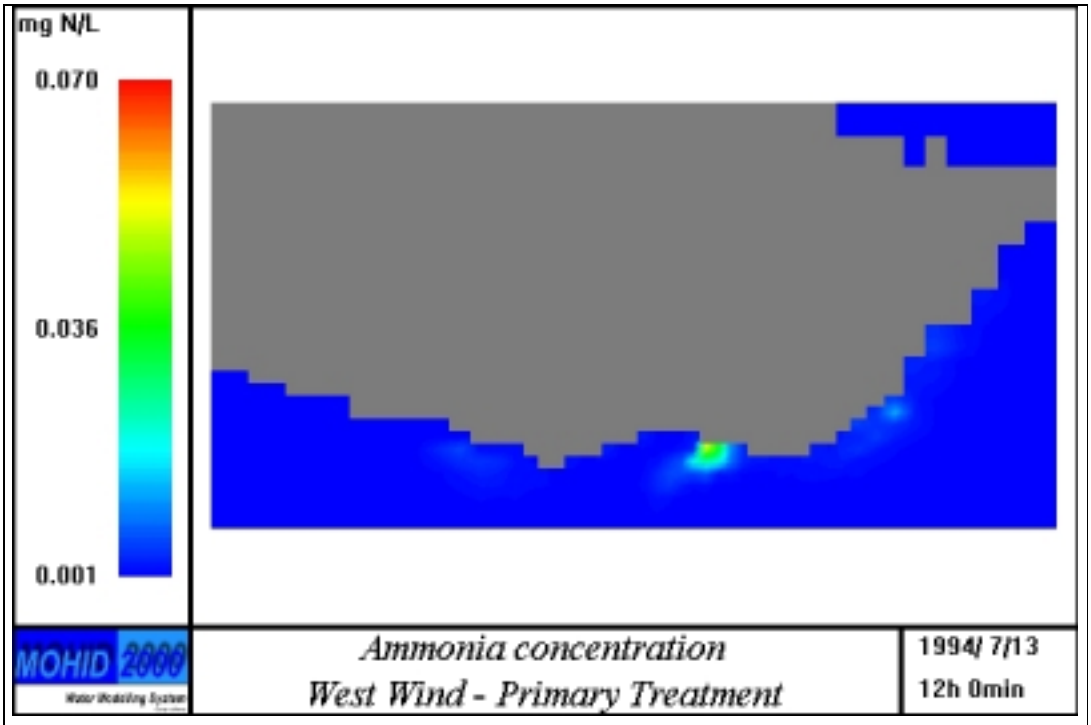


**Figure 72- Simulation with West wind. Increase ammonia concentration caused by wastewater discharge after primary treatment.**

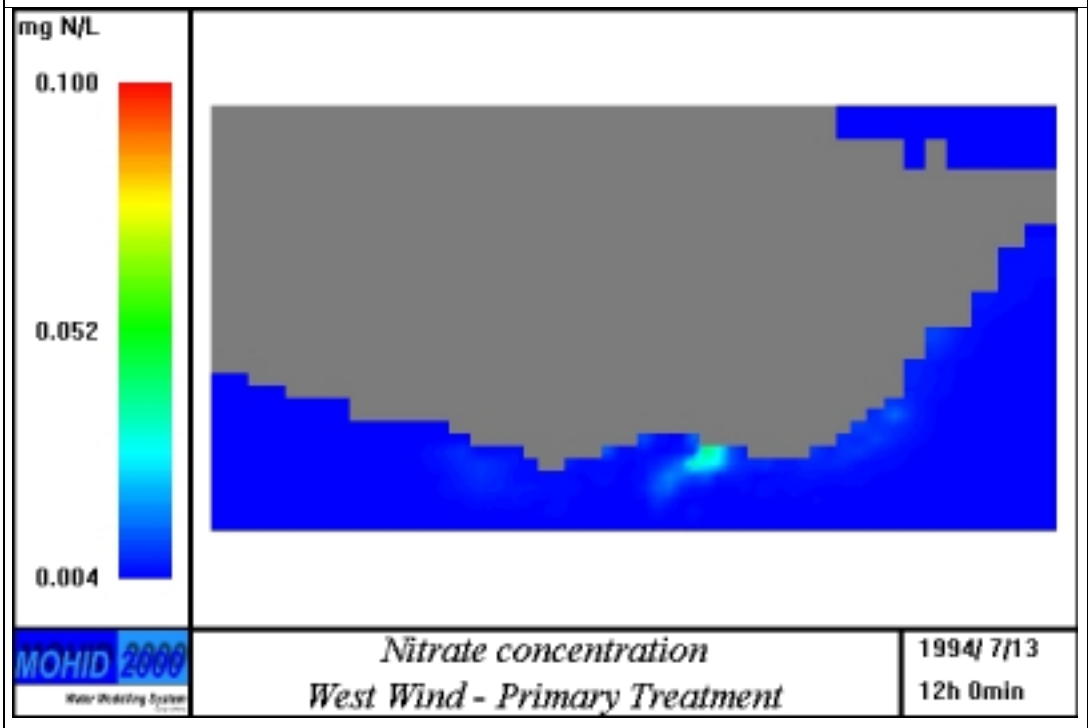


**Figure 73 Simulation with West wind. Increase nitrate concentration caused by wastewater discharge after primary treatment.**

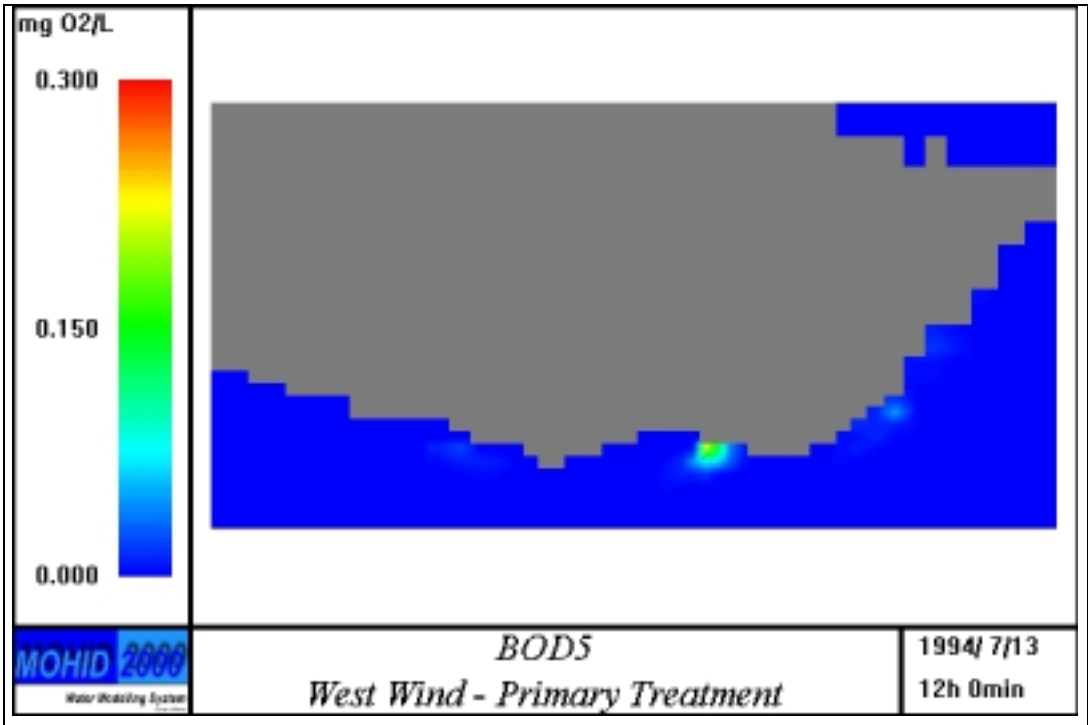


**Figure 74 Simulation with West wind. Increase $BOD_5$ concentration caused by wastewater discharge after primary treatment.**

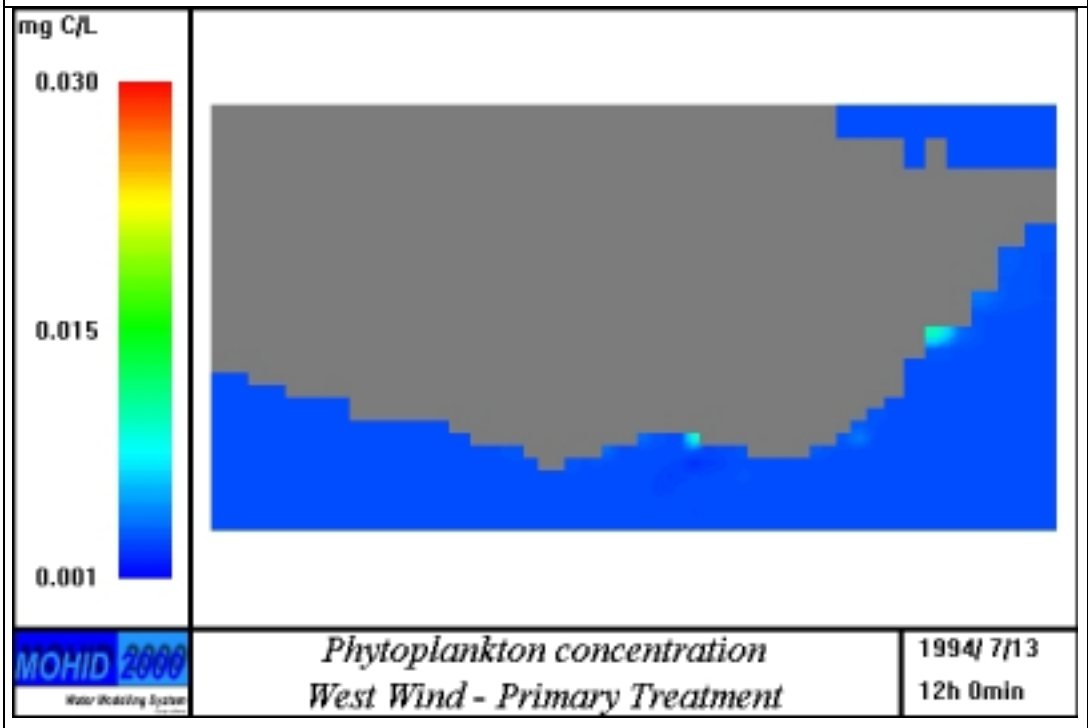


**Figure 75 Simulation with West wind. Increase phytoplankton concentration caused by wastewater discharge after primary treatment.**

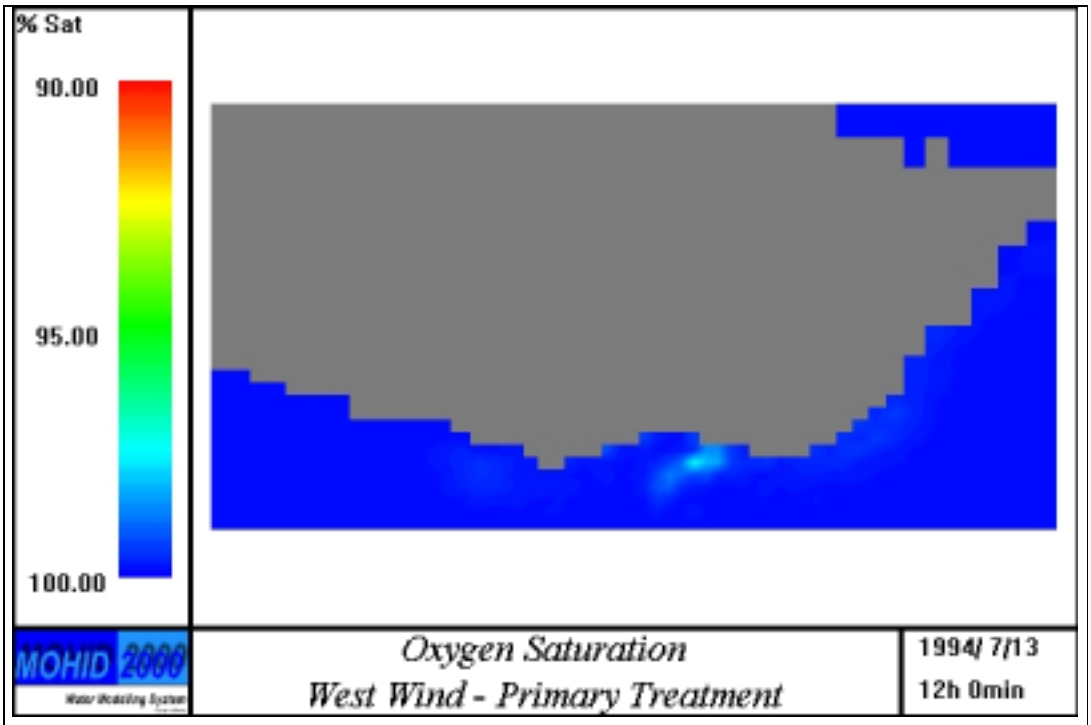


**Figure 76 Simulation with West wind. Decrease oxygen (percentage) caused by wastewater discharge after primary treatment.**

East wind simulation

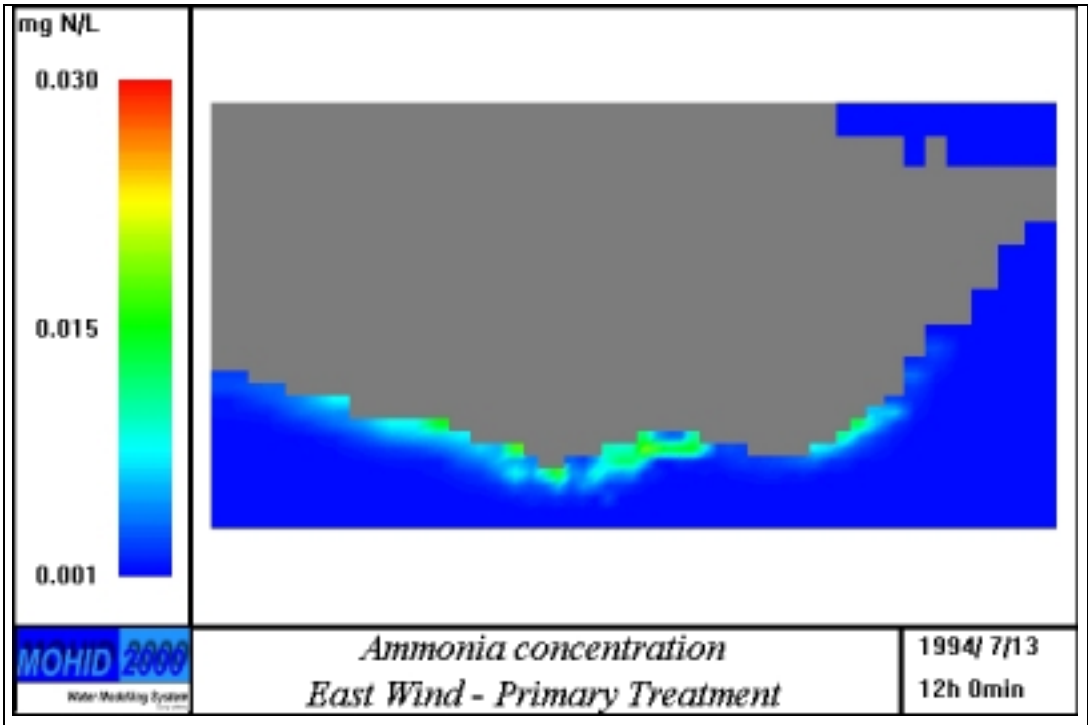


**Figure 77- Simulation with East wind. Increase ammonia concentration caused by wastewater discharge after primary treatment.**

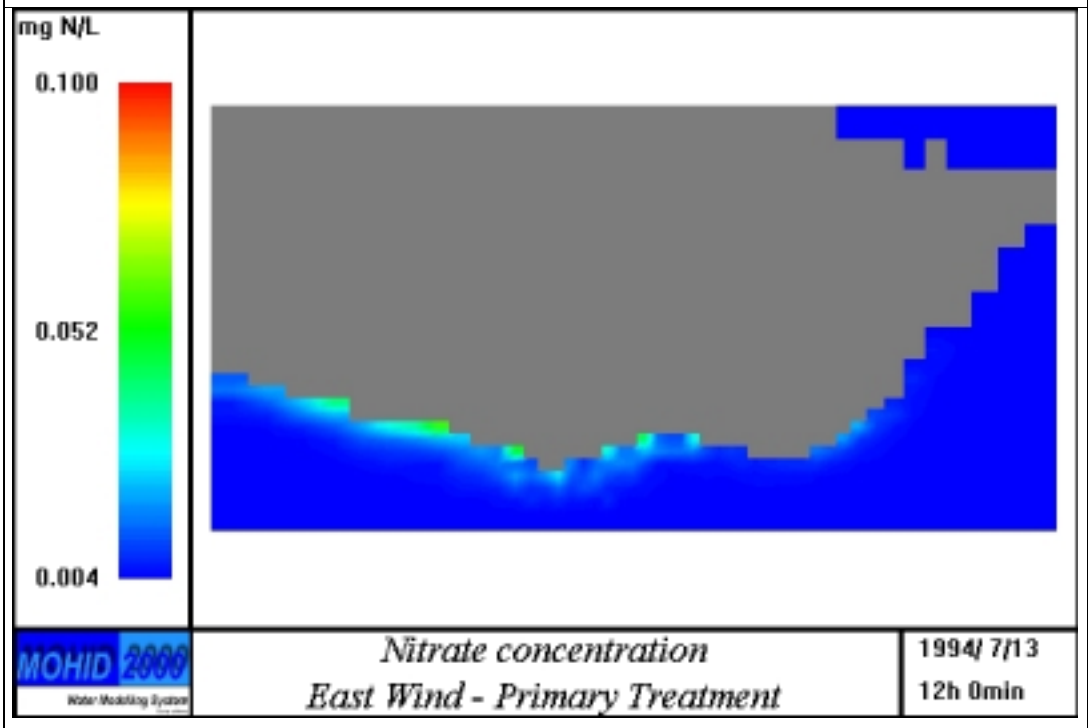


**Figure 78 Simulation with East wind. Increase nitrate concentration caused by wastewater discharge after primary treatment.**

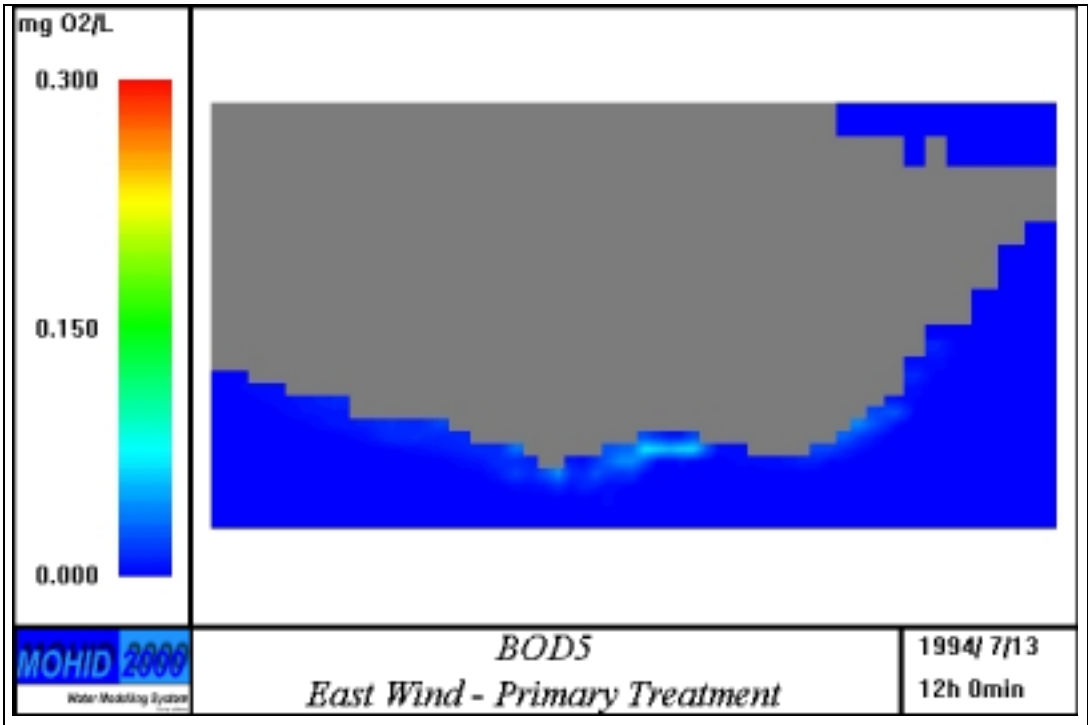


**Figure 79 Simulation with East wind. Increase $BOD_5$ concentration caused by wastewater discharge after primary treatment.**

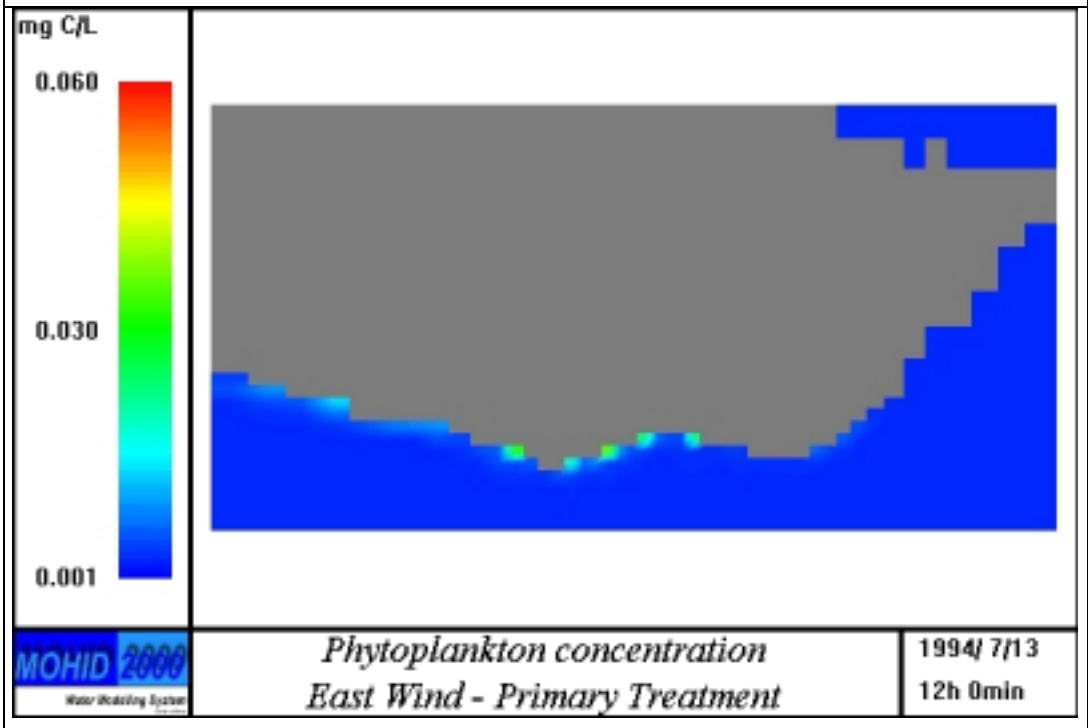


**Figure 80 Simulation with East wind. Increase phytoplankton concentration caused by wastewater discharge after primary treatment.**

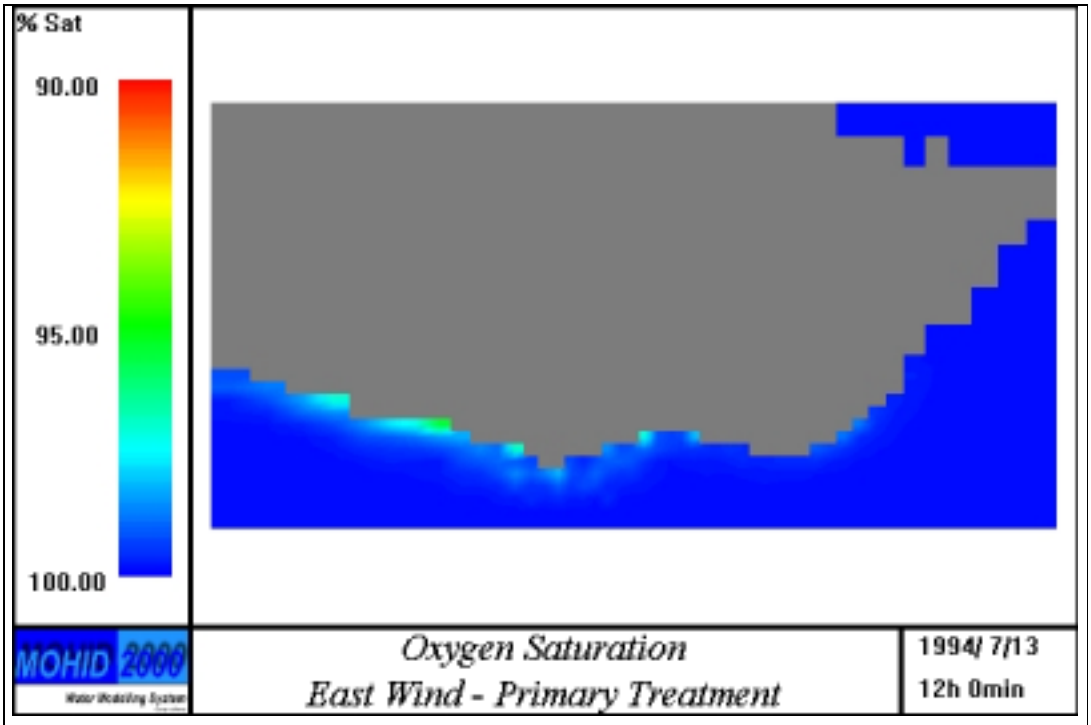


**Figure 81 Simulation with East wind. Decrease oxygen (percentage) caused by wastewater discharge after primary treatment.**

No wind simulation

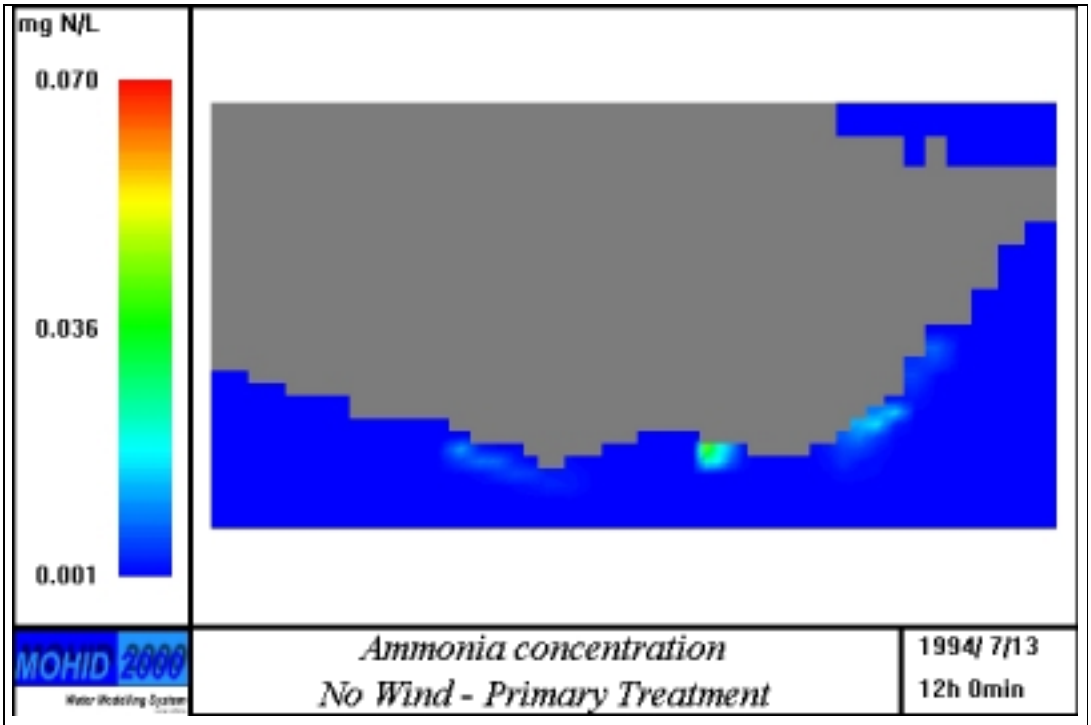


**Figure 82- Simulation with no wind. Increase ammonia concentration caused by wastewater discharge after primary treatment.**

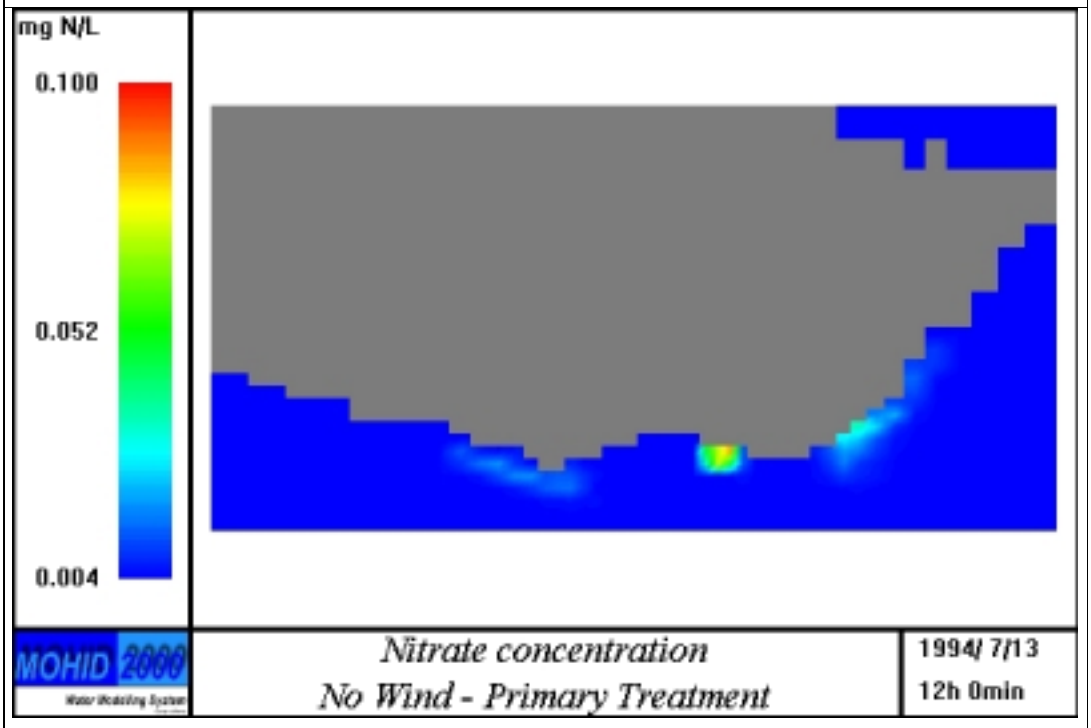


**Figure 83 Simulation with no wind. Increase nitrate concentration caused by wastewater discharge after primary treatment.**

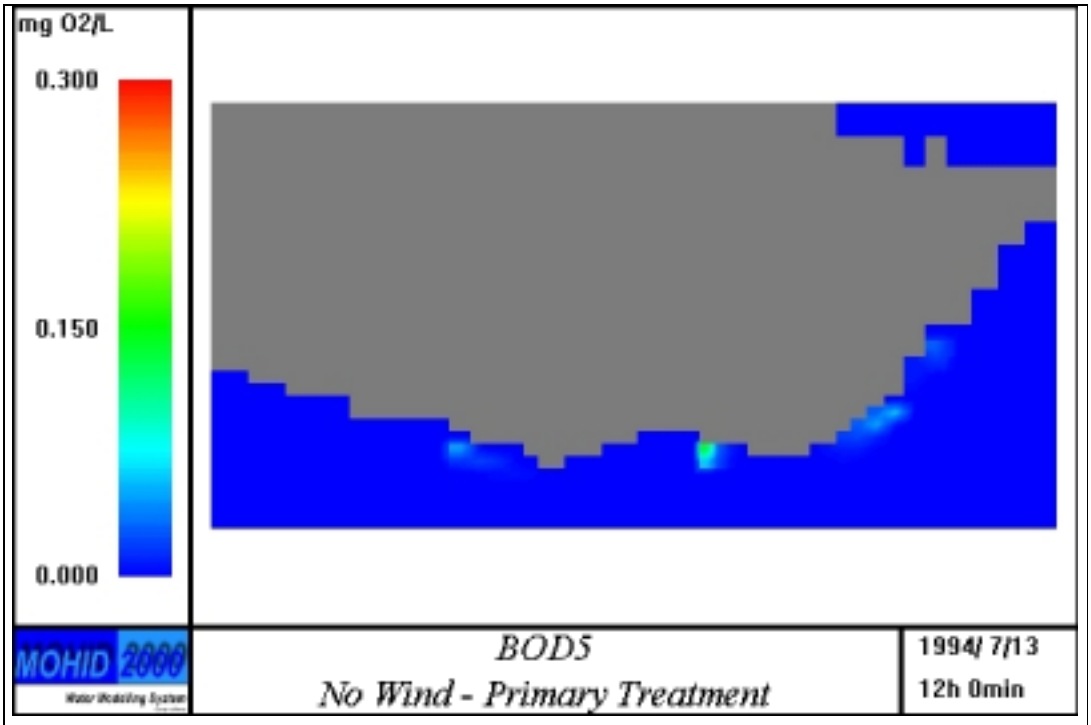


**Figure 84 Simulation with East wind. Increase $BOD_5$ concentration caused by wastewater discharge after primary treatment.**

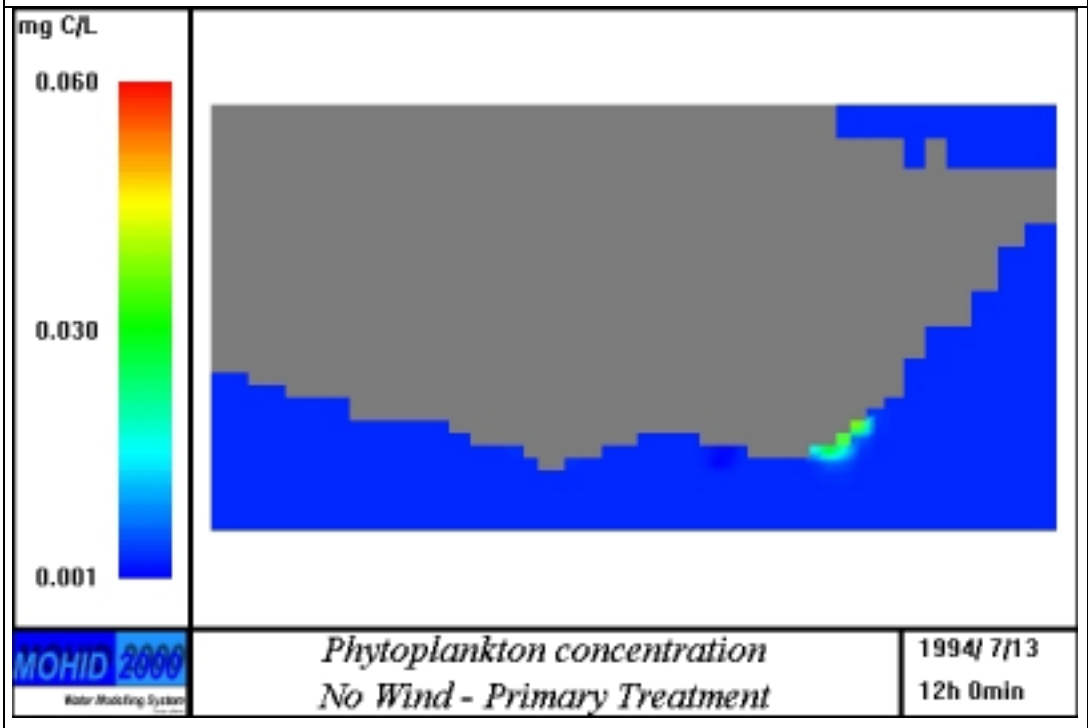


**Figure 85 Simulation with no wind. Increase phytoplankton concentration caused by wastewater discharge after primary treatment.**

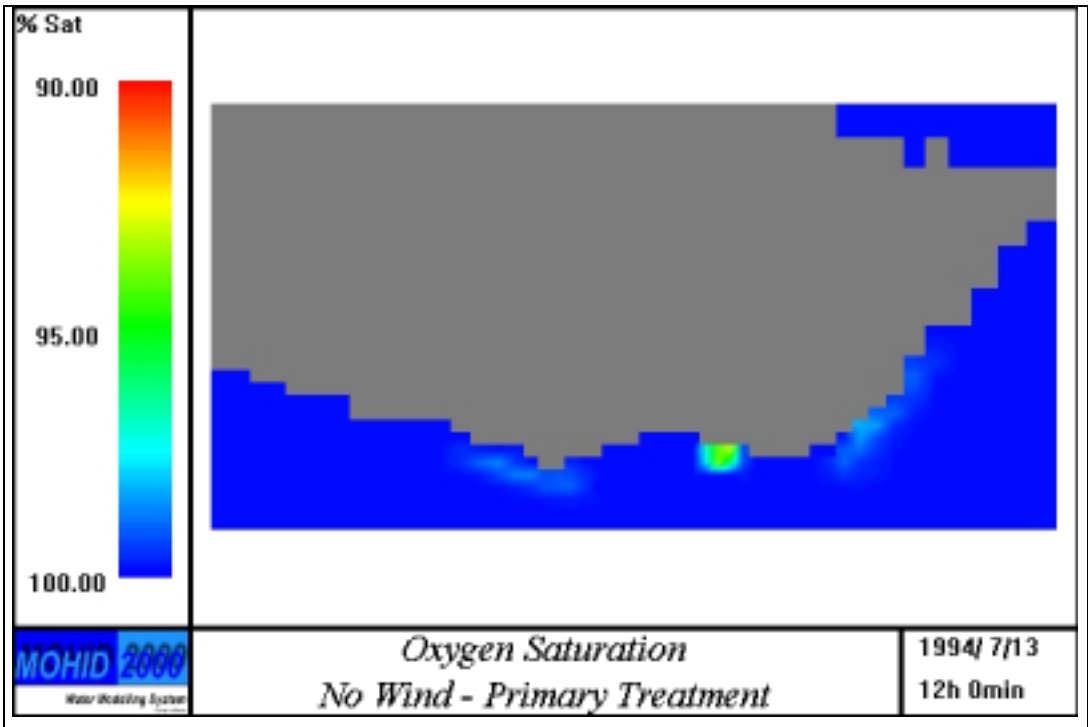


**Figure 86 Simulation with no wind. Decrease oxygen (percentage) caused by wastewater discharge after primary treatment.**

## Microbiological effects on bathing waters

This chapter describes results of simulations of the plumes of Madeira's submarine outfalls in different hydrodynamic, and mortality scenarios The next figures present the variations in the concentration of faecal coliforms in the receiving waters, with the current pattern influenced not only by the tides but also by 5 wind regimes.

It should be noted that in this simulation coliforms have no decay time. Considering these unrealistic hypotheses of T90 infinity only the beaches near Funchal suffer some contamination, and all other outfalls have negligible impact.

T90 of 2, 6hours and infinity were considered. A initial concentration of $10^3$coli./100mL was considered in all the cases. This concentration corresponds to a concentration of $10^6$coli./100mL in the treatment plant and a dilution of 1/1000 in the submarine outfall.

Simulations show that the plume never reaches shoreline unless an unrealistic infinite T90 is assumed.

North wind simulation

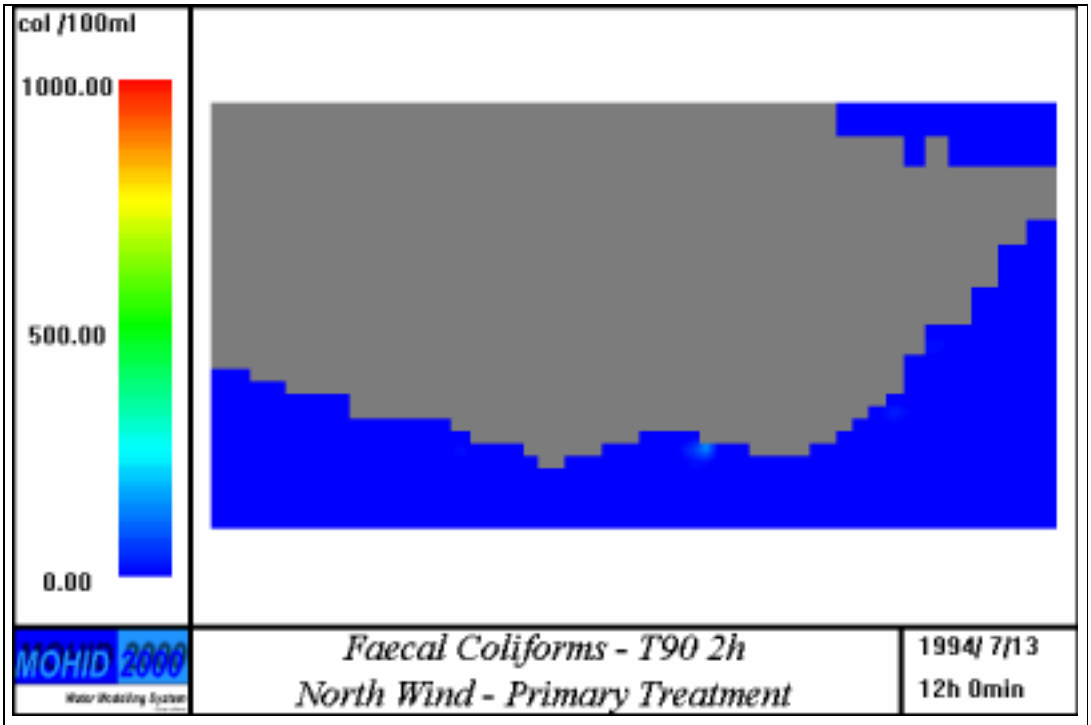


**Figure 87Faecal coliforms concentration after an 8 days run with North wind. The characteristics of the effluent are: a concentration of $10^3$ coliforms/ 100 ml after initial dilution and a $T_{90}$ of 2 hours.**

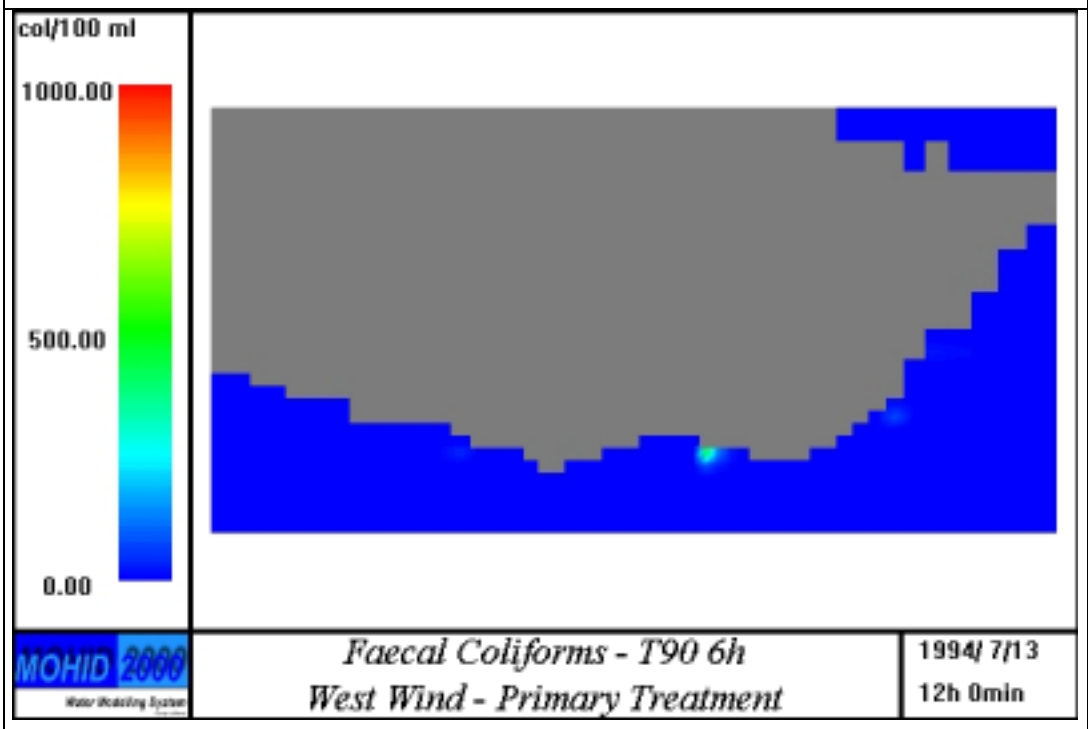


**Figure 88 Faecal coliforms concentration after an 8 days run with North wind. The characteristics of the effluent are: a concentration of $10^3$ coliforms/ 100 ml after initial dilution and a $T_{90}$ of 6 hours.**

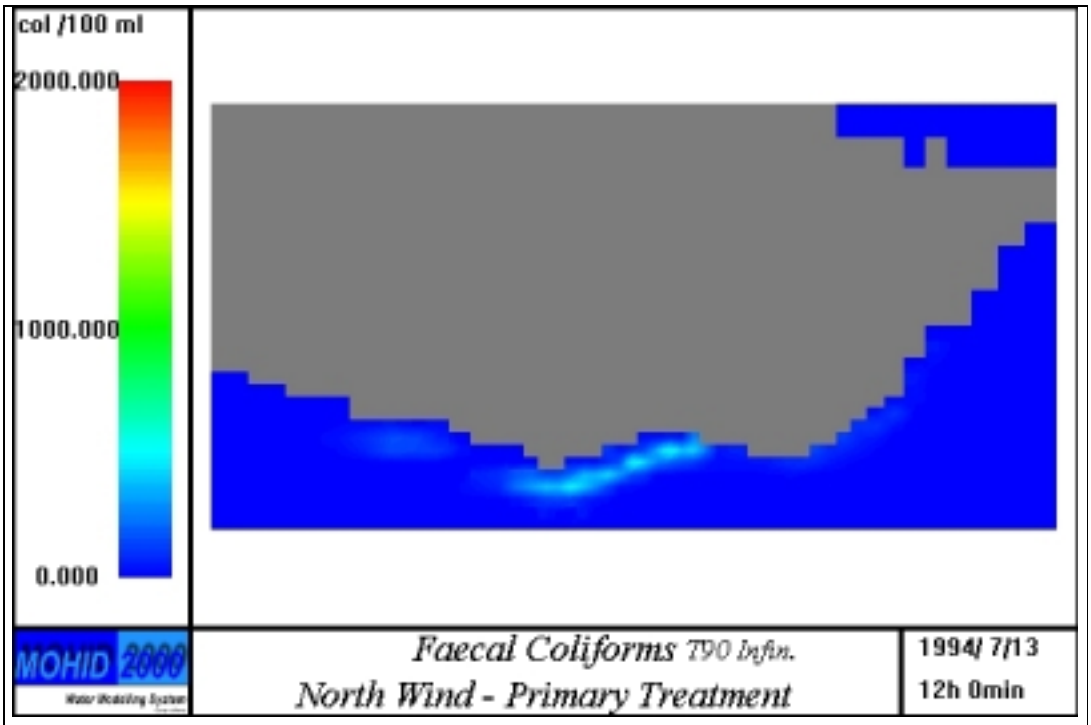


**Figure 89 Faecal coliforms concentration after an 8 days run with North wind. The characteristics of the effluent are: a concentration of $10^3$ coliforms/ 100 ml after initial dilution and a $T_{90}$ infinite.**

South wind simulation

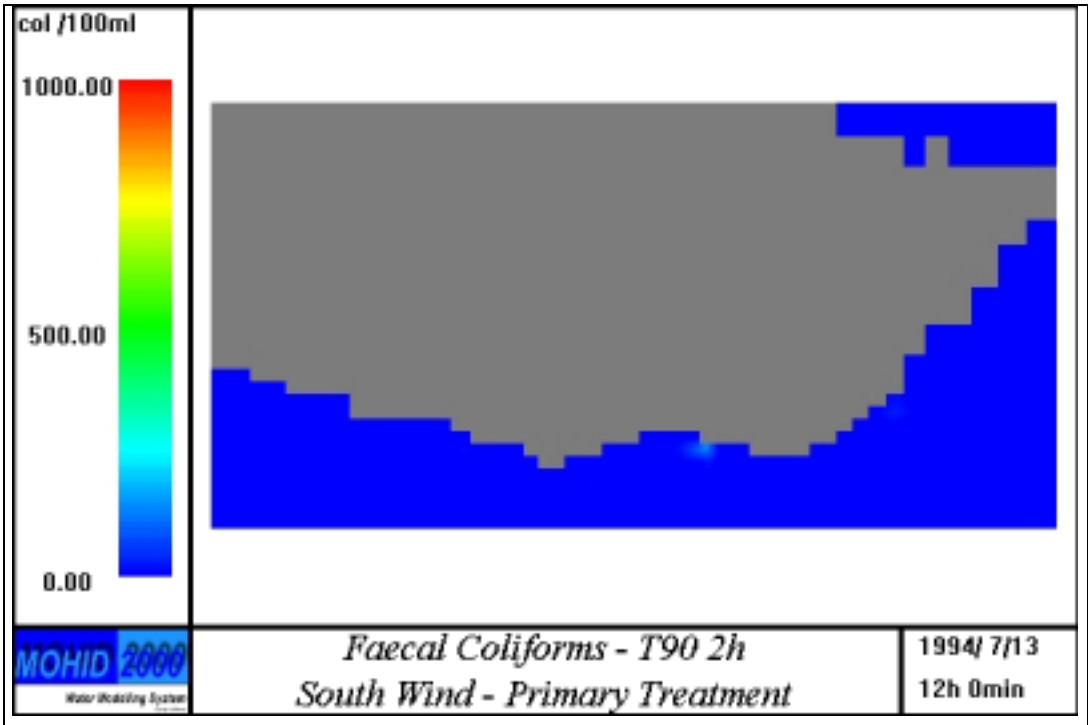


**Figure 90Faecal coliforms concentration after an 8 days run with South wind. The characteristics of the effluent are: a concentration of $10^3$ coliforms/ 100 ml after initial dilution and a $T_{90}$ of 2 hours.**

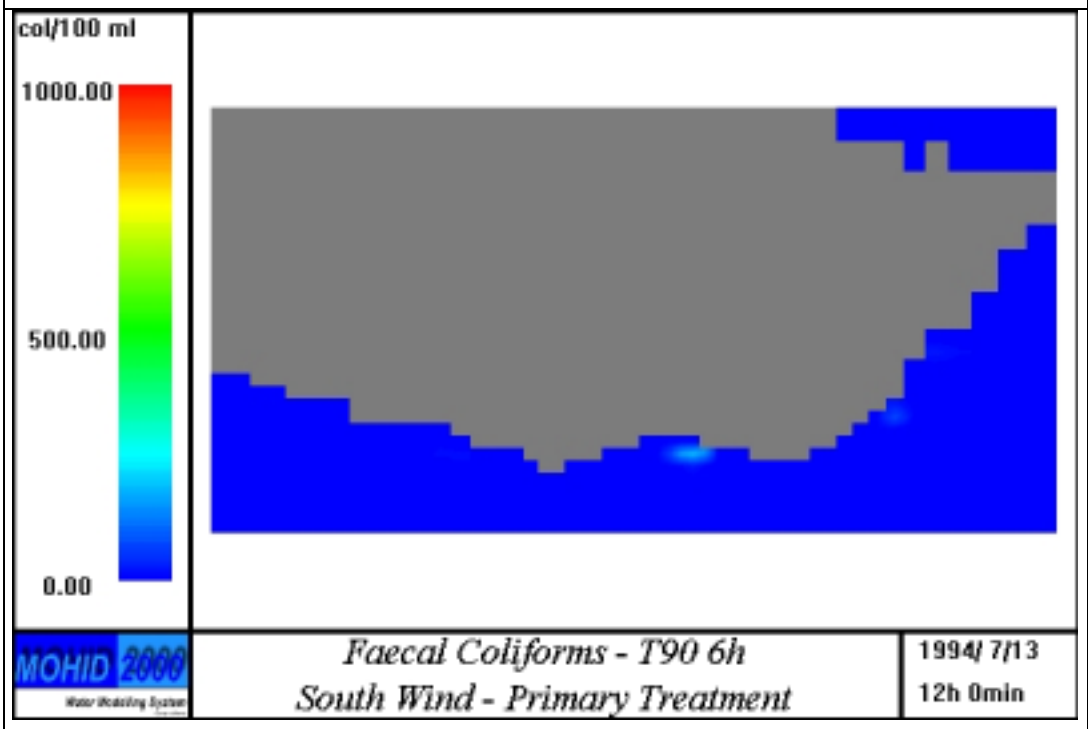


**Figure 91 Faecal coliforms concentration after an 8 days run with South wind. The characteristics of the effluent are: a concentration of $10^3$ coliforms/ 100 ml after initial dilution and a $T_{90}$ of 6 hours.**

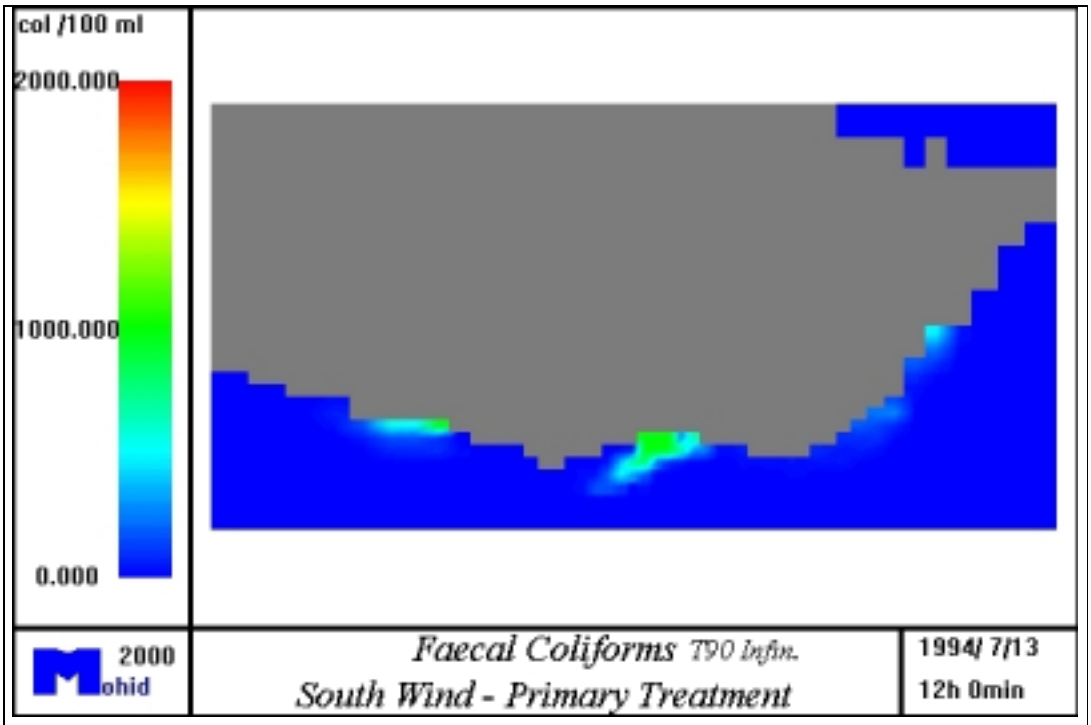


**Figure 92 Faecal coliforms concentration after an 8 days run with South wind. The characteristics of the effluent are: a concentration of $10^3$ coliforms/ 100 ml after initial dilution and a $T_{90}$ infinite.**

West wind simulation

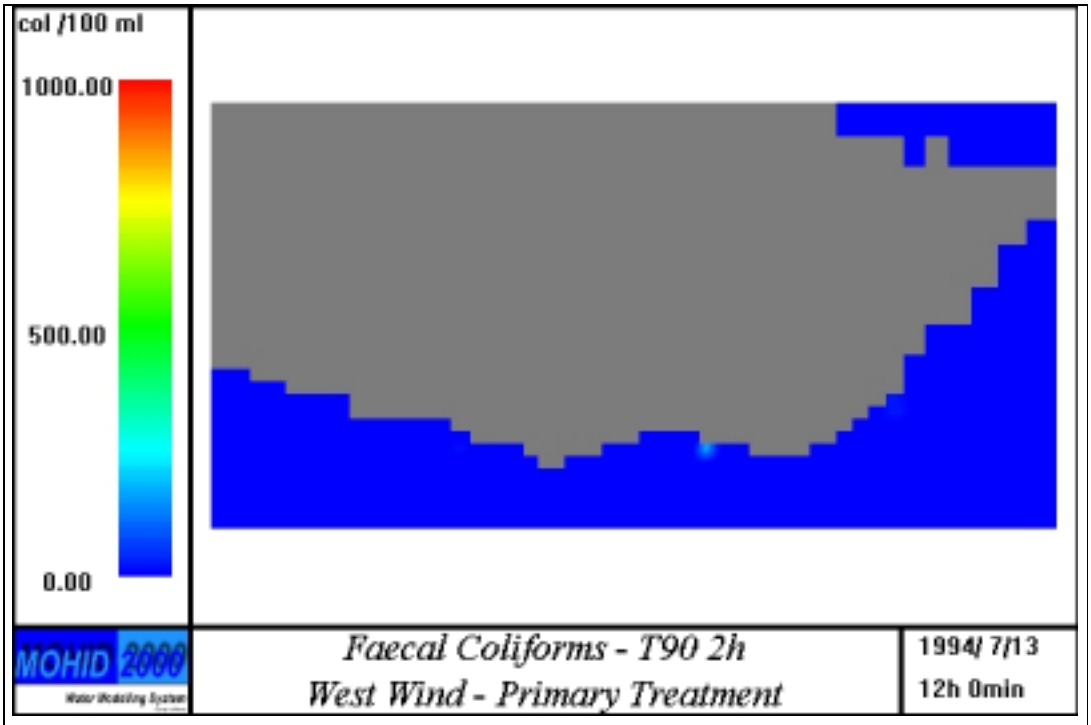


**Figure 93Faecal coliforms concentration after an 8 days run with West wind. The characteristics of the effluent are: a concentration of $10^3$ coliforms/ 100 ml after initial dilution and a $T_{90}$ of 2 hours.**

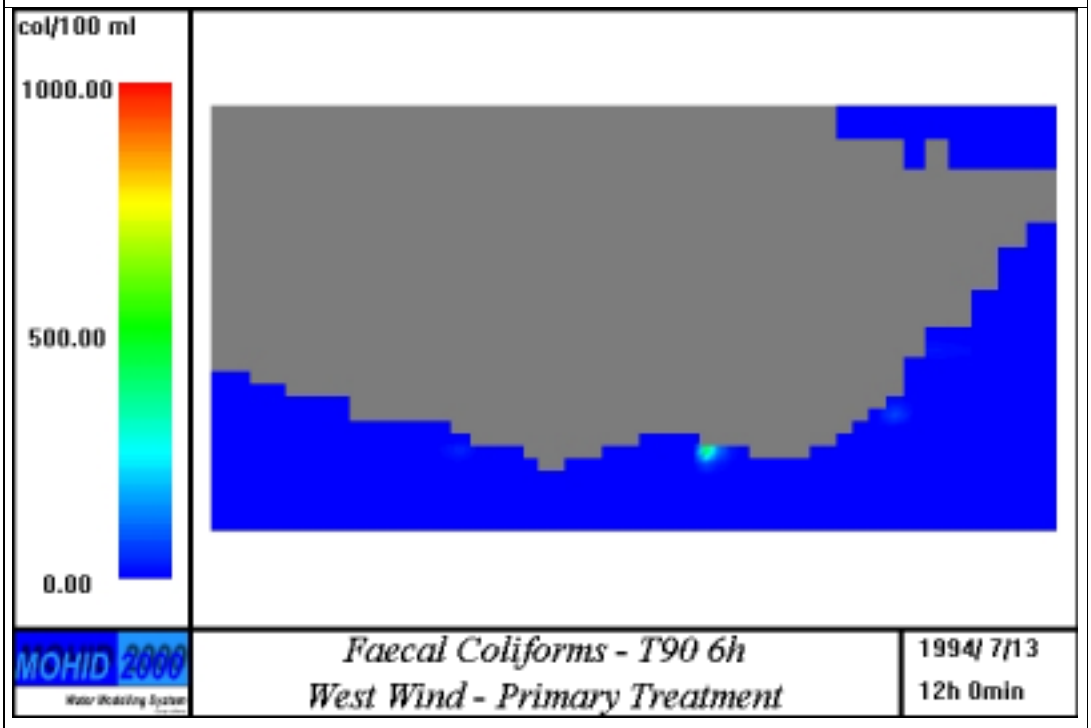


**Figure 94 Faecal coliforms concentration after an 8 days run with West wind. The characteristics of the effluent are: a concentration of $10^3$ coliforms/ 100 ml after initial dilution and a $T_{90}$ of 6 hours.**

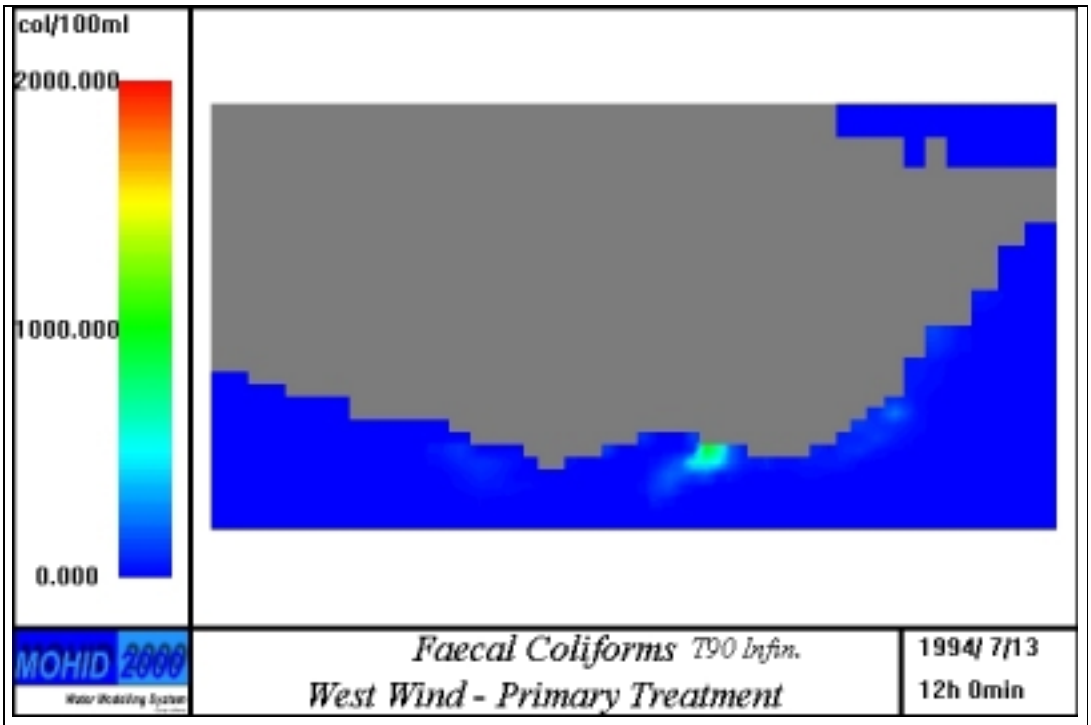


**Figure 95 Faecal coliforms concentration after an 8 days run with West wind. The characteristics of the effluent are: a concentration of $10^3$ coliforms/ 100 ml after initial dilution and a $T_{90}$ infinite.**

East wind simulation

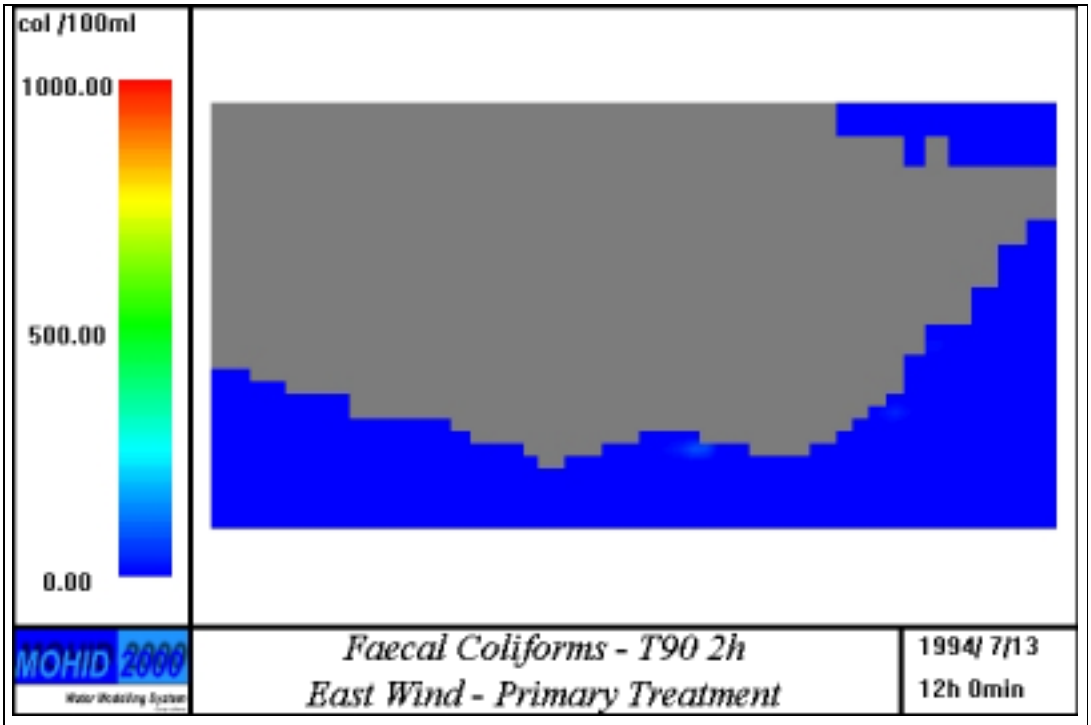


**Figure 96Faecal coliforms concentration after an 8 days run with East wind. The characteristics of the effluent are: a concentration of $10^3$ coliforms/ 100 ml after initial dilution and a $T_{90}$ of 2 hours.**

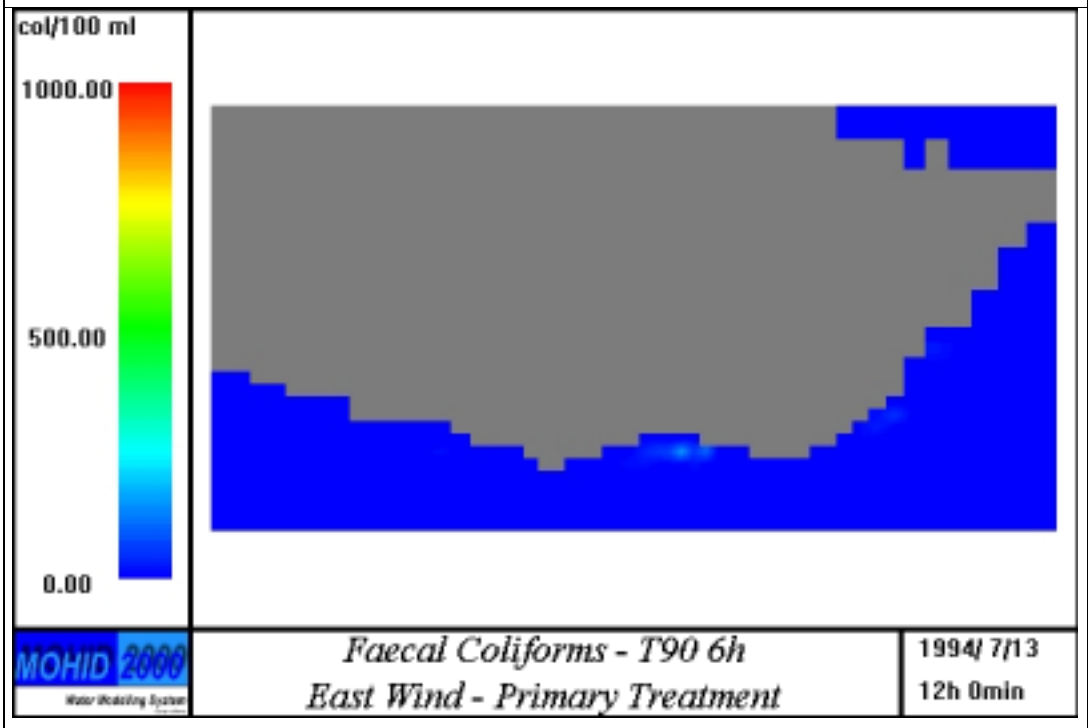


**Figure 97 Faecal coliforms concentration after an 8 days run with East wind. The characteristics of the effluent are: a concentration of $10^3$ coliforms/ 100 ml after initial dilution and a $T_{90}$ of 6 hours.**

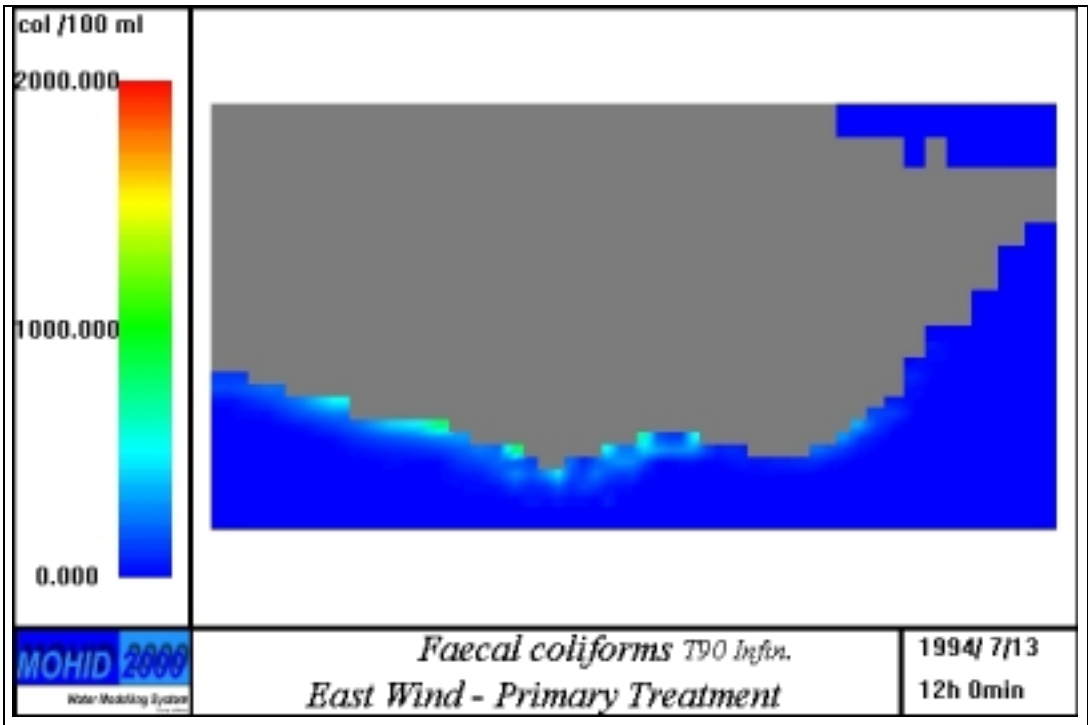


**Figure 98 Faecal coliforms concentration after an 8 days run with East wind. The characteristics of the effluent are: a concentration of $10^3$ coliforms/ 100 ml after initial dilution and a $T_{90}$ infinite.**

No wind simulation

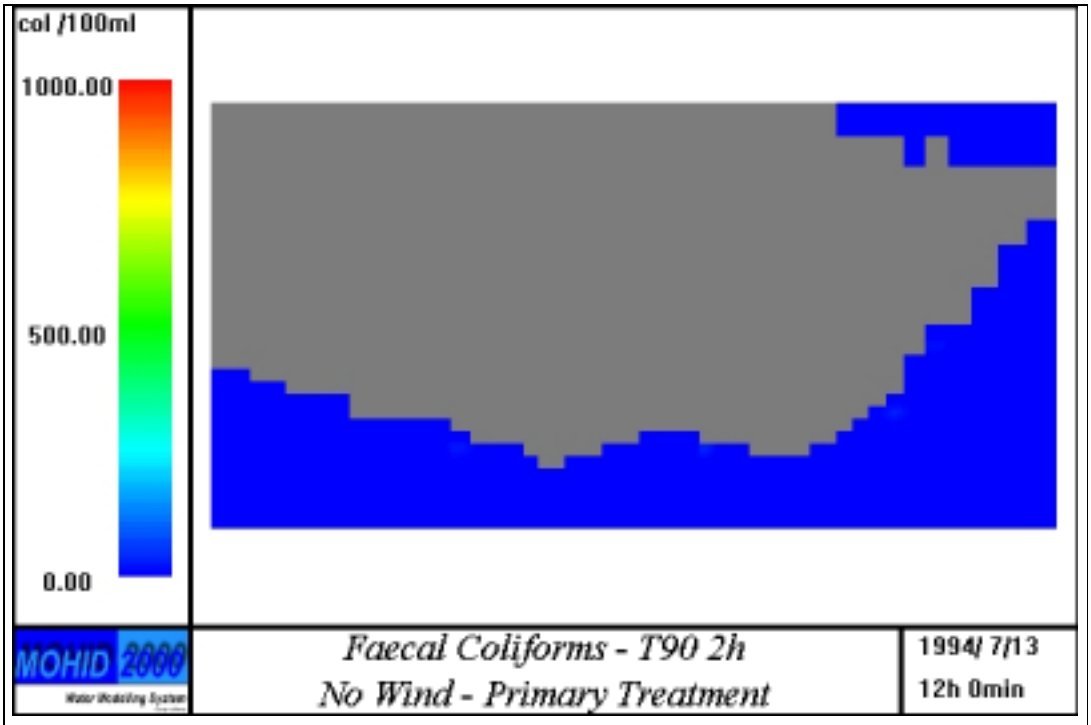


**Figure 99Faecal coliforms concentration after an 8 days run without wind. The characteristics of the effluent are: a concentration of $10^3$ coliforms/ 100 ml after initial dilution and a $T_{90}$ of 2 hours.**

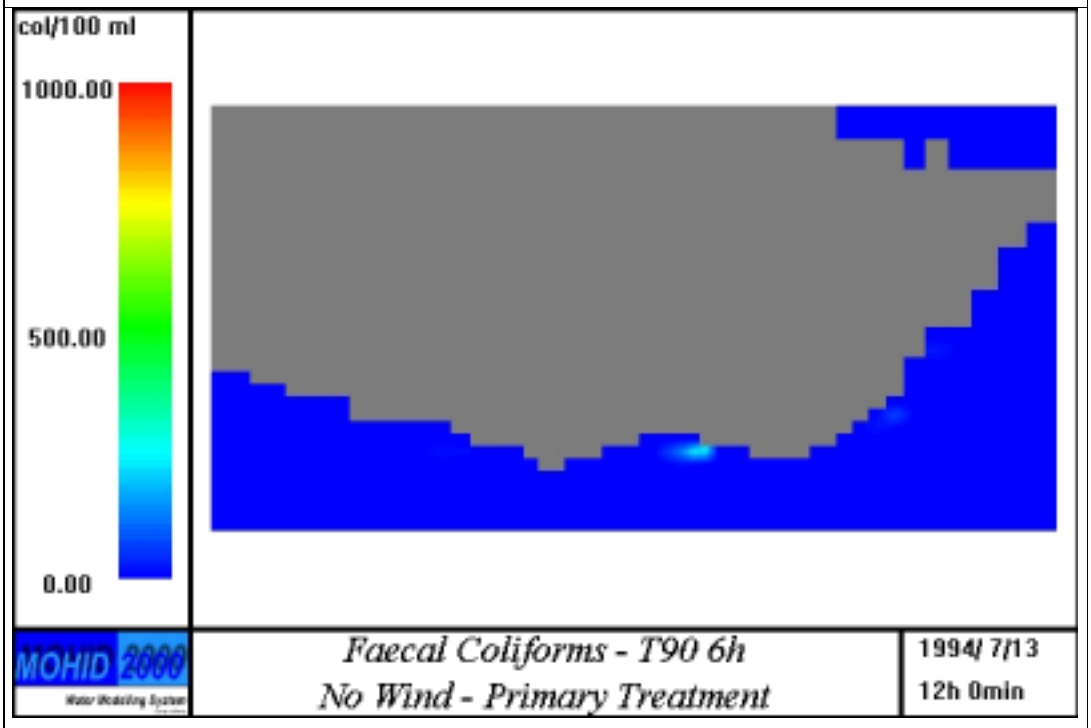


**Figure 100 Faecal coliforms concentration after an 8 days run without wind. The characteristics of the effluent are: a concentration of $10^3$ coliforms/ 100 ml after initial dilution and a $T_{90}$ of 6 hours.**

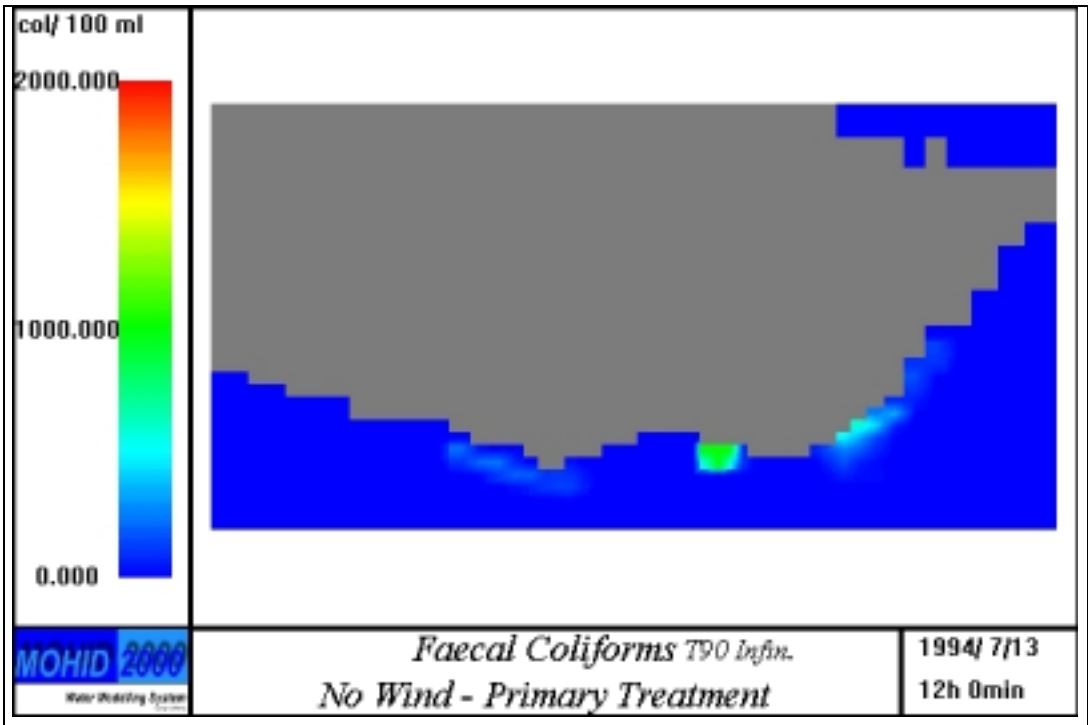


**Figure 101 Faecal coliforms concentration after an 8 days run without wind. The characteristics of the effluent are: a concentration of $10^3$ coliforms/ 100 ml after initial dilution and a $T_{90}$ infinite.**

## Assessment of the Effects of the Systems as Regards Compliance with EU Directives

Council Directive 91/271/EEC, of 21 May 1991, establishes that urban wastewater discharges from agglomerations of between 10,000 and 150,000 population equivalent (p.e.) to coastal waters, in less sensitive areas, may be subjected to treatment less stringent than a secondary treatment if technical studies indicate that such discharges will not adversely affect the environment.

From the analysis of the experimental results and the modulation of the evolution of water quality, it is considered to be congregated the technical conditions that satisfy the legal requirements established in the previous paragraph.

In the base of these affirmations are oceanographic conditions that occur near Madeira's archipelago, such as high transparencies (values of about 30 meters in depth) and high coastal edge slopes (of about 20%).

The results of this study guarantees fulfillment of the conditions stabilized in the Council Directive 76/160/EEC – Bathing Waters, as presented in chapter "Description of Receiving Waters". Indeed the discharge of treated effluents by diffuser in the ocean

at a distance of more than 2,000 meters of the beaches ensure water quality compatible with its use for direct leisure.

In Madeira Island there are no sea areas appointed in the scope of Council Directive 79/923/EEC of 30 October 1979, relative to the required quality of shellfish waters. In this region, the commercial exploration of bivalve's clams is practically inexistent, due to the following main factors: reduced size, weak abundance and occurrence at great depths. It exists, however, some capture of lapas and caramujos, but these clams haven't got any particular protection status. This capture is, however, little significant. So, it is considered that this Directive does not cover these seawaters.

Council Directive 92/43/EEC of 21 May 1992, vulgarly known as "Habitats Directive", has the main propose of contribute for the preservation of biodiversity of species in the European Union. In the scope of this directive, special areas of conservation shall be set up under the title Natura 2000 Network.

In the Madeira's autonomous region there have been declared sites of Community importance those, which preserves the features of the Macaronesian region. The Macaronesian region is extended exclusively throughout a set of Atlantic islands, corresponding to the archipelagoes of Azores, Madeira, Savages, the Canaries and Cape Verde. These islands have three important features in common. They are all Atlantic islands, of volcanic origin that had been never matched to the continent.

In the scope of the Habitats Directive, the region of the Pináculo was declared site of Community importance. Pináculo, with a total area of about 30 hectares, locates marginally to the area of implantation of the Funchal's wastewater system. This site of Community importance is constituted mostly by gravel hillsides colonized by small herbaceous and arbustive vegetation. In accordance with the indicated in the Annex I of the Directive, this site of Community importance only presents two types of protected natural habitats: Vegetated sea cliffs of the Macaronesian coasts (1250) and low formations of euphorbia close to cliffs (5331). This site, however, does not present any special protection status.

The Natura 2000 network integrates, beyond the classified sites established by the Habitats Directive, the classified sites established by the Birds Directive. Council Directive 79/409/EEC, of 2 April 1979, known as the "Birds Directive", relates to the conservation of all species of naturally occurring birds in the wild state in the European Community territory. The Pináculo region lodges two species of birds from the Annex I of this directive: *Calonectris diomedea* and *Sterna hirundo*, which use the site to

reproduction. Some birds of the *Ardea cinerea* specie also use this site, during its pass for the archipelago. These birds are migratory species not enclosed in the Annex I.

It seems that, since that the Funchal and Câmara de Lobos sewage systems transport the effluent to a distance of more than 500 meters of the coast edge, this systems don't cause damage to the region habitats, such as Pináculo's habitats.

## Summary and conclusion

The exceptional hydrodynamic conditions in the zone (namely in terms of current pattern), contribute to an increase in the initial dispersion and subsequent dispersion of pollutant loads, and to minimise the impact of the discharge of effluent (whether primary effluent, or secondary effluent) in the receiving waters.

The abiotic conditions of the system (light, vertical mixing), the acceptable concentrations of nitrogen for the two treatment scenarios considered, and the reduced concentrations obtained from chlorophyll-a, confirm that the zone of influence of the submarine outfall will not become subject to eutrophication.

The complementary treatment of the effluent (secondary treatment instead of primary treatment), does not appear to bring any additional benefit, in terms of water quality, since the corresponding reduction in the concentration of nutrients in the receiving waters is much reduced.

## References

Adélio, A.J.R., J.P. Delfino, J.C. Leitão, P.C. Leitão, P. Pina & R. Neves (2000). Operational models-a tool to improve coastal Management. Eighth International Conference on Hydraulic Engineering Software. Ed. Blain, W. R., C. A. Brebbia. WITPress 2000.

Barkley, R. A. (1972) Johnston Atoll's wake. *Journal of Marine Research* **30**, 201-216.

Barton, E., G. Basterretxea, P. Flament, E. G. Mitchelson-Jacob, B. Jones, J. Arístegui and F. Herrera (2000). Lee region Gran Canaria. Journal of Geophysical Research, vol. 105, No. C7, pages 17,173-17,193, July 15, 2000.

Coelho, H. S., R. J. J. Neves, P. C. Leitão, H. Martins and A. Santos, 1999: The slope current along the Western European Margin: a numerical investigation. Oceanography of the Iberian Continental Margin. Bol. Inst. Esp. Oceanogr., 15, 61-72.

Drena 1991. Interceptor, Estação de tratamento preliminar, emissário de águas residuais do funchal. Emissário Submarino. Volume 1. Estudo de Impacte Ambiental. Secretaria Regional do Equipamento Social Câmara Municipal do Funchal, Julho 1991.

INSTITUTO DA ÁGUA, 1998 – *Urban Wastewater Discharge – Council Directive 91/271/EEC and DECREE LAW 152/97 – Metodic Orientation Lines to the Elaboration of Necessary Techical Studies to Fulfill Artº 6, of DL 152/97 – Discharge em Less Sensitive Zones*. Lisbon, March 1998.

Instituto de Meteorologia (IM)

Instituto Hidrográfico (IH). Roteiro do Arquipélago da Madeira e Ilhas Selvagens, Lisboa, 1979.

INSTITUTO NACIONAL DE INVESTIGAÇÃO DE PESCAS (Actual IPIMAR) – Programa de Apoio às Pescas na Madeira – I. Cruzeiro de reconhecimento de Pescas e Oceanografia 020080779. Lisbon, 1980.

INSTITUTO NACIONAL DE INVESTIGAÇÃO DE PESCAS (Actual IPIMAR) – Programa de Apoio às Pescas na Madeira – II. Cruzeiro de reconhecimento de Pescas e Oceanografia 020170680 e 020241180. Lisbon, 1982.

INSTITUTO NACIONAL DE INVESTIGAÇÃO DE PESCAS (Actual IPIMAR) – Programa de Apoio às Pescas na Madeira – III. Cruzeiro de reconhecimento de Pescas e Oceanografia 020330981. Lisbon, 1984.

INSTITUTO NACIONAL DE INVESTIGAÇÃO DE PESCAS (Actual IPIMAR) – Programa de Apoio às Pescas na Madeira – IV. Cruzeiro de reconhecimento de Pescas e

Oceanografia 020390582. Lisbon, 1984.

INSTITUTO NACIONAL DE INVESTIGAÇÃO DE PESCAS (Actual IPIMAR) – Programa de Apoio às Pescas na Madeira – V. Cruzeiro de reconhecimento de Pescas e Oceanografia 020451182. Lisbon, 1984.

Le Provost, C., F. Lyard, J.M. Molines, M.L. Genco and F. Rabilloud, 1998. A Hydrodynamic Ocean Tide Model Improved by assimilating a satellite altimeter derived dataset. *J. Geophys. Res. V*ol. 103 N. C3, 1998.

Levitus, S. and., T. P. Boyer, 1994. World Ocean Atlas 1994. Volume 4: NOAA Atlas NESDIS 4, 117pp.

Levitus, S., R. Burgett and T. P. Boyer, 1994. World Ocean Atlas 1994. Volumes 1 and 2: NOAA Atlas NESDIS 3, 99pp.

Martins F., P. Leitão, A. Silva and R. Neves. 3D modelling in the Sado estuary using a new generic vertical discretization approach, in press Oceanological Acta.

Martins, F.A., R.J. Neves, P.C. Leitão, 1998. A three-dimensional hydrodynamic model with generic vertical coordinate. Proceedings of Hidroinformatics98, 2, V. Babovic and L. C. Larsen eds., Balkerna/Rotterdam, Copenhague, Denmark, August 1998.1403-1410

Martins, H, A. Santos, E. F. Coelho, R. Neves and T. L. Rosa, 1999: Numerical Simulation of Internal Tides. Journal of Mechanical Engineering Science

METCALF and EDDY, 1991 – *Wastewater Engineering. Treatment, Disposal and Reuse*. McGraw-Hill, United States.

Miranda R., F. Braunschweig, P. Leitão, R. Neves, F. Martins & A. Santos (2000). MOHID2000 - A coastal integrated object oriented model. Eighth International Conference on Hydraulic Engineering Software. Ed. Blain, W. R., C. A. Brebbia. WITPress 2000.

Miranda, R., R. Neves, H. Coelho, H. Martins, P. C. Leitão and A. Santos, 1999: Transport and Mixing Simulation Along the Continental Shelf Edge Using a Lagrangian Approach, Bol. Inst. Esp. Oceanogr., 15,39-60

NASA (1968) *Earth photographs from Gemini VI through XII.* NASA publication SP-171, U.S. Government Printing Office, Washington, D.C.

Parsons, Timothy R.; Takahashi, Masayuki; Hargrave, Barry (1995) Biological Oceanographic Processes. Butterworth Heinemann, 3rd Ed.

Santos A. J. P., 1995: Modelo hidrodinâmico de circulação oceânica e estuarina (in portuguese). PhD Thesis, IST Lisbon. 273 pp.

Santos, A. and R. Neves, 1991: R. Radiative artificial boundaries in ocean barotropic

models. Proc. of the 2nd Int. Conf. On Computer Modelling in Ocean Engineering, September, Barcelona.

Siedler, G., and R. Onken, 1996 : Eastern recirculation. The Warmwater sphere of the North Atlantic Ocean (edit. W. Krauss), Gebrüder Borntraeger. Berlin. Stuttgart, 339-360.

Taboada, J. J., R. Prego, M. Ruiz-Villarreal, M. Gómez-Gesteira, P. Montero, A. P. Santos, V. Pérez-Villar, 1998: Evaluation of the Seasonal Variations in the Residual Circulation in the Ria of Vigo (NW Spain) by means of a 3D baroclinic model. Estuarine, Coastal and Shelf Science.

Tomczak M. (1996) Island wakes in deep and shallow water. http://gaea.es.flinders.edu.au/~mattom/ShelfCoast/chapter07.html.

Trenberth, K. E., W. G. Large and J. G. Olsen, 1990: The mean annual cycle in global wind stress. *J. Phys. Oceanogr*., **20**, 1742-1760.

Visbeck, M., J. Marshall, T. Haine and M. Spall, 1997: Representation of topography by sahved cells in a height coordinate ocean model. *Mon. Wea. Rev*., **125**, 2293-2315.